

UNICAMP

REJANE DE CASTRO SANTANA

**SISTEMAS AUTO-ORGANIZÁVEIS FORMADOS POR TCM,
ETANOL E SURFACTANTES DE GRAU ALIMENTÍCIO: EFEITO DA
TEMPERATURA E DAS CONCENTRAÇÕES DE SURFACTANTE,
CO-SURFACTANTE E ÁGUA**

CAMPINAS

2014



UNIVERSIDADE ESTADUAL DE CAMPINAS
FACULDADE DE ENGENHARIA DE ALIMENTOS

REJANE DE CASTRO SANTANA

SISTEMAS AUTO-ORGANIZÁVEIS FORMADOS POR TCM, ETANOL E
SURFACTANTES DE GRAU ALIMENTÍCIO: EFEITO DA TEMPERATURA E DA
CONCENTRAÇÃO DE SURFACTANTE, CO-SURFACTANTE E ÁGUA

Tese apresentada à Faculdade de Engenharia de Alimentos da Universidade Estadual de Campinas como parte dos requisitos exigidos para a obtenção do título de Doutora em Engenharia de Alimentos

Orientador(a): Profa. Dra. Rosiane Lopes da Cunha

Este exemplar corresponde à versão final da tese defendida pela aluna Rejane de Castro Santana e orientada pela Profa Dra Rosiane Lopes da Cunha

Assinatura da Orientadora

CAMPINAS

2014

Ficha catalográfica
Universidade Estadual de Campinas
Biblioteca da Faculdade de Engenharia de Alimentos
Claudia Aparecida Romano - CRB 8/5816

Santana, Rejane de Castro, 1983-
Sa59s Sistemas auto-organizáveis formados por TCM, etanol e surfactantes de grau alimentício: efeito da temperatura e das concentrações de surfactante, co-surfactante e água / Rejane de Castro Santana. – Campinas, SP : [s.n.], 2014.

Orientador: Rosiane Lopes da Cunha.
Tese (doutorado) – Universidade Estadual de Campinas, Faculdade de Engenharia de Alimentos.

1. Microemulsão. 2. Cristal líquido. 3. Estrutura. 4. Reologia. I. Cunha, Rosiane Lopes. II. Universidade Estadual de Campinas. Faculdade de Engenharia de Alimentos. III. Título.

Informações para Biblioteca Digital

Título em outro idioma: Self-assembly structures formed by MCT, ethanol, and food-grade surfactants: effect of temperature, surfactant, co-surfactant and water concentration

Palavras-chave em inglês:

Microemulsion

Liquid crystal

Structure

Rheology

Área de concentração: Engenharia de Alimentos

Titulação: Doutora em Engenharia de Alimentos

Banca examinadora:

Rosiane Lopes da Cunha [Orientador]

Antônio Augusto Vicente

Carolina Siqueira Franco Picone

Jane Selia dos Reis Coimbra

Lucimara Gaziola de la Torre

Data de defesa: 01-07-2014

Programa de Pós-Graduação: Engenharia de Alimentos

COMISSÃO EXAMINADORA

Profa. Dra. Rosiane Lopes da Cunha – Orientadora (FEA / UNICAMP)
Titular

Prof. Dr. António Augusto Vicente (Universidade do Minho)
Titular

Dra. Carolina Siqueira Franco Picone (FEA / UNICAMP)
Titular

Profa. Dra. Jane Sélia dos Reis Coimbra (DTA / UFV)
Titular

Profa. Dra. Lucimara Gaziola de La Torre (FEQ / UNICAMP)
Titular

Fabiana de Assis Perrechil (UNIFESP – Campus Diadema)
Suplente

Antonio José de Almeida Meirelles (FEA / UNICAMP)
Suplente

Roberta Ceriani (FEQ / UNICAMP)
Suplente

RESUMO

Microemulsões (ME) e cristais líquidos (CL) são sistemas auto-organizáveis com potencial capacidade de solubilização de compostos lipofílicos e hidrofílicos. Microemulsões são formadas por gotas de tamanho reduzido e apresentam aspecto translúcido, enquanto os cristais líquidos apresentam estrutura mais complexa, com fases lamelares, hexagonais ou cúbicas. Entretanto, o estudo de ME e CL compostos por ingredientes biocompatíveis ainda é restrito, assim como a avaliação dos efeitos de cada componente e da temperatura na estrutura e reologia dos sistemas. Desta maneira, o objetivo deste trabalho foi avaliar a estrutura e reologia de ME e CL compostos por água, misturas de surfactantes (Tween 80, Tween 20, Span 80, Span 20 e lecitina), triacilglicerol de cadeia média (TCM) e etanol, em diferentes proporções de TCM:etanol (1:0, 2:1 e 1:2). Diferentes estruturas e comportamentos reológicos foram obtidos dependendo da concentração de água, etanol, tipo de surfactante e temperatura. Inicialmente, o estudo de sistemas contendo somente Tween 80 como surfactante mostrou que o incremento de etanol diminuiu a região de cristal líquido e aumentou a área de microemulsão no diagrama de fases, expandindo a região de micelas reversas para maiores concentrações de água. Além disso, maiores concentrações de etanol produziram sistemas com menor tamanho de partícula (DLS), menor distância (d) entre os planos das estruturas (SAXS) e baixa pseudoplasticidade. Já a avaliação de sistemas contendo inicialmente 70 % (m/m) de Tween 80 como surfactante único e diluídos em água (linha de diluição 7) mostrou que a baixas concentrações de água formaram-se microemulsões A/O com comportamento Newtoniano e tamanho de gota nanométrico. Em concentrações intermediárias de água, cristais líquidos com elevada distância (d) entre os planos das estruturas e de reologia complexa foram produzidos, incluindo fluidos viscoelásticos e com comportamento dependente do tempo de cisalhamento (tixotrópico e anti-tixotrópico). Sistemas com concentração intermediária de água com ausência ou baixa concentração de etanol apresentaram temperatura de transição próximo a 50 °C. Estruturas cúbicas e hexagonais com comportamento do tipo gel foram

produzidas a 25 °C, enquanto sistemas desordenados com menor distância (d) entre os planos da estrutura e comportamento do tipo solução diluída foram observados a altas temperaturas. Na última etapa, sistemas compostos por diferentes misturas de surfactantes foram avaliados. Estruturas do tipo micelar e hexagonal prevaleceram em sistemas compostos por Tween, enquanto estruturas lamelares foram também observadas em sistemas de Tween/Span e Tween/Lecitina. Estruturas cúbicas foram observadas somente nos sistemas Tween 80/Lecitina. Uma relação entre os parâmetros estruturais, comportamento reológico e propriedades das misturas de surfactantes (parâmetro crítico de empacotamento - P, e balanço hidrofílico-lipofílico - BHL) foi observada. Misturas de surfactantes com menor BHL produziram cristais líquidos pseudoplásticos e viscoelásticos em elevadas concentrações de surfactante. A maior pseudoplasticidade foi associada à estrutura cristalina ordenada susceptível à quebra ou reorientação sob cisalhamento. Além disso, as propriedades das misturas de surfactantes influenciaram no fenômeno de partição do etanol, levando a maiores parâmetros de cela (a) em sistemas de menor BHL. Conhecendo os efeitos da temperatura, composição, concentração e interação entre componentes, as propriedades dos sistemas, como estrutura e reologia, podem ser preditas ou moduladas de acordo com o interesse tecnológico.

Palavras-chave: microemulsão, cristal líquido, estrutura, reologia.

ABSTRACT

Microemulsions (ME) and liquid-crystals (LC) are self-assembly structures with potential ability to solubilise both lipophilic and hydrophilic components. Microemulsions are translucent systems formed by small swollen micelles, while liquid crystalline phases exhibit a more complex structure, as lamellar, hexagonal and cubic phases. However, the use of biocompatible ingredients in these systems was scarcely explored, as well as the effect of each component and temperature on the system structure and rheology. Thus, the aim of this work was to evaluate the structure and rheology of ME and LC systems formed by water, surfactant mixtures (Tween 80, Tween 20, Span 80, Span 20 and lecithin), medium-chain triacylglycerol (MCT) and ethanol, at different MCT:ethanol ratios (1:0, 2:1 and 1:2). Systems with different structures and rheology were produced according to water and ethanol concentration, surfactant type and temperature. In the first part of this work systems composed by Tween 80 as surfactant showed that the ethanol increment decreased the liquid crystalline area and increased microemulsion area in the pseudo-ternary diagram, expanding micelles production up to higher water content. Moreover, higher ethanol content produced systems with smaller particle size (DLS), smaller correlation distance (d) (SAXS) and lower pseudoplasticity. The evaluation of dilution line 7 of systems with only Tween 80 as surfactant showed that at W/O microemulsions with Newtonian behavior were produced at low water content. At intermediary water contents, liquid crystalline phases with larger correlation distance (d) and complex rheology were produced, including viscoelastic, thixotropic and anti-thixotropic behavior. Systems with intermediary water content and low water content (or absence) of ethanol showed temperature transition around 50 °C. Cubic and hexagonal structures with gel behavior were produced at 25°C, while disordered systems with smaller correlation distance and dilution solution behavior were produced at high temperatures. In the last part of this study, systems composed of different surfactant mixtures were evaluated. Micelle and hexagonal were the main phases observed on systems composed of Tween, while lamellar structures were also observed in Tween/Span and

Tween/lecithin systems. Cubic structures were observed only in Tween 80/lecithin systems. A relationship between structural parameters, rheological behavior and surfactant mixture properties (critical packing parameter - CPP, and hydrophilic-lipophilic balance – HLB) was observed. Surfactant mixtures with lower HLB produced pseudoplastic and viscoelastic liquid crystalline phases at high surfactant concentrations. The higher pseudoplasticity was associated with a structure susceptible to reorientation or to the structure broken under shear. In addition, characteristics of surfactant mixture affected the ethanol partition phenomenon, leading to higher lattice parameters (a) in systems with lower HLB. This discussion concerning the effects of temperature, composition, concentration and components interactions could be used to predict and design system properties, as structure and rheology, according to a variety of technological interest.

Keywords: microemulsion, liquid crystal, structure, rheology.

SUMÁRIO

- CAPÍTULO 1 -	1
INTRODUÇÃO E OBJETIVO	1
1.1. INTRODUÇÃO	3
1.2. OBJETIVOS	5
1.3. ORGANIZAÇÃO DA TESE EM CAPÍTULOS	5
1.4. REFERÊNCIAS BIBLIOGRÁFICAS	7
- CAPÍTULO 2 -	9
REVISÃO BIBLIOGRÁFICA	9
2.1 CRISTAL LÍQUIDO E MICROEMULSÃO	11
2.1.1 Cristal líquido	11
2.1.2 Microemulsão	13
2.1.2.1. Comportamento das fases	14
2.1.2.2. Teoria termodinâmica de formação das microemulsões	15
2.1.2.3. Diagrama de fase	15
2.1.2.4. Método de emulsificação espontânea	16
2.2 INGREDIENTES BIOCAMPATÍVEIS	17
2.2.1. Fase polar	21
2.2.2. Fase apolar	21
2.2.3. Surfactantes	21
2.2.4. Misturas de surfactantes	24
2.2.5. Co-surfactantes	24
2.3 EFEITO DA TEMPERATURA NA PRODUÇÃO DE MICROEMULSÃO E CRISTAL LÍQUIDO	25
2.4 REFERÊNCIAS BIBLIOGRÁFICAS	27
- CAPÍTULO 3 -	33
EFEITO DA CONCENTRAÇÃO DE ETANOL E DO CISALHAMENTO EM SISTEMAS COMPOSTOS POR TWEEN 80, ÁGUA E TRIACILGLICEROL DE CADEIA MÉDIA	33
3.1. INTRODUCTION	36
3.2. MATERIALS AND METHODS	38
3.2.1. MATERIALS	38

3.2.2.	METHODS	38
3.2.2.1.	Phase-diagram construction and characterisation.....	38
3.2.2.2.	Characterisation of ME, LC and EM phases.....	39
3.2.2.3.	Particle-size measurements	40
3.2.2.4.	Rheological measurements.....	40
3.3.	RESULTS AND DISCUSSION	41
3.3.1.	ELECTRICAL CONDUCTIVITY	41
3.3.2.	PHASE DIAGRAMS	43
3.3.3.	MICROSTRUCTURE AND PARTICLE SIZE	46
3.3.4.	RHEOLOGY.....	48
3.3.4.1.	Steady-state measurements.....	48
3.3.4.2.	Transient-state measurements.....	51
3.3.4.3.	Oscillatory measurements	53
3.4.	CONCLUSIONS	56
3.5.	ACKNOWLEDGEMENTS	57
3.6.	REFERENCES.....	57
	- CAPÍTULO 4 -	63
	EFEITO DA CONCENTRAÇÃO DE ETANOL E DA TEMPERATURA EM SISTEMAS COMPOSTOS POR TWEEN 80, ÁGUA E TRIACILGLICEROL DE CADEIA MÉDIA.....	63
	ABSTRACT.....	65
4.1.	INTRODUCTION.....	66
4.2.	MATERIAL AND METHODS.....	67
4.2.1.	MATERIAL	67
4.2.2.	METHODS	68
4.2.2.1.	Spontaneous emulsification method.....	68
4.2.2.2.	Small-angle scattering (SAXS)	68
4.2.2.3.	Differential scanning calorimeter (DSC)	69
4.2.2.4.	Rheological measurements	70
4.3.	RESULTS AND DISCUSSION.....	70
4.3.1.	SAXS.....	70
4.3.2.	DIFFERENTIAL SCANNING CALORIMETRY (DSC)	75
4.3.3.	RHEOLOGY.....	80
4.4.	CONCLUSION	84

4.5.	ACKNOWLEDGEMENTS	85
4.6.	REFERENCES.....	85
- CAPÍTULO 5 -.....		89
EFEITO DO TIPO DE SURFACTANTE NA ESTRUTURA E REOLOGIA DE SISTEMAS COMPOSTOS POR ÁGUA, TRIACILGLICEROL DE CADEIA MÉDIA E ETANOL.....		89
ABSTRACT.....		91
5.1.	INTRODUCTION.....	92
5.2.	MATERIAL AND METHODS.....	94
5.2.1.	MATERIAL	94
5.2.2.	METHODS	94
5.2.2.1.	Surfactants mixture properties.....	94
5.2.2.2.	Phase-diagrams construction and characterisation.....	96
5.2.2.3.	Characterisation of ME and LC phases.....	96
5.2.2.4.	Small angle X-ray scattering (SAXS).....	97
5.2.2.5.	Rheology	98
5.3.	RESULTS.....	99
5.3.1.	PHASE DIAGRAM AND VISUAL APPEARANCE.....	99
5.3.2.	SAXS.....	101
5.3.3.	FLOW CURVES.....	105
5.3.4.	OSCILLATORY RHEOLOGY.....	108
5.4.	DISCUSSION.....	110
5.4.1.	EFFECT OF WATER AND SURFACTANT CONCENTRATION ON SYSTEM STRUCTURE AND RHEOLOGY.....	110
5.4.2.	EFFECT OF SURFACTANT TYPE ON SYSTEMS STRUCTURE AND RHEOLOGY.....	111
5.5.	CONCLUSIONS.....	113
5.6.	ACKNOWLEDGEMENTS	114
5.7.	REFERENCES.....	114
CAPÍTULO 6 -.....		119
CONCLUSÕES GERAIS		119

AGRADECIMENTOS

A Deus, pela vida e por todas minhas realizações.

Aos meus pais, Romeu e Elisa, irmãos Cristiane e Romeu Vinícius, e sobrinhas Aline e Júlia. Obrigada pelo amor, apoio e carinho de sempre.

Ao meu marido César, pelo amor, paciência, companheirismo e, principalmente pela nossa nova família.

À Profa Dra Rosiane Lopes da Cunha, pela orientação, compreensão e incentivo.

À UNICAMP, funcionários e professores, que viabilizaram a realização deste trabalho.

Ao CNPq, pelo apoio financeiro.

À banca examinadora, pelas valiosas correções e sugestões que contribuíram para a melhoria deste trabalho.

Aos colegas do Laboratório de Engenharia de Processos, e demais amigos de pós do Dea pelo agradável ambiente de trabalho e pelos bons momentos em Campinas.

E a todos os amigos especiais que acompanharam este trabalho e continuam hoje participando da minha vida.

ÍNDICE DE FIGURAS

Capítulo 2

- Figura 1. Auto-associações dos surfactantes de acordo com o parâmetro crítico de empacotamento (P). Adaptado de Holmberg et al. (2003), Lawrence e Rees (2000) e Formariz et al. (2005). 12
- Figura 2. Esquema representativo da microestrutura das microemulsões. 14
- Figura 3. Sistema de classificação de Winsor. Fonte: Flanagan e Singh (2006)... 15
- Figura 4. Diagrama de fases esquemático de um sistema pseudo-ternário composto por água, surfactante, óleo e co-surfactante, identificando as regiões de estruturas do tipo A/O, bicontínuas (BC) e O/A, e 2 fases. 16
- Figura 5. Exemplo de fosfatidilcolina, um fosfolipídio presente na lecitina de soja. 23
- Figura 6. Estrutura química de um estearato de sorbitana (Span) (a) e estearato de sorbitana polietoxilado (Tween) (b). 24

Capítulo 3

- Fig. 1 Systems produced to phase diagram construction. Filled symbols (\bullet) are initial mixtures of Tween 80, MCT and ethanol and open symbols (\circ) are samples obtained over dilution lines. 38
- Fig. 2. Electrical conductivity along the dilution lines of the systems A, B and C. Initial surfactant content (% w/w): 10 (\blacksquare), 20 (Δ), 30 (\blacktriangle), 40 (\diamond), 50 (\blacklozenge), 60 (+), 70 (x), 80 (\circ), 90 (\bullet). Limits of structural transition: Φ_c (maximum water content in a W/O ME), Φ_b (initial water content of bicontinuous ME region) and Φ_m (final water content of bicontinuous ME region). 42

Fig. 3. Phase diagram of systems A, B and C. Phases: LC is liquid crystal, O/W ME is O/W microemulsion, W/O ME is W/O microemulsion, EM is milked-like emulsion and multiphase represents Winsor I, II or III systems.	44
Fig. 4. Visual appearance and microstructure of the systems A, B and C. ME: microemulsion, EM: emulsion, LC: liquid crystalline, and GEL: liquid crystalline with gel-like structure.	46
Fig. 5. Particle size distribution of systems A, B and C over dilution line 7. Water content (% w/w): 0 (—), 10 (—), 20 (—), 30 (—), 40 (—), 50 (—), 70 (••••), 80 (—), 90 (—).	48
Fig. 6. Flow curves of systems A, B and C over dilution line 7. Water content (% w/w): 0 (□), 10 (■), 20 (Δ), 30 (▲), 40 (◇), 50 (◆), 60 (+), 70 (x), 80 (○), 90 (●).	49
Fig. 7. Complex modulus (G^*) of the systems A, B and C. Water content (% w/w): 0 (□), 10 (■), 20 (Δ), 30 (▲), 40 (◇), 50 (◆), 60 (+), 70 (x), 80 (○), 90 (●).	53
Fig. 8. Representative mechanical spectrum of systems A, B, and C. Viscoelastic moduli: loss modulus G'' (□) and storage modulus G' (○).	55
Fig. 9. Elastic modulus (G') (filled symbols) and main peak mean from intensity particle size distribution (open symbols) over the dilution line 7 of systems A (■, □), B (●, ○) and C (▲, Δ).	56

Capítulo 4

Figure 1. SAXS patterns of systems with different MCT:ethanol ratios, A (1:0), B (2:1), and C (1:2), at 25 °C.	71
Figure 2. SAXS patterns of systems composed by different MCT:ethanol ratios, A (1:0), B (2:1), and C (1:2), with (30, 40, 50 and 60) % (w/w) of water at 50 °C and 70 °C.	74
Figure 3. Characteristic length of structure ($d / \text{Å}$) obtained from SAXS of systems with different MCT:ethanol ratio A (1:0) (●), B (2:1) (◆), and C (1:2) (▲) at 25, 50, and 70 °C.	74

Figure 4. Thermal behavior of pure components (water, MCT and Tween 80).	75
Figure 5. Thermal behavior of systems A, B, and C with low (0 to 30 % w/w), and intermediary to high (40 to 90 % w/w) water concentration.....	79
Figure 6. Effect of temperature on complex viscosity (η^*) of systems A, B and C. Process: first heating H1 (•••••), first cooling C1 (— —), second heating H2 (—). Water concentration % (w/w): 0 (■), 10 (■), 20 (■), 30 (■), 40 (■), 50 (■), 60 (■), 70 (■), 80 (■) and 90 (■).....	81

Capítulo 5

Figure. 1. Formula of (a) phosphatidylcholine, (b) Span 20 and Span 80 monosorbates and (c) Tween 20 and Tween 80 polysorbates. R is C_nH_{2n+1} with $n=11$ for Span 20 and Tween 20 and $n=17$ for Span 80 and Tween 80.....	93
Figure. 2. Pseudo-ternary diagrams of systems composed by water, MCT, ethanol, and surfactant mixtures. 1-P: one phase; 2-TP: two transparent phases, WP: white phase. A_{1-P} : area of one-phase region obtained from pseudo-ternary diagrams.	100
Figure. 3. Visual appearance of the different systems formed by surfactants mixtures, MCT, ethanol and water. Final water concentration from 30 to 60 (% w/w) and initial surfactant mixture concentration (% S) varied from 60 to 80 % (w/w).	101
Figure. 4. SAXS patterns of T8, T8T2, T8Lec, T8S2 and T8S8 systems at different water concentrations	103
Figure. 5. Flow curves of systems composed by different surfactants mixtures (T8, T8T2, T8S2, T8S8 and T8Lec), with 60, 70 and 80 % (w/w) of initial surfactant concentration and 30 (—), 40 (●), 50 (▲) and 60 (×) % (w/w) of water. S: initial surfactant concentration.....	107

Figure. 6. Complex viscosity of systems T8, T8T2, T8S2, T8S8 and T8Lec with 60, 70 and 80 % (w/w) of initial surfactant concentration and 30 (—), 40 (●), 50 (▲) and 60 (×) % (w/w) of water. S: initial surfactant concentration..... 110

ÍNDICE DE TABELAS

Capítulo 2

Tabela 1. Estudos recentes de microemulsões compostas por ingredientes de grau alimentício.....	19
Tabela 2. Alguns surfactantes de grau alimentício e seus valores de BHL (Fonte: WALSTRA, 2003; ARAÚJO, 2001).....	22

Capítulo 3

Table 1. Composition of systems A, B and C evaluated by particle size distribution and rheological measurements.....	40
Table 2. Parameters calculated from phase diagrams of systems A, B and C. $A_{O/W ME}$ is the area of the region of O/W microemulsion, $A_{W/O ME}$ is the area of W/O microemulsion, A_{LC} is the liquid crystal area and W_m is maximal amount of water dispersed in an W/O microemulsion.....	45
Table 3. Rheological parameters of systems over dilution line 7 with a non-Newtonian behavior. σ_0 is the yield stress, k is the consistency index and n is the flow index.....	49
Table 4. Viscosity at 3 s^{-1} (η_3) of the systems A, B and C over the dilution line 7.	50
Table 5. Hysteresis between the curves without prior shearing and at steady state (thixotropy) and ratio of the concentration of more non-polar (surfactant + oil) and polar (water + ethanol) components.....	52

Capítulo 4

Table. 1. Structural parameters obtained from SAXS measurements. d : structure repetition distance, a : lattice parameter of H_1 , H_2 , $Ia3d$, $Pn3m$ and, $Im3m$, and r_{hc} : radius of cylindrical micelle of H_1 or H_2	72
---	----

Table. 2. Freezing and melting temperatures and enthalpy of pure components and systems (A, B, and C) with different MCT:ethanol ratios and water content. ... 76

Table. 3. Viscoelastic properties (η^*) and transition temperatures of the first heating (H1), first cooling (C1), and second heating (H2) cycles. 83

Capítulo 5

Tab. 1. Critical packing parameter (CPP) of surfactants. 95

Tab. 2. Surfactant mixtures properties (*HLB* and *CPP*)..... 96

Tab. 3. Composition (% w/w) of the systems evaluated by rheological and SAXS measurements. 97

Tab. 4. Structural parameters obtained by SAXS measurements. *d*: structure repetition distance, *a*: lattice parameter of H_1 , H_2 , L_α or $Pn3m$, d_{hc} : hydrophobic thickness of L_α , d_w : hydrophilic thickness of L_α and r_{hc} : radius of cylindrical micelle of H_1 or H_2 104

Tab. 5. Rheological properties of systems. *n*: behavior index, *k*: consistency index, η_3 : apparent viscosity at 3 s^{-1} , μ : Newtonian viscosity. 106

**- CAPÍTULO 1 -
INTRODUÇÃO E OBJETIVO**

1.1. INTRODUÇÃO

Moléculas de surfactantes se auto-organizam em diferentes tipos de estruturas, incluindo microemulsões e cristais líquido. Microemulsões são sistemas isotrópicos formados por micelas incorporadas de óleo ou água dispersas em um meio contínuo (FLANAGAN; SINGH, 2006). Já os cristais líquidos apresentam estruturas complexas, como lamelar, hexagonal e cúbica. Na fase lamelar as moléculas de surfactante formam bicamadas sobrepostas (BINKS; FLETCHER; TIAN, 2010), enquanto a fase hexagonal se organiza em cilindros e a fase cúbica apresenta uma estrutura tridimensional altamente viscosa (ALAM et al., 2010).

Estes sistemas podem ser preparados por processos de baixa energia, apresentando custo reduzido e facilidade de produção (SAGALOWICZ; LESER, 2010; ANTON; VANDAMME, 2009). Além disso, propriedades como elevada área interfacial e regiões hidrofóbicas e hidrofílicas bem definidas têm despertado um grande interesse na aplicação destes sistemas na veiculação (“delivery”) de substâncias nas áreas farmacêutica, cosmética e de alimentos (SAGALOWICZ; LESER, 2010). A principal aplicação das microemulsões em alimentos tem sido a solubilização de substâncias (AMAR; ASERIN; GARTI, 2003; FENG et al., 2009; LEE et al., 2009; FLANAGAN; SINGH, 2006; LIN et al., 2009) com o intuito de aumentar a biodisponibilidade de compostos com propriedades benéficas à saúde.

Apesar das propriedades diferenciadas e potencialidades mencionadas, as microemulsões e os cristais líquidos apresentam restrições quanto aos ingredientes usualmente utilizados na sua produção. Estes sistemas são compostos por uma fase apolar e uma polar (como óleo e água, respectivamente), além de surfactantes (como lecitina, ésteres de açúcar e éter de polioxietileno) e co-surfactantes (alcoóis de cadeia curta ou média, como etanol, butanol e pentanol), componentes essenciais para o ajuste da flexibilidade do filme de surfactante (FENG et al., 2009). Os óleos mais utilizados em alimentos contém triacilgliceróis de cadeia longa (como o óleo de soja, girassol, canola, etc), pois eles apresentam elevada disponibilidade e compatibilidade com a matriz alimentar. Porém, estes óleos são mais difíceis de solubilizar do que os triacilgliceróis de cadeia média e curta, apresentando

dificuldades tecnológicas na produção de microemulsões (FLANAGAN; SINGH, 2006). Além disso, alguns surfactantes e co-surfactantes são parcialmente tóxicos, tornando a produção de microemulsões com ingredientes biocompatíveis um grande desafio para pesquisadores das áreas farmacêutica, cosmética e alimentícia. Apesar das exigências serem ainda maiores para alimentos, pois existe a obrigatoriedade de se trabalhar com componentes de grau alimentício, preferencialmente GRAS (generally recognized as safe) (CHEN et al., 2006), poucos estudos têm sido realizados neste sentido (FLANAGAN; SINGH, 2006; FLANAGAN et al., 2006; LEE et al., 2009; FENG et al., 2009; FASOLIN; SANTANA; CUNHA, 2012).

Dentre os surfactantes biocompatíveis, a lecitina comercial é composta por uma mistura de fosfolipídios de caráter anfótero e considerados GRAS. Surfactantes não-iônicos, como polissorbatos (Tweens) e monossorbatos (Spans), são menos tóxicos que surfactantes iônicos e sofrem menor influência do pH e força iônica (MATSARIDOU et al., 2012). Polissorbatos e monossorbatos se diferenciam quanto ao tipo de ácido graxo, grau de esterificação e comprimento da cadeia de polietoxietileno (ZHANG et al., 2010). Tais variações estruturais resultam em microemulsões e cristais líquidos com diferentes microestruturas e propriedades reológicas.

A combinação de surfactantes lipofílicos e hidrofílicos modifica a curvatura espontânea e elasticidade ou rigidez do filme de surfactante, resultando em sistemas diferenciados (PAUL; MITRA, 2005). O uso de misturas de surfactantes pode também aumentar a capacidade de solubilização de bioativos (MOHAMMADY; POUZOT; MEZZENGA, 2009) e reduzir a concentração de surfactante e co-surfactante necessária para a formação de microemulsões, aumentando a co-solubilização da água e do óleo através de um efeito sinérgico (PAUL; MITRA, 2005).

Além da composição, a estrutura das microemulsões e cristais líquidos é fortemente influenciada pelas condições do meio, como pH, força iônica e temperatura (LIU; HAO, 2011; BERNI; LAWRENCE; MACHIN, 2002; LAWRENCE, 1994). A temperatura aumenta a flexibilidade do filme de surfactante e provoca a desidratação de grupos da cabeça polar dos surfactantes não-iônicos (MOHAMMADY; MATTHIEU; MEZZENGA, 2009). Desta forma, o estudo da transição de fases com a variação da temperatura

pode ser usada para simular processos industriais e biológicos em condições de temperaturas específicas (KULKARNI, 2011).

1.2. OBJETIVOS

1.2.1. Objetivos específicos

Produzir microemulsões e cristais líquidos compostos por ingredientes biocompatíveis e avaliar os efeitos da composição e temperatura na estrutura e reologia dos sistemas formados.

1.2.2. Objetivos específicos

Os objetivos específicos deste trabalho foram:

- Avaliar o efeito da adição de etanol, da taxa e tempo de cisalhamento na microestrutura e reologia de sistemas compostos de água, triacilglicerol de cadeia média (TCM) e Tween 80;
- Entender o efeito da temperatura na microestrutura e reologia de sistemas compostos de água, TCM e Tween 80;
- Avaliar a influência da substituição parcial do Tween 80 por outro surfactante (Tween 20, Span 20, Span 80 e lecitina) na microestrutura e reologia de sistemas compostos de água, TCM, Tween 80 e etanol.

1.3. ORGANIZAÇÃO DA TESE EM CAPÍTULOS

A apresentação deste trabalho foi organizada em seis capítulos, como descrito a seguir:

Capítulo 1: Introdução e objetivos

Capítulo 2: Revisão bibliográfica

Neste capítulo foram abordados aspectos teóricos da estrutura e formação das microemulsões e cristais líquidos, apresentando alguns trabalhos recentes e relevantes sobre o tema.

Capítulo 3: Efeito da concentração de etanol e do cisalhamento em sistemas compostos por Tween 80, água e triacilglicerol de cadeia média

Este capítulo avaliou sistemas compostos por Tween 80, água, TCM e etanol em diferentes proporções de TCM:etanol (1:0, 2:1 e 1:2). Diagramas de fases foram construídos a partir da análise visual, microscopia de luz polarizada e condutividade elétrica. A transição estrutural em uma linha de diluição foi avaliada a partir de análises de condutividade elétrica, tamanho de partícula e reologia em estado estacionário e oscilatório. Os resultados foram publicados na *Colloids and Surfaces A: Physicochemical and Engineering Aspects* (2012), v. 398, p. 54-63.

Capítulo 4: Efeito da concentração de etanol e da temperatura em sistemas compostos por Tween 80, água e triacilglicerol de cadeia média

Este capítulo deu continuidade ao estudo dos sistemas compostos por Tween 80, água, TCM e etanol em diferentes proporções de TCM:etanol (1:0, 2:1 e 1:2). A estrutura destes sistemas foi avaliada por meio de espalhamento de raios X a baixos ângulos (SAXS) e calorimetria. Além disso, o efeito da temperatura (25-70°C) na transição de fases foi avaliado a partir de análises de reologia oscilatória e SAXS.

Capítulo 5: Efeito do tipo de surfactante na estrutura e reologia de sistemas compostos por água, triacilglicerol de cadeia média e etanol

Os sistemas avaliados anteriormente foram parcialmente modificados a partir da substituição do Tween 80 por uma mistura de surfactantes contendo Tween 80 e Tween 20, Span 80, Span 20 ou lecitina. Estes sistemas foram avaliados em medidas reológicas e SAXS com o intuito identificar a relação entre as propriedades das misturas de surfactantes e o comportamento reológico e estrutural do sistema.

Capítulo 6: Conclusões gerais

1.4. REFERÊNCIAS BIBLIOGRÁFICAS

- ALAM et al. (2010). Phase behavior and rheology of oil swollen micellar cubic phase and gel emulsions in nonionic surfactant systems. **Journal of Colloid and Interface Science**, 341, 267–272.
- AMAR, A.; ASERIN, A.; GARTI, N. (2003). Solubilization pattern of lutein and lutein esters in food grade nonionic microemulsion. **Journal of Agricultural and Food Chemistry**, 51, 4775–4781.
- ANTON, N.; VANDAMME, T. F. (2009). The universality of low-energy nano-emulsification. **International Journal of Pharmaceutics**, 377, 142–147.
- BERNI, M.G.; LAWRENCE, C.J.; MACHIN, D. (2002). A review of the rheology of the lamellar phase in surfactant systems. **Advances in Colloid and Interface Science**, 98, 217–243.
- BINKS, B. P.; FLETCHER, P. D. I.; TIAN, L. (2010). Influence of nanoparticle addition to Winsor surfactant microemulsion systems. **Colloids and Surfaces A: Physicochemical and Engineering Aspects**, 363, 8-15.
- CHEN, et al. (2006). Microemulsion-based hydrogel formulation of ibuprofen for topical delivery. **International Journal of Pharmaceutics**, 315, 52–58.
- FASOLIN, L.H.; SANTANA, R.C.; CUNHA, R.L. (2012). Microemulsion and liquid crystalline formulated with triacylglycerols: Effect of ethanol and oil unsaturation. **Colloids and Surfaces A: Physicochemical and Engineering Aspects**, 415, 31–40.
- FENG, et al. (2009). Study on food-grade vitamin E microemulsions based on non-ionic emulsifier. **Colloids and Surfaces A: Physicochemical and Engineering Aspects**, 339, 1–6.
- FLANAGAN, J.; SINGH, H. (2006). Microemulsions: A Potential Delivery System for Bioactives. **Critical Reviews in Food Science and Nutrition**, 46, 221–237.
- FLANAGAN, et al. (2006). Solubilisation of soybean oil in microemulsions using various surfactants. **Food Hydrocolloids**, 20, 253–260.
- KULKARNI, C. V. (2011). Nanostructural studies on monoelaidin – water systems at low temperatures. **Langmuir**, 27, 11790-11800.
- LAWRENCE, M. J. (1994). Surfactant systems: their use in drug delivery. **Chemical Society Reviews**, 23, 417-424.

- LEE, et al. (2009). Enhancement of the encapsulation and transmembrane permeation of isoflavone-containing red clover extracts in phospholipid-based microemulsion using different extraction processes. **Journal of Agricultural and Food Chemistry**, 57, 9489–9495.
- LIN, et al. (2009). Stability and characterisation of phospholipid-based curcumin-encapsulated microemulsion. **Food Chemistry**, 116, 923–928.
- LIU, C.; HAO, J. (2011). Shear-induced structural transition and recovery in the salt-free cationic surfactant systems containing deoxycholic acid. **Journal of Physical Chemistry B**, 115, 980–989.
- MATSARIDOU et al. (2012). The influence of surfactant HLB and oil/surfactant ratio on the formation and properties of self-emulsifying pellets and microemulsion reconstitution. **AAPS PharmSciTec**, 13:1319-1330.
- MOHAMMADY, S. Z.; POUZOT, M.; MEZZENGA, R. (2009). Oleoylethanolamide-based lyotropic liquid crystals as vehicles for delivery of amino acids in aqueous environment. **Biophysical Journal**, 96, 1537-1546.
- PAUL, B. K.; MITRA, R. K. (2005). Water solubilization capacity of mixed reverse micelles: Effect of surfactant component, the nature of the oil, and electrolyte concentration. **Journal of Colloid and Interface Science**, 288, 261-279
- SAGALOWICZ L.; LESER M.E. (2010) Delivery systems for liquid food products. **Current Opinion in Colloid & Interface Science**, 15:61–72.
- ZHANG et al. (2010). Characterization and antimicrobial activity of pharmaceutical microemulsions. **International Journal of Pharmaceutics**, 395, 154-160.

**- CAPÍTULO 2 -
REVISÃO BIBLIOGRÁFICA**

2.1 CRISTAL LÍQUIDO E MICROEMULSÃO

Cristais líquidos e microemulsões são sistemas produzidos a partir da auto-organização de moléculas de surfactante dispersas em um meio contínuo de óleo ou água. Em baixas concentrações, os surfactantes se localizam na interface entre o domínio dos dois líquidos. Acima de uma concentração específica, conhecida como concentração micelar crítica (CMC), os surfactantes se auto-organizam, formando estruturas ordenadas caracterizadas por regiões hidrofóbicas e hidrofílicas alternadas. A associação das moléculas anfifílicas é um fenômeno termodinamicamente favorável que busca a otimização da solvatação da molécula e a redução da energia de Gibbs do sistema (LAWRENCE; REES, 2000).

2.1.1 CRISTAL LÍQUIDO

Os cristais líquidos (fases lamelar, hexagonal e cúbica) são estruturas altamente organizadas formadas em sistemas com quantidades relevantes de surfactantes (FORMARIZ et al., 2005; LAWRENCE; REES, 2000), apresentando viscosidade elevada e características elásticas de sólidos (HYDE, 2001). Além da concentração de surfactante, o tipo de cristal líquido formado depende das características da molécula de surfactante, temperatura e composição das fases polares e apolares (MCCLEMENTS et al., 2009). O tipo de estrutura pode ser estimado a partir do parâmetro crítico de empacotamento (P) do surfactante (Equação 1 e Figura 1) (MYERS, 2006).

$$P = \frac{v}{a_0 l} \quad (1)$$

sendo v e l o volume e o comprimento da parte hidrofóbica, respectivamente, e a_0 a área seccional ocupada pelo grupo polar.


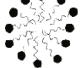

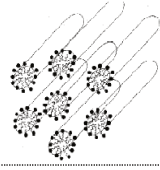

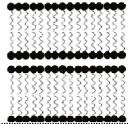


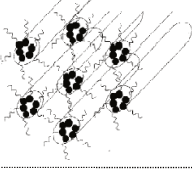

Parâmetro crítico de empacotamento (P)		Estrutura do agregado	Denominação da fase
$P < 1/3$			Micela normal
$P < 1$	$1/3 < P < 1/2$		Hexagonal normal
			Cúbica Normal
$P \sim 1$			Lamelar
			Cúbica Reversa
$P > 1$			Hexagonal reversa
			Micela reversa

Figura 1. Auto-associações dos surfactantes de acordo com o parâmetro crítico de empacotamento (P). Adaptado de Holmberg et al. (2003), Lawrence e Rees (2000) e Formariz et al. (2005).

A estrutura esférica micelar típica é transformada em uma estrutura micelar mais alongada ou do tipo bastão com o aumento da concentração inicial de surfactante. Um aumento ainda maior na concentração pode causar a orientação e o empacotamento rígido da micela alongada em formações hexagonais infinitas, nas quais compartimentos aquosos podem ser separados por camadas lipídicas (fase hexagonal reversa, H_1) ou vice-versa (normal, H_2). Dependendo do surfactante utilizado, um aumento adicional da concentração resulta em uma estrutura lamelar (L_α), constituída por bicamadas lipídicas intercaladas por fases aquosas. Já a fase cúbica, que ocorre entre as condições de estrutura hexagonal e lamelar, é uma estrutura contínua complexa com curvaturas positivas e negativas na interface, tridimensional, transparente, viscosa (do tipo gel) e isotrópica (ATTWOOD, FLORENCE, 2003). De acordo com a repetição das unidades formadoras dos cristais, as

estruturas cúbicas contínuas são denominadas do tipo diamante ($Pn3m$), primitiva ($Im3m$) ou tipo giróide ($Ia3d$) (KULKARNI, 2011).

2.1.2 MICROEMULSÃO

As emulsões são constituídas por dois líquidos imiscíveis, como óleo e água, sendo que um dos líquidos encontra-se disperso no outro na forma de pequenas gotas esféricas. As emulsões são classificadas como micro (10-100 nm), mini/nano (100-1000 nm) e macroemulsões (0,5-100 μm) (WINDHAB et al., 2005), de acordo com o tamanho de suas gotas. As microemulsões são caracterizadas como sistemas opticamente isotrópicos (translúcidas) e termodinamicamente estáveis. Já as nanoemulsões possuem aparência transparente a leitosa e são termodinamicamente instáveis assim como as mini e macroemulsões, podendo eventualmente apresentar separação de fases ao longo do tempo de estocagem (JAFARI et al., 2008).

As microemulsões são consideradas micelas inchadas (pela incorporação de óleo ou água) formadas por surfactantes organizados em monocamadas com seus grupos polares orientados na direção da água e suas caudas na direção do óleo. Microemulsões A/O são constituídas por micelas contendo água em sua parte central (Figura 2a), sendo produzidas quando pequenas concentrações de fase aquosa estão presentes, formando micelas reversas. A microemulsão bicontínua existe quando quantidades similares das fases aquosa e oleosa estão presentes. O óleo e a água coexistem como uma fase contínua na presença de uma interface estabilizada por um filme de surfactante contínuo e flutuante cuja curvatura é zero (Figura 2b). Já as microemulsões O/A são constituídas por micelas contendo óleo em sua parte central (Figura 2c), sendo formadas principalmente em elevadas concentrações de água e baixas concentrações de fase oleosa (LAWRENCE; REES, 2000).

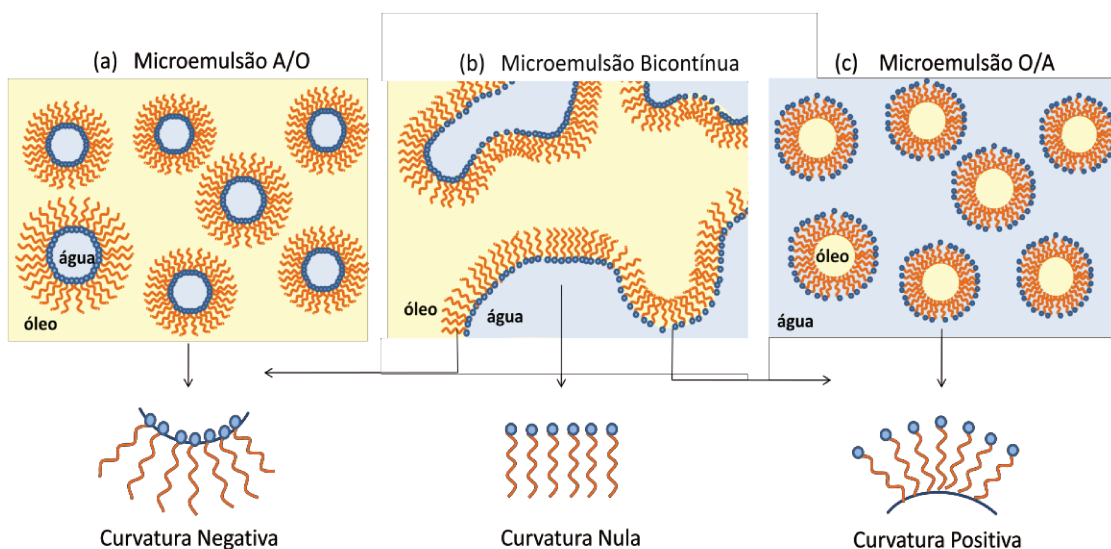


Figura 2. Esquema representativo da microestrutura das microemulsões.

2.1.2.1. Comportamento das fases

As microemulsões podem estar presentes em um sistema multifásico, convenientemente descrito pela classificação de Winsor (Figura 3). O sistema Winsor I consiste em uma microemulsão O/A em equilíbrio com uma fase superior com excesso de óleo. O sistema Winsor II representa uma microemulsão A/O em equilíbrio com uma fase inferior com excesso de água. Quando volumes iguais de óleo e água estão presentes, uma estrutura bicontínua é formada, juntamente com uma fase superior de óleo e uma fase inferior de água pode existir (FLANAGAN; SINGH, 2006), sendo este sistema classificado com Winsor III. Finalmente, o sistema Winsor IV define macroscopicamente o sistema simples de microemulsão O/A ou A/O.

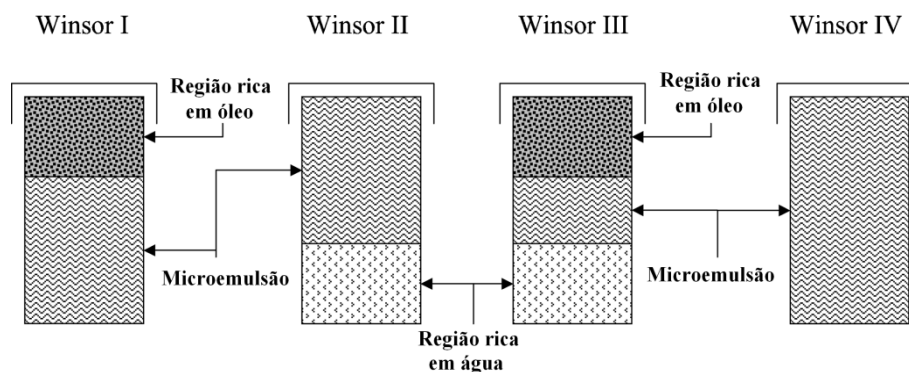


Figura 3. Sistema de classificação de Winsor. Fonte: Flanagan e Singh (2006).

2.1.2.2. Teoria termodinâmica de formação das microemulsões

A energia de Gibbs de formação de emulsões (ΔG_f) pode ser descrita pela equação 2 (MCCLEMENTS, 2005; ANTON, BENOIT, SAULNIER, 2008):

$$\Delta G_f = \gamma \cdot \Delta A - T \cdot \Delta S_f \quad (2)$$

Onde ΔG_f é a energia de Gibbs de formação, γ a tensão interfacial, ΔA a variação na área interfacial, T a temperatura e ΔS_f a variação da entropia de formação.

Durante a formação das microemulsões, a variação da área interfacial ΔA é muito grande, já que ocorre a formação de gotas de tamanho reduzido. Entretanto, a presença de uma mistura adequada de surfactantes e co-surfactantes reduz a tensão interfacial γ a valores extremamente baixos, tornando-se desprezível o primeiro termo da equação ($\gamma \cdot \Delta A$). Quando as fases aquosa e oleosa são misturadas, o surfactante se difunde na interface óleo-água e as gotas se formam, aumentando a entropia do sistema ($T \cdot \Delta S_f \gg 0$). Desta maneira, a energia de Gibbs de formação é negativa ($\Delta G_f < 0$) e o processo de emulsificação torna-se espontâneo, ou seja, o sistema resultante é termodinamicamente favorável (LAWRENCE; REES, 2000).

2.1.2.3. Diagrama de fase

Diagramas de fases permitem definir a extensão e a natureza das regiões de formação de microemulsões e cristal líquido de acordo com a composição dos sistemas (Figura 4). Sistemas simples compostos por água, óleo e surfactante são avaliados em diagramas de fases ternários. Quando os

sistemas são compostos por mais substâncias, como co-surfactante e bioativos dissolvidos, diagramas de fases pseudo-ternários são utilizados, tendo um ou mais vértices do diagrama representado por uma mistura binária, como surfactante/co-surfactante, água/bioativo ou óleo/bioativo (LAWRENCE; REES, 2000).

Em um diagrama de fases, cada um dos vértices do triângulo equilátero representa a proporção de 100 % em massa de um componente. A quantidade de cada componente de uma mistura representada dentro do triângulo é dada pelo comprimento da linha perpendicular que une um ponto ao cateto oposto ao vértice que representa o componente puro.

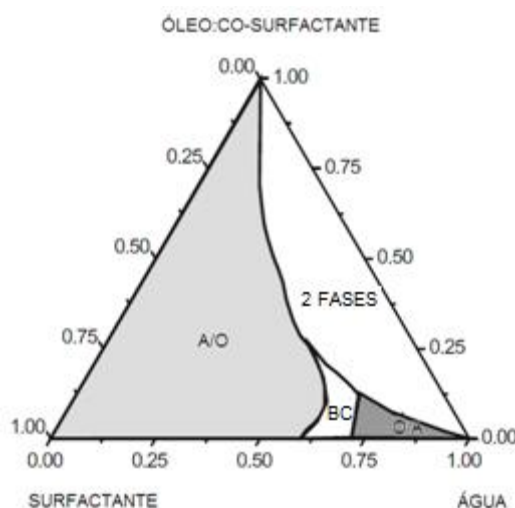


Figura 4. Diagrama de fases esquemático de um sistema pseudo-ternário composto por água, surfactante, óleo e co-surfactante, identificando as regiões de estruturas do tipo A/O, bicontínuas (BC) e O/A, e 2 fases.

2.1.2.4. Método de emulsificação espontânea

Microemulsões e cristais líquidos são produzidos principalmente por processos de baixa energia, em que condições adequadas de processo levam a uma mudança de curvatura na interface óleo-água e à transição de fases, formando gotas dispersas em um meio contínuo.

O método de temperatura de inversão de fases promove o ajuste de curvatura do filme de surfactante a partir da mudança de temperatura, a composição constante (SAGALOWICZ; LESER, 2010). Já o método de

emulsificação espontânea se baseia na mistura de componentes (óleo, água, surfactante e co-surfactante) em concentração específica a determinada temperatura constante (ANTON; VANDAMME, 2009). Estes processos de emulsificação são de simples realização e possuem potencial uso em escala industrial, baixo custo de produção e condições de processamento compatíveis para a veiculação de substâncias sensíveis ao cisalhamento e temperatura (SAGALOWICZ; LESER, 2010; ANTON; VANDAMME, 2009).

Processos de alta energia, ou seja, que utilizam uma elevada quantidade de energia mecânica são tradicionalmente utilizados na indústria para a formação de sistemas estruturados, incluindo macro, mini ou nano-emulsões. A estabilidade cinética destes sistemas pode ser alcançada com a adição de baixas concentrações de surfactantes (até 2 %), enquanto as microemulsões formadas por emulsificação espontânea necessitam de 20% ou mais de surfactante (RAKSHIT; MOULIK, 2008). As interações e as características de cada componente na estrutura de sistemas auto-organizáveis serão apresentadas com o intuito final de otimizar a composição destes sistemas, ou seja, reduzir a concentração de surfactante e co-surfactante necessária à formação de microemulsões para a posterior aplicação em sistemas alimentícios, farmacêuticos e cosméticos.

2.2 INGREDIENTES BIOCAMPATÍVEIS

As propriedades das substâncias que compõem o sistema (água, óleo, surfactante e co-surfactante) influenciam diretamente no comportamento das fases, assim como na sua capacidade de solubilização do bioativo (YAGHMUR; ASERIN; GARTI, 2002). Além disso, os sistemas devem ser compostos por ingredientes biocompatíveis, sendo esta a principal limitação da aplicação das microemulsões em alimentos. Estudos recentes vêm sendo desenvolvidos com o intuito de avaliar o uso de alguns ingredientes de grau alimentício na produção de microemulsões, como apresentado na Tabela 1. A fase polar compatível com uma matriz alimentícia é tradicionalmente constituída de água, enquanto a fase apolar pode ser composta por óleos essenciais, triacilglicerol de cadeia média e longa e monoglicerídeos de glicerol. Os surfactantes biocompatíveis mais avaliados nestes estudos foram

mono e polisorbatos, lecitina, ésteres de açúcar, mono e di-glicerídeos etoxilados. Já os co-surfactantes biocompatíveis são restritos e como exemplo tem-se o etanol e ácidos orgânicos. Alguns dos componentes das microemulsões e cristais líquidos serão discutidos a seguir.

Tabela 1. Estudos recentes de microemulsões compostas por ingredientes de grau alimentício.

Autores	Composição dos sistemas		Surfactante / Co-surfactantes
	Fase polar	Fase apolar	
Fasolin, Santana e Cunha (2012)	água	óleo de girassol	Tween 80 / etanol
Fan et al. (2011)	água, propileno glicol	triacilglicerol de cadeia media (TCM)	Tween 80, Span 80, lecitina de soja
Gurfinkel, Aserin e Garti (2011)	água	monooleato de glicerol	oleyl lactato
Liu, Chang e Hung (2011)	água	terpenos (limoneno, 1,8-cineol, α -terpineol)	Tween 80 / etanol
Tavano et al. (2011)	água	miristato de isopropila (IPM)	Tween 80, Span 80 / etanol
Zheng et al. (2011)	água	óleo de peixe /oleato de etila	Tween 80
Zhang et al. (2011)	água	monolaurato de glicerol	Tween 80 / ácido propiônico
Liu e Wang (2010)	água	ácido linolênico	Span 80, ester de óleo de rícino de polioxietileno (EL 35)
Fanun (2010a, b)	água	óleo de menta	monolaurato de sacarose (L1695), mono-di glicerídeo etoxilado (EMDG) / etanol
Fanun (2010c)	água, propileno glicol	limoneno	monolaurato de sacarose (L1695), mono-di glicerídeo etoxilado (EMDG)
Hickey et al. (2010)	água	oleato de etila	Span 20, Tween 80
Zhang et al. (2010)	água	monolaurato de glicerol	Tween 40/ etanol
Zhang et al. (2009)	água	monolaurato de glicerol	Tween 80 / ácido orgânico
Zhong et al. (2009)	água	óleo de menta	lecitina, Tween 20, Span 20, di-(2-etilhexil) sulfosuccinato de sódio (AOT), polioxil (35), Brij-35 / etanol
Lin et al. (2009)	água	óleo de menta, óleo de soja, oleato de etila, miristato de isopropila (IPM)	lecitina, Tween 80

Tabela 1. Estudos recentes de microemulsões compostas por ingredientes de grau alimentício.

Autores	Composição dos sistemas		
	Fase polar	Fase apolar	Surfactante / Co-surfactantes
Fanun (2009)	água	óleo de menta, miristato de isopropila (IPM)	monolaurato de sacarose (L1695), mono-di glicerídeo etoxilado (EMDG)
Feng et al. (2009)	água, propileno glicol	butirato de etila, caprilato de etila, oleato de etila, octano	polioxil (35) / etanol
Lee et al. (2009)	água	oleato de etila	lecitina, Tween 80
Cho et al. (2008)	água	óleo de canola	Tween 20, 40, 60 and 80, Span 20, 40, 60 and 80.
Papadimitriou et al. (2008)	água, propileno glicol	limoneno	lecitina / propanol
Polizelli, Santos e Feitosa (2008)	água	óleo de soja	di-(2-etilexil) sulfosuccinato de sódio (AOT), monooleína (MO), lecitina
Dave et al. (2007)	água	limoneno	laurato de sacarose, oleato de sacarose, sacarose e trealose desidratada
Flanagan et al. (2006)	água	óleo de soja	lecitina, mono- di-glicerídeos etoxilados (EMDG), Brij 97 / etanol
Polizelli et al. (2006)	água	óleo de soja	bis 2-etilexil sulfosuccinato de sódio (AOT), monooleína (MO)
Patel, Schmid e Lawrence (2006)	água, propileno glicol	óleo de soja, óleo de girassol, etil ester, etil oleato, tributirina, miristato de isopropila (IPM), triacilglicerol de cadeia média (TCM)	lecitina, Tween 80 / etanol

2.2.1. FASE POLAR

A água é o solvente polar mais adequado para uso em alimentos. Entretanto, pela Tabela 1, observa-se que alguns autores vêm substituindo parcialmente ou totalmente a água por propileno glicol ou glicerol. Estes solventes modificam a polaridade da fase aquosa e penetram com mais facilidade na interface, aumentando a flexibilidade do filme de surfactante e desestabilizando a fase de cristal líquido, favorecendo a formação de microemulsão (YAGHMUR; ASERIN; GARTI, 2002). Eles podem ser utilizados com o intuito de diminuir a concentração de surfactante e co-surfactante e eliminar o uso de ingredientes não permitidos em alimentos.

2.2.2. FASE APOLAR

Dependendo da natureza do óleo, em particular do tamanho da cadeia de carbônica, o óleo pode penetrar em diferentes extensões no filme de surfactante que envolve a gota. Óleos essenciais possuem massa molar pequena, sendo caracterizados por uma mistura complexa de hidrocarbonetos (geralmente cíclicos e insaturados), alcoóis e compostos carbonílicos (ARAÚJO, 2001). Óleos essenciais, como o limoneno e óleo de menta, têm sido extensivamente utilizados no preparo de microemulsões de grau alimentício (Tabela 1). Óleos vegetais são compostos por uma longa cadeia de ácidos graxos, são semi-polares e muito volumosos para penetrar facilmente no filme interfacial e viabilizar a curvatura ótima de formação da microemulsão (FLANAGAN et al., 2006). Triacilgliceróis de cadeia média são uma boa alternativa para a produção de microemulsões, apresentando maior solubilização que óleos vegetais (FLANAGAN; SINGH, 2006).

2.2.3. SURFACTANTES

Surfactantes são moléculas anfífilas responsáveis pela redução da tensão interfacial e estabilidade de sistemas estruturados. A formação de microemulsões pode requerer uma quantidade elevada de surfactante, limitando sua aplicação em alimentos devido aos baixos níveis permitidos pela legislação, à qualidade sensorial e à inviabilidade econômica (RAO;

MCCLEMENTS, 2011). Além disso, muitos dos surfactantes usualmente utilizados não são de grau alimentício. Desta forma, os surfactantes devem ser criteriosamente estudados com o intuito de aumentar a aplicação destes sistemas.

Os surfactantes podem ser classificados quanto ao balanço hidrofílico-lipofílico (BHL), determinado a partir de sua estrutura molecular, ou melhor, seus grupamentos lipofílicos e hidrofílicos. Os surfactantes mais hidrofóbicos apresentam um baixo valor de BHL, sendo solúveis em óleo, enquanto que os compostos com elevado valor de BHL possuem um caráter hidrofílico mais pronunciado, sendo solúveis em água. Como regra geral, surfactantes com valores de BHL de 3 - 6 são apropriados para a estabilização de emulsões A/O, enquanto que aqueles com valores de 8 – 18 atuam como emulsificantes de emulsões O/A (ARAÚJO, 2001). Os surfactantes são também classificados de acordo com a natureza de sua porção polar, podendo ser catiônicos, aniônicos, não iônicos ou zwitteriônicos (também denominados como anfóteros). Alguns surfactantes e seus respectivos valores de BHL estão apresentados na Tabela 2.

Tabela 2. Alguns surfactantes de grau alimentício e seus valores de BHL (Fonte: WALSTRA, 2003; ARAÚJO, 2001).

Tipo de Surfactante	Exemplos	BHL
<i>Aniônicos</i>		
Éster de ácido láctico	Estearoil 2-lactil lactato de sódio	21,0
<i>Zwiteriônicos</i>		
Fosfolipídios	Lecitina	~ 9
<i>Não-iônico</i>		
Monoglicerídios	Monoesterato de glicerol	3,8
Ester de monoglicerídios	Monopalmitato de lactoil	8,0
Span 80	Monooleato de sorbitana	4,3
Span 60	Monoestearato de sorbitana	4,7
Span 40	Monopalmitato de sorbitana	6,7
Span 20	Monolaurato de sorbitana	8,6
Tween 80	Monooleato de polioxietileno de sorbitana	15,0
Tween 60	Monoestearato de polioxietileno de sorbitana	14,9
Tween 40	Monopalmitato de polioxietileno de sorbitana	15,6
Tween 20	Monolaurato de polioxietileno de sorbitana	16,7

Os surfactantes aniônicos contêm geralmente um dos quatro grupos polares solúveis carboxilato, sulfonato, sulfato ou fosfato. Os surfactantes

catiônicos são muito utilizados em agentes de limpeza e cosméticos em geral, sendo compostos por um ou vários grupos amônio terciários ou quaternários. Já os zwitteriônicos são constituídos por dois grupos carregados, um positivo e outro negativamente (KIRK; OTHMER; HOWE-GRANT, 1996).

Os fosfolipídios são surfactantes zwitteriônicos considerados GRAS, encontrados naturalmente na gema de ovo e na soja. A lecitina comercial é uma mistura de fosfolipídios, incluindo a fosfatidilcolina (Figura 5), a fosfatidiletanolamina e a fosfatidilinositol (ARAÚJO, 2001).

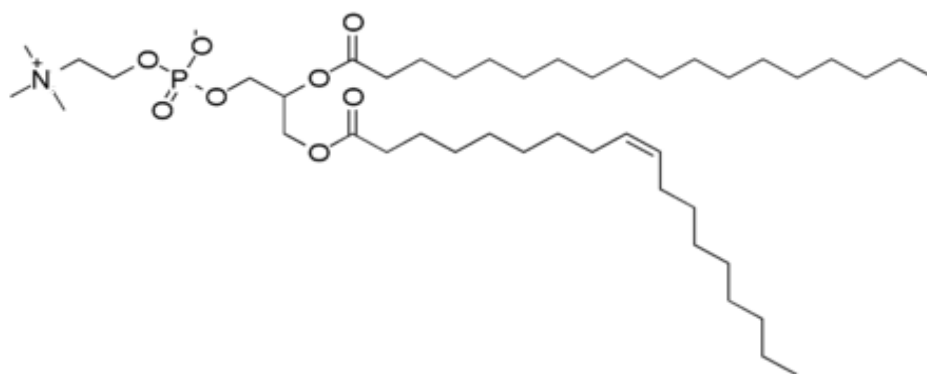


Figura 5. Exemplo de fosfatidilcolina, um fosfolipídio presente na lecitina de soja.

Já os surfactantes não iônicos não se dissociam em meios aquosos, e sua afinidade com a água é dada pelos grupos amida, amina, éteres e hidroxilas (KIRK; OTHMER; HOWE-GRANT, 1996). Estes compostos vêm sendo utilizados intensamente na indústria farmacêutica em função de sua baixa toxicidade. Dentre os surfactantes não-iônicos estão os Spans e Tweens (FLANAGAN; SINGH, 2006).

O Span (Figura 6a) é obtido a partir da esterificação do sorbitol com um ácido graxo, enquanto que o Tween (Figura 6b) é obtido a partir da esterificação do sorbitol polietoxilado com um ácido graxo. Dependendo do tipo de ácido graxo e do grau de etoxilação, os produtos obtidos apresentam diferentes valores de BHL. Pelas características moleculares, o Span possui maior afinidade com materiais lipídicos e o Tween com aquosos.

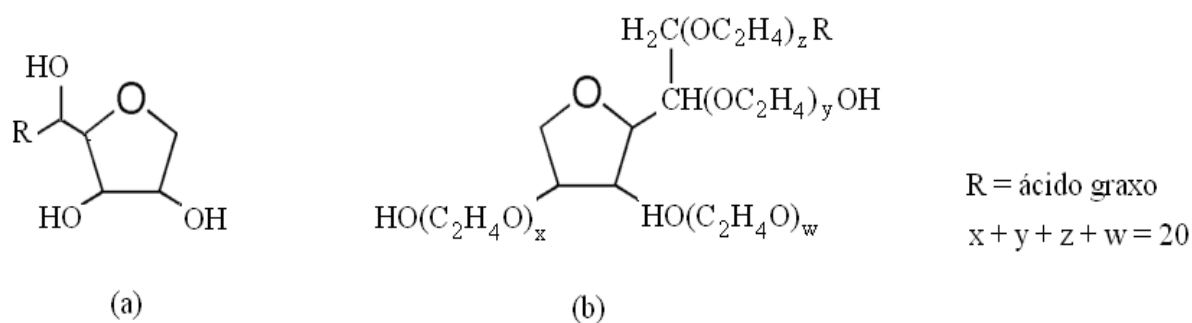


Figura 6. Estrutura química de um estearato de sorbitana (Span) (a) e estearato de sorbitana polietoxilado (Tween) (b).

2.2.4. MISTURAS DE SURFACTANTES

Misturas de surfactantes podem ser utilizadas com o intuito de melhorar a eficiência da formulação e diminuir o conteúdo de surfactante e co-surfactante necessário para a formação de microemulsões (LIN et al., 2009). A combinação de surfactantes hidrofílicos e lipofílicos leva a auto-associações especiais através de modificações na curvatura e flexibilidade do filme de surfactante que pode aumentar a co-solubilização do óleo e da água (PAUL; MITRA, 2005) e diminuir a susceptibilidade de precipitação dos componentes (FANUN 2010c). Além disso, o uso de misturas de surfactantes pode aumentar a capacidade de solubilização de bioativos (MOHAMMAD; POUZOT; MEZZENGA, 2009).

Neste sentido, misturas de surfactantes incluindo um ou mais ingredientes GRAS pode ser explorado com o intuito de melhorar a eficiência da formulação e vislumbrar a aplicação de microemulsões e cristais líquidos em indústrias de alimentos. Por exemplo, a mistura de lecitina e surfactantes não iônicos tem apresentado bons desempenhos na formação de microemulsões sem o uso de co-surfactantes (PATEL; SCHMID; LAWRENCE, 2006).

2.2.5. CO-SURFACTANTES

Os co-surfactantes são moléculas anfífilas que se estendem na interface óleo-água juntamente com os surfactantes (MILLER; NEOGI, 2008). O co-surfactante atua de duas formas: modificando a polaridade das fases polar e apolar e aumentando a solubilidade entre elas; e penetrando no filme

interfacial como um surfactante e aumentando a sua flexibilidade (FENG et al., 2009). Assim, o co-surfactante é capaz de influenciar a curvatura espontânea da interface, desestabilizar a fase líquida cristalina e, então, favorecer a formação de uma microemulsão (YAGHMUR; ASERIN; GARTI, 2002).

Os principais co-surfactantes utilizados são alcoóis de massa molar pequena ou média, com cadeia contendo entre dois a dez carbonos. O etanol é um co-surfactante permitido em alguns alimentos (FENG et al., 2009; PATEL; SCHMID; LAWRENCE, 2006), mas sua eficiência é inferior aos alcoóis de grau não alimentício comumente utilizados na formação de microemulsões (butanol, propanol, pentanol e hexanol) (MENDONÇA, 2005). Apesar disso, alguns estudos relataram a formação de microemulsões contendo 10 % a 20 % de etanol, com potencial uso em bebidas alcoólicas (FLANAGAN; SINGH, 2006).

2.3 EFEITO DA TEMPERATURA NA PRODUÇÃO DE MICROEMULSÃO E CRISTAL LÍQUIDO

Além da composição, a formação das microemulsões é influenciada pela temperatura. Yaghmur, Aserin e Garti. (2002) avaliaram o efeito da temperatura em sistemas compostos por água, limoneno, etanol, propileno glicol e surfactantes não-iônicos (Tween 60 and Brij 96v). Sistemas compostos por Tween 60 e propileno glicol não foram sensíveis a mudanças de temperaturas entre 25 °C e 60 °C, enquanto sistemas compostos por Brij 96v e propileno glicol apresentaram um aumento na região monofásica em 45 °C e 60 °C. O aumento da temperatura em sistemas compostos por Tween 60 e glicerol provocou o aumento da região de 2 fases, a redução da região de cristal líquido e o aumento da região de microemulsão A/O. O aumento da temperatura provoca a desidratação de surfactantes não-iônicos, aumentando a sua solubilidade em óleo e favorecendo a curvatura espontânea negativa do filme de surfactante. Além disso, a temperatura pode aumentar a movimentação dos surfactantes na película, aumentando a flexibilidade interfacial que eventualmente leva à redução da ordenação molecular dos surfactantes em sistemas líquido cristalinos, podendo favorecer a formação da microemulsão (MOHAMMADY; MATTHIEU; MEZZENGA, 2009; SANTANA; PERRECHIL; CUNHA, 2013)

Por outro lado, Flanagan et al. (2006) e Feng et al. (2009) observaram a redução da área de microemulsão com o aumento da temperatura em sistemas compostos por água, etanol, sacarose, óleo de soja e Brij 97 e, sistemas compostos por água, etanol, butirato de etila, e polioxil 35 (surfactante não-iônico), respectivamente. Nestes casos, maiores temperaturas levaram à redução da solubilidade dos surfactantes não-iônicos em água e aumentaram a solubilidade dos surfactantes em óleo, e esta variação de solubilidade reduziu a área de microemulsão destes sistemas.

A temperatura não afeta somente a formação da microemulsão, mas também a transição de fases líquidas cristalinas. Desta forma, o estudo da transição de fases com o aumento ou redução da temperatura pode simular processos industriais ou biológicos de interesse (KULKARNI, 2011). Visto que os alimentos, bebidas, cosméticos e fármacos precisam ser estáveis na temperatura de armazenamento, a identificação da estrutura numa faixa de temperatura é importante.

Leser et al. (2006) discutiram a influência da temperatura no comportamento de fases de monoglicerídeos. O aquecimento pode ser usado no preparo de sistemas que apresentam elevada viscosidade em baixas temperaturas (como fases cúbicas) e baixa viscosidade em temperaturas elevadas. Em altas temperaturas, os sistemas são eficientemente homogeneizados por agitadores magnéticos ou vortex, e o processo de resfriamento final originará um sistema homogêneo de elevada viscosidade. A mudança de viscosidade com o aumento da temperatura se deve à redução da viscosidade da fase contínua e à fluidização térmica induzida na fase líquida cristalina (AHMED; ARAMAKI, 2009), indicando uma transição de fases.

Pouzot et al. (2007) observaram que sistemas compostos por monooleína, limoneno e água apresentaram fases cúbicas a 25 °C, enquanto sistemas micelares (L_2), também chamadas de microemulsões inchadas, foram produzidos a 45 °C. Já em temperaturas intermediárias, fases cúbicas e micelares coexistiam. O aumento da temperatura provoca um desordenamento da estrutura, a redução dos parâmetros estruturais (parâmetro de cela) (KULKARNI, 2011; MEZZENGA et al., 2005; POUZOT et al., 2007) e o encolhimento das fases, expulsando a água absorvida (KULKARNI, 2011), o que é explicado pelo aumento da flexibilidade do filme, pelo rearranjo das

cadeias hidrofóbicas com a temperatura, e pela desidratação progressiva dos grupos polares dos surfactantes (MOHAMMADY; POUZOT; MEZZENGA, 2009).

2.4 REFERÊNCIAS BIBLIOGRÁFICAS

- AHMED, T.; ARAMAKI, K. (2009). Temperature sensitivity of wormlike micelles in poly(oxyethylene) surfactant solution: Importance of hydrophilic-group size. **Journal of Colloid and Interface Science**, 336, 335–344.
- ALAM, et al. (2010). Phase behavior and rheology of oil-swollen micellar cubic phase and gel emulsions in nonionic surfactant systems. **Journal of Colloid and Interface Science**, 341, 267-272.
- ANTON, N.; VANDAMME, T. F. (2009). The universality of low-energy nano-emulsification. **International Journal of Pharmaceutics**, 377, 142–147.
- ANTON N.; BENOIT J. P.; SAULNIER, P. (2008) Design and production of nanoparticles formulated from nano-emulsion templates - A review. **Journal of Control Release**, 128, 185–199
- ATTWOOD, D.; FLORENCE, A. T. (2003). **Princípios físico-químicos em farmácia**, Vol. 4. São Paulo: EDUSP, 732p.
- ARAÚJO, J. M. A. (2001). **Química de alimentos: Teoria e prática**. Viçosa: Universidade Federal de Viçosa, 2ª ed., 416 p
- BINKS, B. P.; FLETCHER, P. D. I.; TIAN, L. (2010). Influence of nanoparticle addition to Winsor surfactant microemulsion systems. **Colloids and Surfaces A: Physicochemical and Engineering Aspects**, 363, 8-15.
- CHO, et al. (2008). Formulation of a cosurfactant-free o/w microemulsions using nonionic surfactant mixture. **Journal of Food Science**, 73, 121-115.
- DAVE, et al. (2007). Phase behaviour and SANS investigations of edible sugar-limonene microemulsions. **Colloids and Surfaces A: Physicochemical and Engineering Aspects**, 296, 45-50.
- FAN et al. (2011). Improved intestinal delivery of salmon calcitonin by water-in-oil microemulsions. **International Journal of Pharmaceutics**, 330, 416:323.
- FANUN, M. (2009). Properties of microemulsions based on mixed nonionic surfactants and mixed oils. **Journal of Molecular Liquids**, 150, 25-32.

FANUN, M. (2010a). Microemulsions with mixed non-ionic surfactants and flavour oil. **Journal of Surfactants and Detergents**, 13, 321-328.

FANUN, M. (2010b). Formulation and characterization of microemulsions based on mixed non-ionic surfactants and peppermint oil. **Journal of Colloid and Interface Science**, 343, 496-503.

FANUN, M. (2010c). Properties of microemulsions with mixed non-ionic surfactants and citrus oil. **Colloids and Surfaces A: Physicochemical and Engineering Aspects**, 369, 246-252.

FASOLIN, L. H.; SANTANA, R. C.; CUNHA, R. L. (2012). Microemulsion and liquid crystalline formulated with triacylglycerols: Effect of ethanol and oil unsaturation. **Colloids and Surfaces A: Physicochemical and Engineering Aspects**, 415, 31–40.

FENG, et al. (2009). Study on food-grade vitamin E microemulsions based on non-ionic emulsifier. **Colloids and Surfaces A: Physicochemical and Engineering Aspects**, 339, 1–6.

FLANAGAN, J.; SINGH, H. (2006). Microemulsions: A Potential Delivery System for Bioactives. **Critical Reviews in Food Science and Nutrition**, 46, 221–237.

FLANAGAN, et al. (2006). Solubilisation of soybean oil in microemulsions using various surfactants. **Food Hydrocolloids**, 20, 253–260.

FORMARIZ, et al. (2005). Microemulsões e fases líquidas cristalinas como sistemas de liberação de fármacos. **Revista Brasileira de Ciências Farmacêuticas**, 41, 301–313.

GURFINKEL J.; ASERIN A.; GARTI N. (2011) Interactions of surfactants in nonionic/anionic reverse hexagonal mesophases and solubilization of a-chymotrypsinogen A. **Colloid Surf A Physicochem Eng Asp** 392:322–328.

HICKEY, et al. (2010). Analysis of phase diagram and microstructural transitions in a ethyl oleate/water/Tween 80/Span 20 microemulsion system using high-resolution ultrasonic spectroscopy. **International Journal of Pharmaceutics**, 388, 213-222.

HYDE, S.T. (2001). **Identification of lyotropic liquid crystalline mesophases**. In. HOLMBERG, K. (Ed.) Handbook of applied surface and colloid chemistry. New York: John Wiley & Sons.

HOLMBERG, K.; JÖNSSON, B.; KRONBERG, B.; LINDMAN, B. (2003). **Surfactants and polymers in aqueous solution**. West Sussex: John Wiley & Sons.

JAFARI, et al. (2008). Re-coalescence of emulsion droplets during high-energy emulsification. **Food Hydrocolloids**, 22, 1191–1202.

KIRK, R. E.; OTHMER, D. F.; HOWE-GRANT, M. (1996). **Kirk-Othmer encyclopedia of chemical technology**. 4 ed. New York: Wiley.

KULKARNI, C.V. (2011). Nanostructural studies on monoelaidin – water systems at low temperatures. **Langmuir**, 27, 11790-11800.

LAWRENCE, M.J.; REES, G.D. (2000). Microemulsion-based media as novel drug delivery systems. **Advanced Drug Delivery Reviews**, 45, 89 –121.

LEE, et al. (2009). Enhancement of the encapsulation and transmembrane permeation of isoflavone-containing red clover extracts in phospholipid-based microemulsion using different extraction processes. **Journal of Agricultural and Food Chemistry**, 57, 9489–9495.

LESER, M. E.; SAGALOWICS, L.; MICHEL, M.; WATZKE, H. J. (2006) Self-assembly of polar food lipids. **Advances in Colloid and Interface Science**, 123–126, 125–136

LIN, et al. (2009). Stability and characterisation of phospholipid-based curcumin-encapsulated microemulsion. **Food Chemistry**, 116, 923–928.

Liu, C. H.; Chang, F. Y.; Hung, D. K. (2011) Terpene microemulsions for transdermal curcumin delivery: effects of terpenes and cosurfactants. **Colloids and Surface B – Biointerfaces**, 82, 63–70

LIU, F.; WANG, Z. W. (2010). Formulation of α -linolenic acid microemulsion free of co-surfactant. *Chinese Chemical Letters*, 21, 105-108.

McClements, D. J. (2005) *Food emulsions: principles, practice, and techniques*. CRC Press, Washington, DC.

MENDONÇA, C. R. B. (2005). Desenvolvimento de metodologias para análise direta de óleos vegetais empregando microemulsões de água em óleo e meios não aquosos. Tese (Doutorado em Química) – Universidade Federal do Rio Grande do Sul.

MEZZENGA et al. (2005). Shear rheology of lyotropic liquid crystals: a case study. **Langmuir**, 21, 3322-3333.

MCCLEMENTS, et al. (2009). Structural design principles for delivery of bioactive components in nutraceuticals and functional foods. **Critical Reviews in Food Science and Nutrition**, 49, 577-606.

MOHAMMADY, S. Z.; POUZOT, M.; MEZZENGA, R. (2009). Oleoylethanolamide-Based lyotropic liquid crystals as vehicles for delivery of amino acids in aqueous environment. **Biophysical Journal**, 96, 1537-1546.

MILLER, C. A.; NEOGI, P. (2008). **Interfacial phenomena: equilibrium and dynamic effects**. New York: M. Dekker, 2 ed. 494 p., (Surfactant science series; v.17).

PAPADIMITRIOU, et al. (2008). Biocompatible microemulsions based on limonene: Formulation, structure, and applications. **Langmuir**, 24, 3380-3386.

PATEL, N.; SCHMID, U.; LAWRENCE, M. J. (2006). Phospholipid-based microemulsions suitable for use in foods. **Journal of Agricultural and Food Chemistry**, 54, 7817–7824.

PAUL, B. K.; MITRA, R. K. (2005). Water solubilization capacity of mixed reverse micelles: Effect of surfactant component, the nature of the oil, and electrolyte concentration. **Journal of Colloid and Interface Science**, 288, 261-279.

POLIZELLI, M. A.; SANTOS, A. L.; FEITOSA, E. (2008). The effect of sodium chloride on the formation of W/O microemulsions in soy bean oil/surfactant/water systems and the solubilization of small hydrophilic molecules. **Colloids and Surface A: Physicochemical and Engineering Aspects**, 315, 130-135.

POLIZELLI, et al. (2006). Formation and characterization of soy bean oil/surfactant/water microemulsions. **Colloids and Surfaces A: Physicochemical Engineering Aspects**, 281, 230-236.

POUZOT, et al. (2007). Structural and rheological investigation of Fd3m inverse micellar cubic phases. **Langmuir**, 23, 9618-9628.

RAO, J.; MCCLEMENTS, D. J. (2011). Food-grade microemulsions, nanoemulsions and emulsions: Fabrication from sucrose monopalmitate & lemon oil. **Food Hydrocolloids**, 25, 1413-1423.

RAKSHIT, A. K.; MOULIK, S. P. (2008). **Physicochemistry of W/O microemulsions**. In: Fanun, M. Microemulsions, Crc Press, 2008.

- SAGALOWICZ, L.; LESER, M. E. (2010). Delivery systems for liquid food products. **Current Opinion in Colloid & Interface Science**, 15, 61–72.
- SANTANA, R. C.; PERRECHIL, F. A.; CUNHA, R. L. (2013). High- and low-energy emulsifications for food applications: a focus on process parameters. **Food Engineering Reviews**, 5, 107-122.
- TAVANO et al. (2011) Niosomes vs microemulsions: new carriers for topical delivery of Capsaicin. **Colloids and Surfaces B – Biointerfaces**, 87, 333–339.
- WALSTRA, P. (2003). **Physical chemistry of foods**. New York: Marcel Dekker, 807 p. (Food science and technology; v. 121).
- WINDHAB, et al. (2005). Emulsion processing—from single-drop deformation to design of complex processes and products. **Chemical Engineering Science**, 60, 2101–2113.
- YAGHMUR, A.; ASERIN, A.; GARTI, N. (2002). Phase behavior of microemulsions based on food-grade nonionic surfactants: effect of polyols and short-chain alcohols. **Colloids and Surface A: Physicochemical and Engineering Aspects**, 209, 71–81.
- ZHANG, et al. (2009). Antimicrobial activity of a food-grade fully dilutable microemulsion against *Escherichia coli* and *Staphylococcus aureus*. **International Journal of Food Microbiology**, 135, 211-215.
- ZHANG, et al. (2010). Characterization and antimicrobial activity of a pharmaceutical microemulsion. **International Journal of Pharmaceutics**, 395,154-160.
- ZHANG et al. (2011) Antibacterial activities of a food-grade dilution-stable microemulsion. **Journal of Food Safety**, 31, 232–237
- ZHENG, et al. (2011). Study on the microstructure and rheological property of fish oil lyotropic liquid crystal. **Colloids and Surfaces A: Physicochemical and Engineering Aspects**, 385, 47-54.
- ZHONG, et al. (2009). Formation and characterization of mint oil/S and CS/water microemulsions. **Food Chemistry**, 115, 539–544.

- CAPÍTULO 3 -
EFEITO DA CONCENTRAÇÃO DE ETANOL E DO
CISALHAMENTO EM SISTEMAS COMPOSTOS POR
TWEEN 80, ÁGUA E TRIACILGLICEROL DE CADEIA
MÉDIA

EFFECTS OF A COSURFACTANT ON THE SHEAR
DEPENDENT STRUCTURES OF SYSTEMS
COMPOSED OF BIOCOMPATIBLE INGREDIENTS

Rejane de Castro Santana, Luiz Henrique Fasolin, Rosiane Lopes da Cunha. Colloids and Surfaces A (2012), v. 398, p. 54-63.

**EFFECTS OF A COSURFACTANT ON THE SHEAR DEPENDENT
STRUCTURES OF SYSTEMS COMPOSED OF BIOCOMPATIBLE
INGREDIENTS**

Rejane de Castro Santana, Luiz Henrique Fasolin, Rosiane Lopes da Cunha

In: Colloids and Surfaces A (2012), v. 398, p.54-63

Department of Food Engineering, Faculty of Food Engineering, University of
Campinas – UNICAMP, 13083862, Campinas, SP, Brazil

* Corresponding author. Tel.: +55 19 3521 40407, fax: +55 19 3521 4027.

Email address: rosiane@fea.unicamp.br (R.L. da Cunha).

ABSTRACT

The phase transitions of systems composed of water, polyoxyethylene sorbitan monooleate (Tween 80), medium-chain triglycerides (MCTs) and ethanol were evaluated based on rheological properties using different proportions of MCT:ethanol (1:0, 2:1 and 1:2). Higher ethanol contents led to a broadened microemulsion (ME) region and a diminished liquid crystalline (LC) region in the phase diagram and resulted in the formation of systems with smaller particle sizes, lower viscosities and less shear-thinning. Different systems were obtained from the water titration of an initial mixture of 70% (w/w) surfactant and 30% (w/w) oil + ethanol. At low water contents, Newtonian W/O MEs were produced. At intermediate water contents, LC phases were observed, including viscous and gel-like structures with viscoelastic properties and complex rheology (shear-thinning, Bingham plastic or Herschel–Buckley behaviour). In addition, these samples exhibited time-dependent behaviours, showing thixotropy in systems rich in amphiphilic and non-polar components and anti-thixotropy in systems with a prevalence of polar (ethanol and water) components. According to oscillatory measurements, cubic phases were most likely formed at 40% (w/w) water in systems with low (or an absence of) ethanol. At higher water contents (>50%, w/w), O/W milk-like emulsions were produced in systems with low ethanol contents, whereas O/W MEs were

produced in the system with a high ethanol content. O/W MEs exhibited larger droplet sizes and lower viscosities than W/O MEs. The different structures depended strongly on the system composition, which enables the production of textures with potential applications in the food, cosmetic and pharmaceutical industries.

Keywords: microemulsion, liquid crystal, rheology, microstructures

3.1. INTRODUCTION

Surfactant molecules self-assemble into a large variety of morphologies, including micelles and liquid-crystalline (LC) phases, such as lamellar, hexagonal, or cubic phases [1]. These systems are prepared using low-energy methods in which a change in surfactant layer curvature and a phase transition occur during the process [2]. In addition to the ease and low cost of their preparation, these systems have oil and water domains with well-defined interfaces from surfactants, which lead to the ability to solubilise a large quantity of both polar and nonpolar additives [3], including food additives, nutraceuticals, aromatic compounds, cosmetic compounds, active ingredients, and drugs [4].

Microemulsions (MEs) are usually optically isotropic, translucent and thermodynamically stable systems with low viscosities. They are formed by small droplets (1–200 nm) stabilised by surfactants, usually in combination with a cosurfactant [1]. In contrast, LC phases exhibit a more complex structure. Surfactant molecules form bilayers that are regularly stacked in a lamellar phase, whereas cylinders are organised on a triangular lattice in a hexagonal phase [1], and a highly viscous three-dimensional structure exists in a cubic phase [5].

ME and LC characterisation can be performed with a large variety of classical methods, such as turbidity, electrical conductivity, light-polarised microscopy, electron microscopy, dynamic light scattering (DLS), small-angle-X-ray-scattering (SAXS), nuclear magnetic resonance (NMR) and viscosity measurements [6,7]. However, in addition to viscosity, other rheological measurements can be used to identify and characterise such systems. Flow curves can reflect changes in macroscopic properties during shearing [8] and are a useful method for monitoring structural transitions during processing. Flow curves also provide information that is important for practical applications. In

addition, oscillatory measurements reflect the system structure and the behaviour of the product during storage.

The structures of MEs and LC phases depend on the system's composition and on the shearing conditions [8,9]. The production of MEs and LC phases with a formulation capable of solubilising specific drugs requires extensive pre-formulation studies [10]. Many recent studies have been performed with the aim of preparing MEs using biocompatible ingredients. However, most of the reported methods have used at least one not-food-acceptable ingredient or cyclic oils (which are highly susceptible to oxidation) [11–13], or the aqueous phase has been replaced with another polar ingredient, such as propylene glycol [11,14,15]. Polyoxyethylene sorbitan fatty acid esters (Tweens) are nonionic surfactants that are extensively used in ME production [12,16–18] because of their non-toxic and biodegradable character [19,20]. Many studies have used systems that contain Tween 80 as a surfactant to improve the solubilisation of active molecules [4,17,21,22]. Regarding cosurfactants, short-chain alcohols are the most commonly used cosurfactants in microemulsion formulations; however, ethanol is the only alcohol suitable for use in food products, such as alcoholic beverages [23]. Medium-chain-triglycerides have been used in biocompatible microemulsions [15,24] as nonpolar phases because they are more stable than cyclic oils and because they have a more apolar structure and a lower molecular weight than long-chain-triglycerides (vegetable oils), which makes medium-chain-triglycerides more easily solubilised [23,25].

This study was aimed at the evaluation of systems composed only of biocompatible ingredients: water as a polar phase, Tween 80 as a nonionic surfactant, a medium-chain-triglyceride (MCT) as an apolar phase, and ethanol as a cosurfactant at different proportions of MCT:ethanol (1:0, 2:1 and 1:2). Different rheological measurements were used to describe the phase transitions of the systems, identifying the phase diagram limits and the effect of ethanol on the shear-dependent structure of the systems. To our knowledge, no studies on the relationship between rheological behaviour and the structure and composition of this type of system have been reported.

3.2. MATERIALS AND METHODS

3.2.1. MATERIALS

Delios V, a medium-chain-triglyceride (MCT) rich in caprylic and capric glycerides, was kindly donated by Cognis (Germany). Tween 80 (polyoxyethylene sorbitan monooleate) and 99.5% ethanol were purchased from Synth (Brazil).

3.2.2. METHODS

3.2.2.1. Phase-diagram construction and characterisation

The four-component systems were described by pseudo-ternary diagrams using different MCT:ethanol ratios (1:0, 2:1 and 1:2, w/w). The diagrams were produced using a spontaneous emulsification method at 25 °C. First, an initial mixture of Tween 80 and MCT + ethanol was prepared at different ratios (10:90; 20:80; 30:70; 40:60; 50:50; 60:40; 70:30; 80:20; 90:10, w/w) (filled symbols in Fig. 1) under continuous magnetic stirring. Deionised water was then titrated under constant stirring in increments of 10% (w/w) (open symbols in Fig. 1). Each formulation was kept stirring for 30 min, and the samples were then stored at 25 °C for at least 15 days before they were examined for the diagram construction.

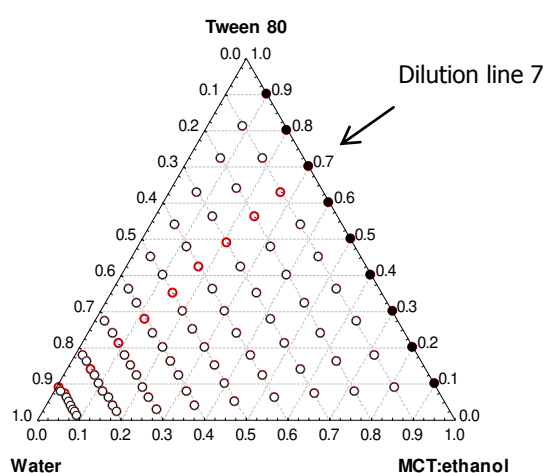


Fig. 1 Systems produced to phase diagram construction. Filled symbols (•) are initial mixtures of Tween 80, MCT and ethanol and open symbols (○) are samples obtained over dilution lines.

Each system was characterised according to its electrical conductivity, microstructure under polarised microscopy and visual appearance. First, the nature of the dispersed phase and the sample structure (W/O ME, LC and O/W ME) were estimated by the electrical conductivity at room temperature (25 °C) using an Orion 3 Star (Thermo Electron, USA) bench-top conductivity meter coupled to a conductivity cell (Orion 013016MD). The characteristics of each system and the phase-diagram limits were confirmed by visual and microscopic analyses. Systems that showed birefringence through cross-polaroids in an Olympus BX51TF optical microscope (Olympus, Japan) were considered liquid-crystalline (LC) phases. Systems with only one phase that was clear and non-birefringent (dark appearance under cross-polarised light microscopy) were classified as microemulsions (MEs). Translucid systems with phase separation were classified as “multiphase” and represented Winsor I, Winsor II or Winsor III systems. Systems with a milky appearance were classified as emulsions (EMs), which included macro, mini or nanoemulsions, depending on their mean droplet size.

Characteristic parameters of the systems were obtained, including the maximal amount of aqueous phase dispersed in the W/O ME (W_m), the total LC region (ALC), the total W/O ME region (AW/O ME) and the total O/W ME region (AO/W ME).

3.2.2.2. Characterisation of ME, LC and EM phases

The samples obtained from water titration of an initial mixture of 70% (w/w) Tween 80 and 30% (w/w) MCT + ethanol (dilution line 7, identified as red open symbols in Fig. 1) were analysed by particle size distribution and by rheological measurements. The composition of these systems is shown in Table 1. Each sample was named according to its formulation: first in accordance to the initial surfactant concentration (70%, w/w), followed by the water content (0–90%, w/w). In addition, the samples were classified according to the MCT:ethanol ratio used: A (1:0), B (2:1) or C (1:2). For example, an initial sample that contained 70% (w/w) Tween 80, 20% (w/w) MCT and 10% (w/w) ethanol (MCT:ethanol = 2:1) diluted with 50% (w/w) water was named as B7050.

Table 1. Composition of systems A, B and C evaluated by particle size distribution and rheological measurements.

% water	% Tween 80	System A (1:0)		System B (2:1)		System C (1:2)	
		% oil	% ethanol	% oil	% ethanol	% oil	% ethanol
0	70	30	0	20	10	10	20
10	63	27	0	18	9	9	18
20	56	24	0	16	8	8	16
30	49	21	0	14	7	7	14
40	42	18	0	12	6	6	12
50	35	15	0	10	5	5	10
60	28	12	0	8	4	4	8
70	21	9	0	6	3	3	6
80	14	6	0	4	2	2	4
90	7	3	0	2	1	1	2

3.2.2.3. Particle-size measurements

Particle-size measurements were performed at 25 °C using dynamic light scattering (DLS) on a ZetaSizer Nano-ZS (Malvern Instruments, UK) with a detection angle of 173°. The intensity size distributions and the main peak mean from the intensity distribution were obtained using the General Purpose algorithm in the instrument software.

3.2.2.4. Rheological measurements.

Flow curves and oscillatory measurements were performed on a Physica MCR301 rheometer (Anton Paar, Austria) using a stainless steel cone-plate geometry (5.0 cm, 2° angle, truncation 208 mm).

Flow curves were obtained at 25 °C by an up-down-up step program using a shear-rate range between 0 and 100 s⁻¹. The results of the samples without prior shearing at the transient state (S1) and at the steady state (S3) were used to estimate the thixotropy of the samples based on the area between curves S1 and S3 (hysteresis) [26].

The flow curves under steady-state conditions were fitted to a Newtonian, power-law, Bingham plastic or Herschel–Buckley model. These models are generally represented by Eq. (1):

$$\sigma = \sigma_0 + k \cdot \dot{\gamma}^n \quad (1)$$

where σ is the shear stress (Pa), σ_0 is the yield stress (Pa), k is the consistency index (Pa s^n), $\dot{\gamma}$ is the shear rate (s^{-1}), and n is the flow index. For $\sigma_0 \neq 0$ and $n = 1$, the fluid is characterized as a Bingham plastic, whereas for $\sigma_0 \neq 0$ and $n < 1$, the fluid is denominated as Herchel–Bukley (HB) type. For $\sigma_0 = 0$ and $n = 1$, the fluid behaviour is Newtonian, and for $\sigma_0 = 0$ and $n < 1$, the fluid shows shear-thinning behaviour. The apparent viscosity at 3 s^{-1} (η_{33}) obtained at the transient state (S1) was also evaluated. This shear rate was chosen because it was the minimum value measured and because it showed little effect of shear on the rheological behaviour.

Oscillatory measurements were performed within the linear viscoelastic region. The complex (G^*), storage (G') and loss (G'') moduli were evaluated using a frequency sweep between 0.01 and 10 Hz at 25 °C.

3.3. RESULTS AND DISCUSSION

3.3.1. ELECTRICAL CONDUCTIVITY

Fig. 2 shows the electrical conductivities of the systems A, B and C. Most of the samples showed a characteristic profile of conductivity over the dilution lines, particularly the samples with higher initial surfactant concentrations. These samples showed high electrical conductivity under the dilution line. Some samples of systems A and B showed high viscosities and gel-like structures, which made measurements of their conductivities nonviable.

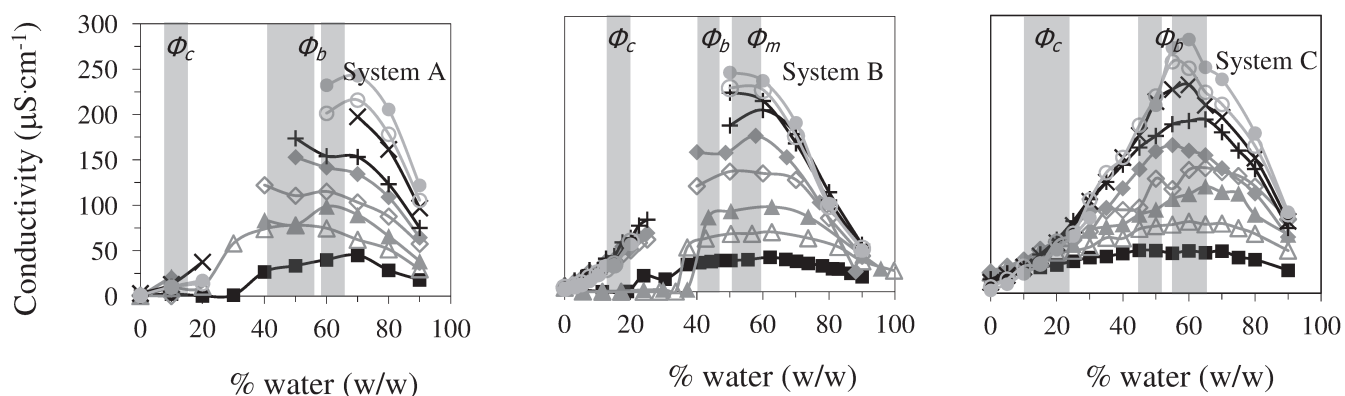


Fig. 2. Electrical conductivity along the dilution lines of the systems A, B and C. Initial surfactant content (% w/w): 10 (■), 20 (△), 30 (▲), 40 (◇), 50 (◆), 60 (+), 70 (x), 80 (○), 90 (●). Limits of structural transition: Φ_c (maximum water content in a W/O ME), Φ_b (initial water content of bicontinuous ME region) and Φ_m (final water content of bicontinuous ME region).

Samples with low water-volume contents exhibited low electrical conductivity values that slightly increased up to a critical water mass fraction ϕ_c (between 10 and 22.5%, w/w water). At the critical water mass fraction, the water droplets are most likely dispersed in the continuous medium as discrete particles with few interactions between them, which results in a low conductivity [27]. An increase in the water content between ϕ_c and ϕ_b (approximately up to 45–55%, w/w of water) resulted in a linear and abrupt increase in the conductivity; this phenomenon is known as percolation. A change in the curvature of the electrical conductivity plot could indicate structural changes from W/O MEs to more complex structures through the self-assembly of surfactant molecules. Collisions between spherical droplets of W/O MEs most likely occurred due to the attractive interactions between the droplets, which resulted in the formation of numerous clusters and water channels (liquid-crystal structures) that increased the electrical conductivity of the systems [28]. For intermediate water volume contents between ϕ_b and ϕ_m , the electrical conductivity increased nonlinearly up to a maximum value (approximately 55–60%, w/w water); under these conditions, a bicontinuous ME (or bicontinuous cubic phase) occurred. At higher water contents, the conductivity decreased abruptly, which suggests the transition of a W/O to an O/W ME. The decrease in conductivity can be explained by the dilution of the O/W ME in the water phase having decreased the concentration of the dispersed oil droplets [29].

3.3.2. PHASE DIAGRAMS

According to the visual appearance, light-polarised microscopy results and electrical conductivity curves, the pseudoternary diagrams of the systems A, B and C were constructed, as presented in Fig. 3.

W/O MEs were obtained at low water concentrations in systems A, B and C, whereas O/W MEs were formed at higher water concentrations only in systems B and C (with ethanol addition). The formation of W/O MEs is more difficult than that of O/W MEs, which makes the solubilisation of hydrophobic active molecules difficult [4]. W/O and O/W ME regions were separated by a liquid-crystalline (LC) phase, which exhibited an opaque appearance and a high viscosity or gel formation. At low surfactant concentrations and high MCT:ethanol concentrations, a “multiphase” system was formed in which a ME phase coexisted with an oil and/or an water phase (Winsor I, II or III). In contrast, at low surfactant concentrations and high water concentrations, a milk-like emulsion (EM) with a cream phase separation (or not) was formed.

Fig. 3 and Table 2 show that the additional of ethanol increased the O/W ME, W/O ME and “multiphase” regions and decreased the EM area. Moreover, the LC area significantly decreased with the first addition of ethanol (MCT:ethanol = 2:1), but further increase in the ethanol content (MCT:ethanol = 1:2) led to a slight decrease in the LC area. As a consequence of the change in the interface between the LC and W/O ME regions, the maximum water dispersed in W/O ME (W_m) increased from 12.5 to 25% (w/w) in system B and was 35% (w/w) in system C; this result is significant with respect to the solubilisation of hydrophilic components in a hydrophobic matrix. Ethanol acts as a cosurfactant that reduces the interfacial tension and increases the fluidity of the interface. Alcohols interact at the interface between oil and water causing the swelling of aqueous channels and the relaxation of surfactant bilayers, which leads to a disordering of the cubic phase and to the formation of phases with flatter interfaces, such as sponge and lamellar phases [30]. As a result, ethanol can avoid the formation of rigid structures, including gels, liquid crystals and precipitates [31]. Furthermore, alcohol influences the solubility properties of the oil and water phases because of its partitioning between the oil and water phases [23].

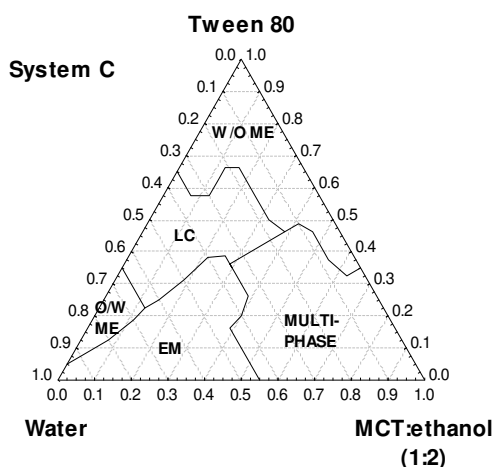
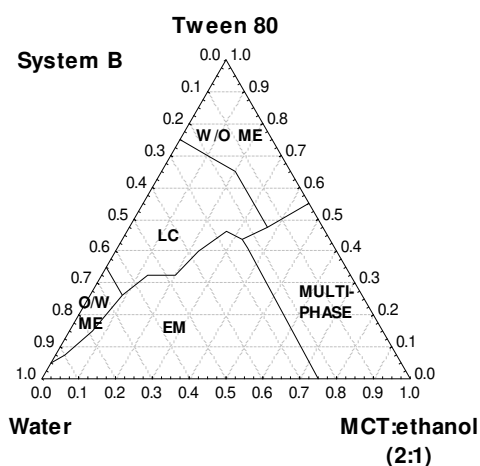
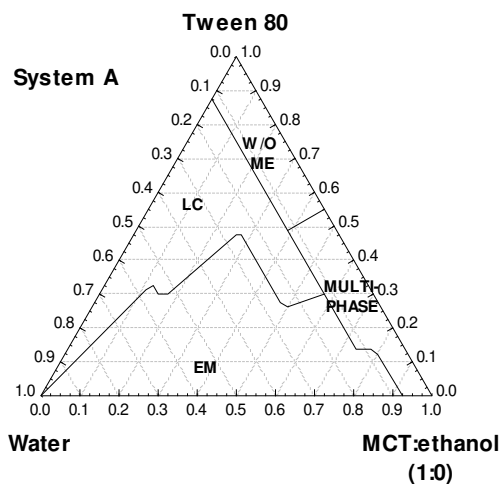


Fig. 3. Phase diagram of systems A, B and C. Phases: LC is liquid crystal, O/W ME is O/W microemulsion, W/O ME is W/O microemulsion, EM is milked-like emulsion and multiphase represents Winsor I, II or III systems.

Table 2. Parameters calculated from phase diagrams of systems A, B and C. $A_{O/W ME}$ is the area of the region of O/W microemulsion, $A_{W/O ME}$ is the area of W/O microemulsion, A_{LC} is the liquid crystal area and W_m is maximal amount of water dispersed in an W/O microemulsion.

Parameters	Systems		
	A	B	C
$A_{W/O ME}$ (%)	10.5	14.4	21.2
$A_{O/W ME}$ (%)	0	2.9	4.2
A_{LC} (%)	31.0	19.1	18.0
W_m	12.5	25	35

Other authors have evaluated the phase diagrams of systems composed of some of the ingredients used in this work. Patel, Schmid and Lawrence [15] obtained between 10 and 72% A_{ME} (total region of W/O and O/W ME) in systems composed of propylene glycol (PG), MCT, ethanol and phospholipids. The highest values were obtained in the presence of ethanol and in absence of water because the replacement of water with PG increased the flexibility of the surfactant film and favoured microemulsion formation [13]. Garti et al. [24] evaluated systems composed of water, limonene and Brij 96 (polyoxyethylene 10 oleyl ether), which exhibited an A_{ME} value of 13%; the addition of ethanol (limonene:ethanol = 1:1) increased the value of A_{ME} to 30.3% in the same manner as observed in this work. Systems composed of MCT, water and Tween 80 showed W/O microemulsion formation over a limited isotropic area (in agreement with our results), whereas the addition of ethanol (MCT:ethanol = 1:1) and PG (water:PG = 1:1) produced a system with an A_{ME} value of 43.3% [24]; this value is greater than that obtained in our work for system C (A_{ME} = 25.4%) because the solubilisation of water is more difficult than that of propylene glycol. The increase of microemulsion area with the addition of ethanol was observed by other authors in a system composed of Tween 40, water and glycerol monolaurate [16] and in a system composed of Brij 96v, water, propylene glycol and limonene [24]. Comparing to others short-chain alcohols with different lengths and shapes (linear or branched) (as propanol, butanol and pentanol), ethanol is less efficiency in promoting microemulsion formation [32–34]. However, ethanol is considered a safe ingredient to some

applications and it is usually chosen as the cosurfactant for biocompatible systems [33].

3.3.3. MICROSTRUCTURE AND PARTICLE SIZE

Fig. 4 shows the visual appearance and microstructure under polarised light of the samples produced by water titration from an initial mixture that contained 70% (w/w) surfactant (dilution line 7). All systems formed LC phases at intermediate water contents and W/O MEs at lower water contents; systems A and B, however, formed LC phases with gel-like structures. Only system C formed an O/W ME at dilution line 7.

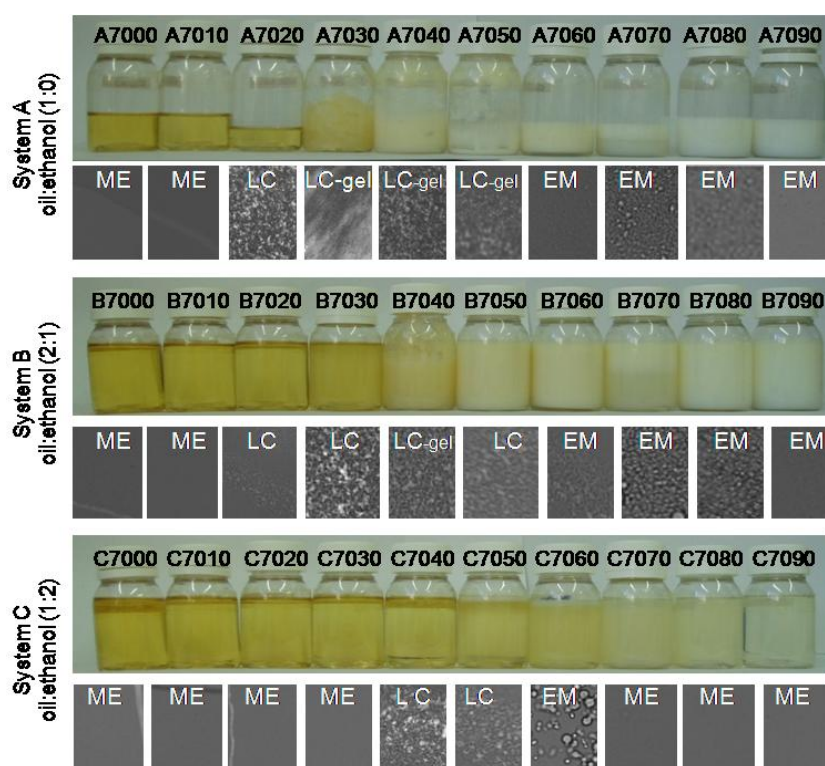


Fig. 4. Visual appearance and microstructure of the systems A, B and C. ME: microemulsion, EM: emulsion, LC: liquid crystalline, and GEL: liquid crystalline with gel-like structure.

The intensity particle size distributions of systems A, B and C are shown in Fig. 5. At intermediate water contents, which correspond to the LC phase, there was a limitation of the technique for evaluate systems with large and polydispersed particle size.

The systems with low water contents (0–40%, w/w water) exhibited higher polydispersity than the samples with high water contents (70–90%, w/w water). These systems with low water contents showed at least two intensity peaks over a wide range of particle sizes (1–10,000 nm). However, a comparison of A, B and C systems with the same water contents reveals that the addition of ethanol decreased the particle size and/or the polydispersity of the systems. The addition of water (0–10%, w/w) led to a decrease in the particle size, which can be expected because the surfactant molecule has an amphiphilic character. A small amount of water increased Tween 80 interactions and produced a W/O ME with a more compact structure than that formed in the absence of water. The increase in water content up to an intermediate value (between 30 and 50%, w/w water) led to an increase in particle size. The increase in particle size to high values (many of them not measured by DLS) most likely means that the structure of the W/O MEs changed to LC phases, as lamellar, hexagonal or cubic structures. At water concentrations greater than 60% (w/w), the particle size decreased as the water content was increased, which suggests a structural transition from an LC phase to an O/W ME or O/W EM. Most of these systems showed a monomodal distribution, except the system with higher ethanol content and 90% (w/w) water (C7090), which showed two peaks at approximately 10 and 100 nm.

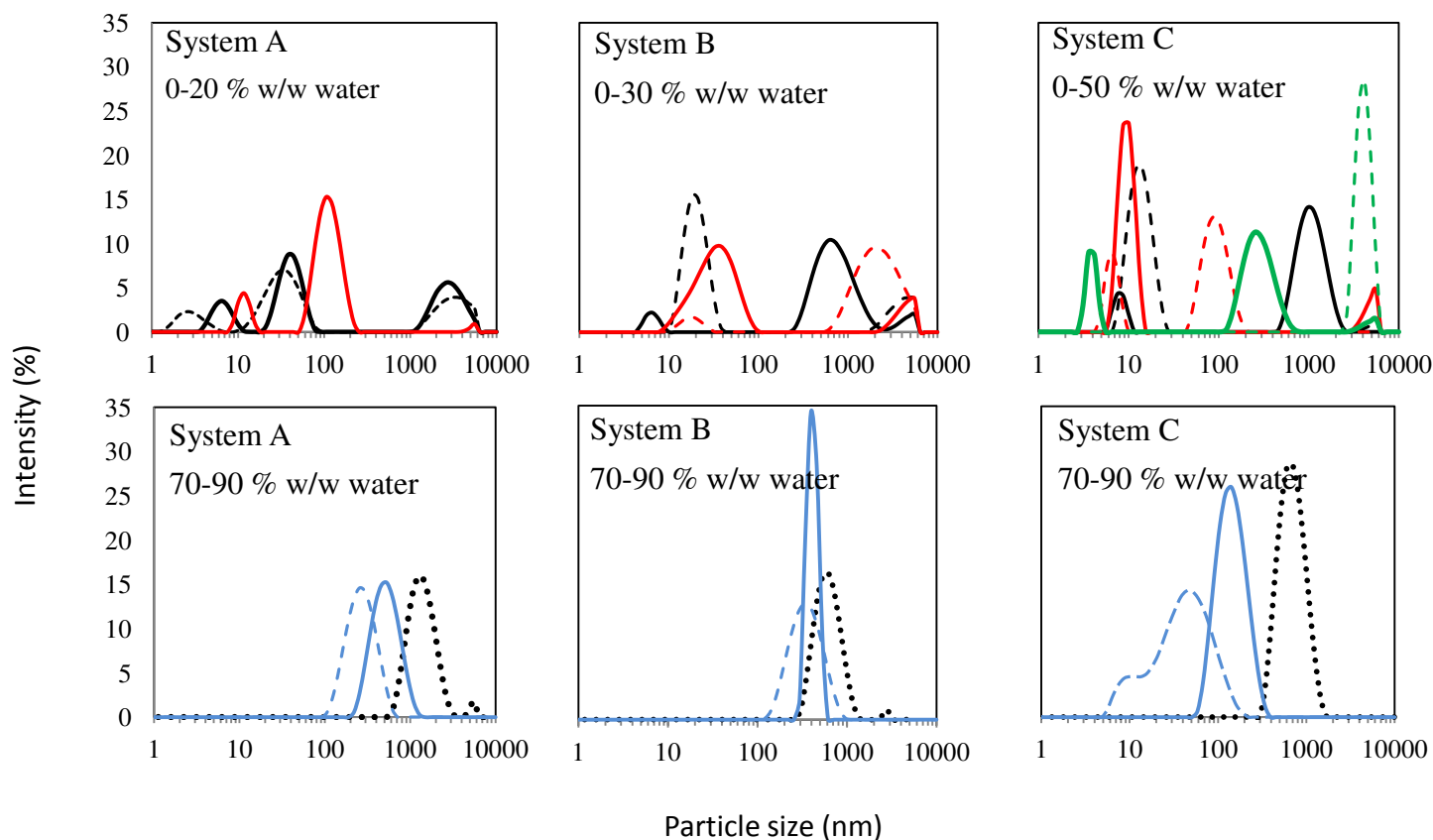


Fig. 5. Particle size distribution of systems A, B and C over dilution line 7. Water content (% w/w): 0 (—), 10 (---), 20 (—), 30 (---), 40 (—), 50 (---), 70 (••••), 80 (—), 90 (---).

3.3.4. RHEOLOGY

3.3.4.1. STEADY-STATE MEASUREMENTS

The flow curves of systems A, B and C over dilution line 7 are shown in Fig. 6. Most samples exhibited Newtonian behavior ($R^2 > 0.98$), including all of the ME systems and LC phases in the boundary with the ME region. Newtonian behaviour is expected in ME systems due to their reduced droplet size and low interaction between them, as reported in other works [24, 25, 35]. The transition from a Newtonian to a complex fluid occurred in systems with low ethanol contents and intermediate water contents. The rheological parameters of the systems that exhibit non-Newtonian behavior are presented in Table 3, and the viscosities of all systems are shown in Table 4.

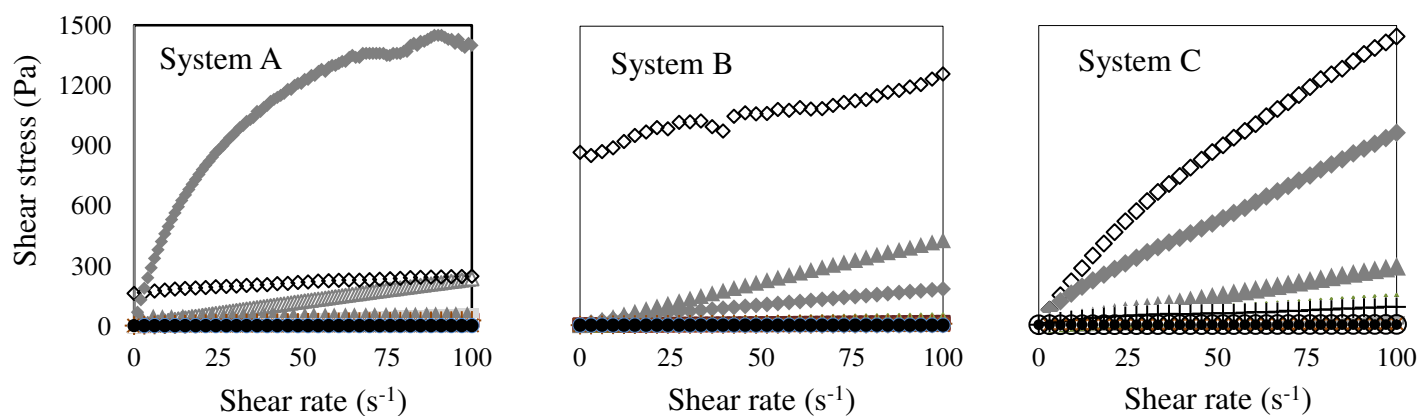


Fig. 6. Flow curves of systems A, B and C over dilution line 7. Water content (% w/w): 0 (□), 10 (■), 20 (Δ), 30 (▲), 40 (◇), 50 (◆), 60 (+), 70 (x), 80 (○), 90 (●).

Table 3. Rheological parameters of systems over dilution line 7 with a non-Newtonian behavior. σ_0 is the yield stress, k is the consistency index and n is the flow index.

System	Rheological parameters			
	σ_0 (Pa)	k (Pa.s ^{<i>n</i>})	n	R^2
A7030	41	0.80	1	0.93
A7040	130 ^A	18.29 ^A	0.40 ^A	0.99
A7050	-	230.42 ^D	0.40 ^A	0.97
A7060	-	0.58 ^B	0.83 ^C	0.99
B7040	1446 ^B	17.85 ^A	0.79 ^B	0.98
B7050	-	8.45 ^C	0.75 ^B	0.99
B7060	-	0.41 ^A	0.75 ^B	0.99

Different superscript letters indicate significant difference ($p > 0.05$) between the parameters of the samples with the same rheological behavior.

Table 4. Viscosity at 3 s^{-1} (η_3) of the systems A, B and C over the dilution line 7.

Systems	η_3 (mPa.s)		
	A	B	C
7000	268 ^{dC}	100 ^{eB}	61.0 ^{dA}
7010	531 ^{eC}	218 ^{fB}	101 ^{eA}
7020	$3.0 \cdot 10^3$ ^{fC}	454 ^{gB}	179 ^{fA}
7030	$1.7 \cdot 10^6$ ^{hC}	$7.7 \cdot 10^4$ ^{iB}	491 ^{gA}
7040	$1.8 \cdot 10^6$ ^{hB}	$1.5 \cdot 10^6$ ^{jB}	$2.2 \cdot 10^3$ ^{iA}
7050	$8.1 \cdot 10^4$ ^{gC}	$2.8 \cdot 10^3$ ^{hB}	$1.8 \cdot 10^3$ ^{hA}
7060	183 ^{dC}	66.2 ^{dA}	95.9 ^{eB}
7070	13.1 ^{cB}	9.6 ^{cA}	10.2 ^{cA}
7080	3.0 ^{bA}	3.2 ^{bA}	3.7 ^{bA}
7090	0.8 ^{aA}	1.6 ^{aB}	1.3 ^{aB}

Different superscript letters indicate significant difference ($p > 0.05$). Small letters compare differences within a column and capital letters compare differences between the systems A, B and C for the same water volume content.

The systems without ethanol and with 30% (w/w) water (A7030) showed Bingham plastic behaviour, whereas samples A7040 and B7040 (40%, w/w water and a lower ethanol content) exhibited HB behaviour. The presence of yield stress in these systems is a reflection of a three-dimensional network and gel-like structure (Fig. 4), as observed in the cubic phases of systems composed of monoolein, ethanol and water [36]. However, systems with 50 and 60% (w/w) water and lower ethanol contents (A7050, A7060, B7050 and B7060) exhibited a shear-thinning behaviour without the presence of yield stress. Fluid pseudoplasticity is attributed to the orientation of particles through the flow caused by shearing of the system, such as through the realignment of the disordered lamellar phase under shearing [8] or the breaking of the wormlike micellar network [20,37]. Shear-thinning decreased with the addition of ethanol in most of the non-Newtonian systems (Table 3). Furthermore, the addition of ethanol decreased the viscosity of systems that contained oil as the continuous phase (Table 4). The decrease in interfacial tension caused by the addition of ethanol led to the formation of microemulsions that exhibited Newtonian behaviour over a large range of water contents.

Evaluation of the samples over dilution line 7 revealed that the viscosity of all systems increased up to an intermediate water volume content and then decreased as the water content was further increased (Table 4), as observed in

other works [24,25,38,39,15]. The increased particle size (Fig. 5) enhanced the attractive interactions between the droplets, which promoted their aggregation and most likely promoted the formation of interconnected structures. Therefore, LC phases with high viscosities and non-Newtonian behaviours were formed at intermediate water contents (Fig. 6 and Table 3). A prevalent water content induced a sudden decrease in the viscosity, which is correlated to the disruption of the liquid-crystal phase into an O/W ME or O/W EM. When an excess of water is added to a lamellar liquid crystal, the increase in the hydration degree of the polyoxyethylene chains of the surfactant (Tween 80) increases the spontaneous curvature, and the flat structure is destabilised and disrupted into small droplets [2].

A comparison of the viscosity (η_3) and droplet size of the systems at lower and higher water contents reveals that O/W emulsions contained larger droplets (Fig. 5) and exhibited a lower viscosity (η_3) than W/O MEs (Table 4). The main reason for the reduced viscosity of the samples at high water contents is the lower viscosity of the continuous phase. The reduction in the viscosity of O/W emulsions could also be attributed to the decrease in the hydrophobic interactions of the surfactant tails and to the migration of surfactant molecules from the bulk to the interface of the oil droplets.

3.3.4.2. TRANSIENT-STATE MEASUREMENTS

The systems with intermediate water contents exhibited time-dependent behaviour. The thixotropy (Table 5) was qualitatively estimated by the area between the flow curves at the transient state (S1) (data not shown) and those at the steady state (S3) (Fig. 6). The systems A7020, A7030, A7040, A7050, B7030 and B7040 showed thixotropic behaviour, with steady-state viscosity values (S3) that were lower than the transient-state viscosity values (S1). In this case, shearing caused deformation and/or rupture of the aggregated particles, which decreased the resistance to flow and therefore reduced the apparent viscosity over time [40]. These systems exhibited higher viscosity values (Table 4) and a gel-like appearance (Fig. 4). The more systems are structured in the gel state, the more sensitive they become to shear, which could induce an alteration of the microstructure [41]. The systems with higher thixotropy (A7030,

A7040 and B7040) have large particle sizes (Fig. 5) and a reduced (or absence) ethanol content in common. These systems consequently exhibit low concentrations of polar components (ethanol and water), which allows the amphiphilic and nonpolar compounds to predominate (Table 5).

Table 5. Hysteresis between the curves without prior shearing and at steady state (thixotropy) and ratio of the concentration of more non-polar (surfactant + oil) and polar (water + ethanol) components.

Systems	Thixotropy (Pa.s ⁻¹)			(surfactant+oil)/(water+ethanol) ratio		
	A	B	C	A	B	C
7000	38.1	-158	-193	-	9	4
7010	148.7	-213	-508	9	4.26	2.57
7020	4888	301	-446	4	2.57	1.78
7030	626283	58987	98.1	2.3	1.7	1.27
7040	911659	324628	-3003	1.5	1.17	0.92
7050	109230	-29465	-18272	1.0	0.82	0.67
7060	-3083	-1378	-1473	0.67	0.56	0.47
7070	-29.6	-11.6	-7.1	0.43	0.37	0.32
7080	-6.0	-1.2	-3.1	0.25	0.22	0.19
7090	0.16	-0.03	0.98	0.11	0.10	0.07

In contrast, the systems A7060, B7050, B7060, C7040, C7050 and C7060 showed anti-thixotropic behaviour with viscosity values higher in the steady state (S3) than in the transient state (S1). These results indicate that a more organised arrangement was formed after the shearing process. Most of these samples were composed by high concentrations of polar (ethanol and water) components (Table 5) and exhibited viscosities lower than those exhibited by the thixotropic systems (Table 4). This finding is important with respect to the self-assembly of surfactant molecules because the formation of more-ordered structures can be favoured by shear and by a high content of nonpolar components.

Zipfel et al. [42] and Liu and Hao [8] have suggested that the anti-thixotropy behaviour is associated with the formation of multilamellar vesicles with a viscosity greater than that of the precursor lamellar phase. At higher shear rates, the size of multilamellar vesicles can increase or the vesicles can be transformed into unilamellar vesicles [43,44]. In the same manner, systems

with a high density of smaller vesicles have also been associated with anti-thixotropic behaviour of surfactant systems [8,42].

3.3.4.3. OSCILLATORY MEASUREMENTS

Oscillatory tests also allowed an evaluation of the structural transition of the colloidal mixture of MCT, water, ethanol and Tween 80. Fig. 7 shows the frequency dependency of complex (G^*) moduli of the systems A, B and C over the dilution line 7. As was the case with viscosity, the G^* values decreased upon addition of ethanol to the systems. In addition, the G^* values increased for water contents up to intermediate levels and decreased at higher water contents. Solè et al. [2] have obtained similar results in systems composed of water, oleic acid, C12C10 (polyoxyethylene 10 lauryl ether) and hexadecane. The transition from a lamellar to a cubic phase was described by a low plateau modulus (G^*) at low water contents, which increased upon the addition of water and achieved a constant high value of G^* at a water content of 50%. The viscoelastic properties (complex viscosity and elastic moduli) have been reported to increase with increasing oil content in gel systems composed of water, Tween 80 and oil (squalane), which was also associated with structural changes; the swelling of the micelles or the shape transition of the micelles from non-spherical to spherical [45]. In our study, the increase of viscoelastic properties can be associated with W/O ME to LC phase transition.

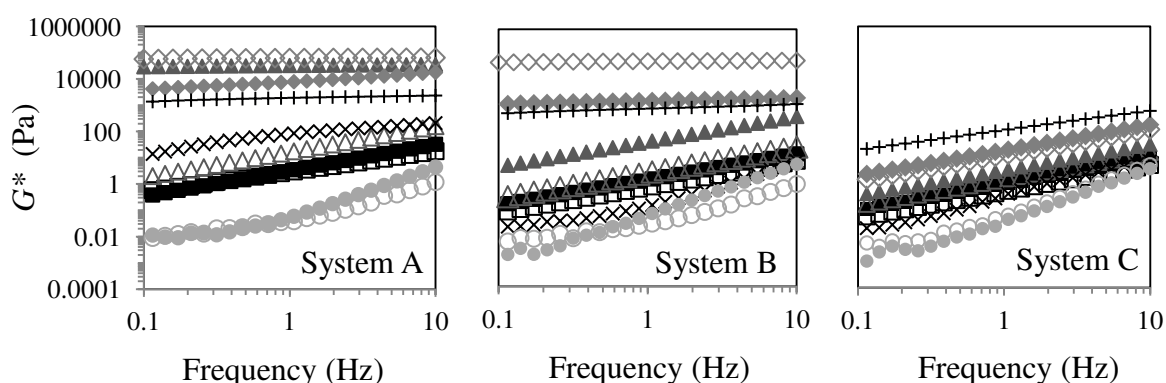


Fig. 7. Complex modulus (G^*) of the systems A, B and C. Water content (% w/w): 0 (□), 10 (■), 20 (Δ), 30 (▲), 40 (◇), 50 (◆), 60 (+), 70 (x), 80 (○), 90 (●).

Fig. 8 shows the frequency dependency of elastic (G') and viscous (G'') moduli of the systems according to their viscoelastic behaviours and water contents. We observed that all the systems exhibited liquid-like behaviour ($G' < G''$) at low water volume contents (Fig. 8) of 0–20%, 0–30% and 0–60% (w/w) water for systems A, B and C, respectively. Systems A and B showed gel-like behaviours ($G' > G''$) at intermediate water volume contents of 30–60% and 40–60%, respectively. Because samples A7030, A7040 and B7040 exhibited gel formation (Fig. 4), yield stress (Table 3) and very high elastic properties [46], with G' values between 25 and 60 kPa (Fig. 9), we estimate that these systems are cubic phases.

At higher water contents, all the systems became less structured and exhibited similar low values of G' and G'' (Fig. 8). System A with a 70% water volume exhibited a concentrated solution behavior (G' and G'' crossover at intermediate frequency). This viscoelastic behaviour has been associated with hexagonal structures [46–48] and wormlike micelles [22,37].

Analysis of the behaviour of G' and particle size over dilution line 7 (Fig. 9) revealed a clear phase transition. Systems A and B with lower ethanol contents showed the highest G' and viscosity values at 40% (w/w) water and formed the most structured phase. However, the addition of ethanol (system C) shifted the phase transition to a higher water content, as evident from the highest value of G' and the particle size at 60% (w/w) water. The highest viscosity of system C, however, was observed at a water content of 40% (w/w). Such a discrepancy may be associated with the shear-dependent rheological behaviour of these LC phases.

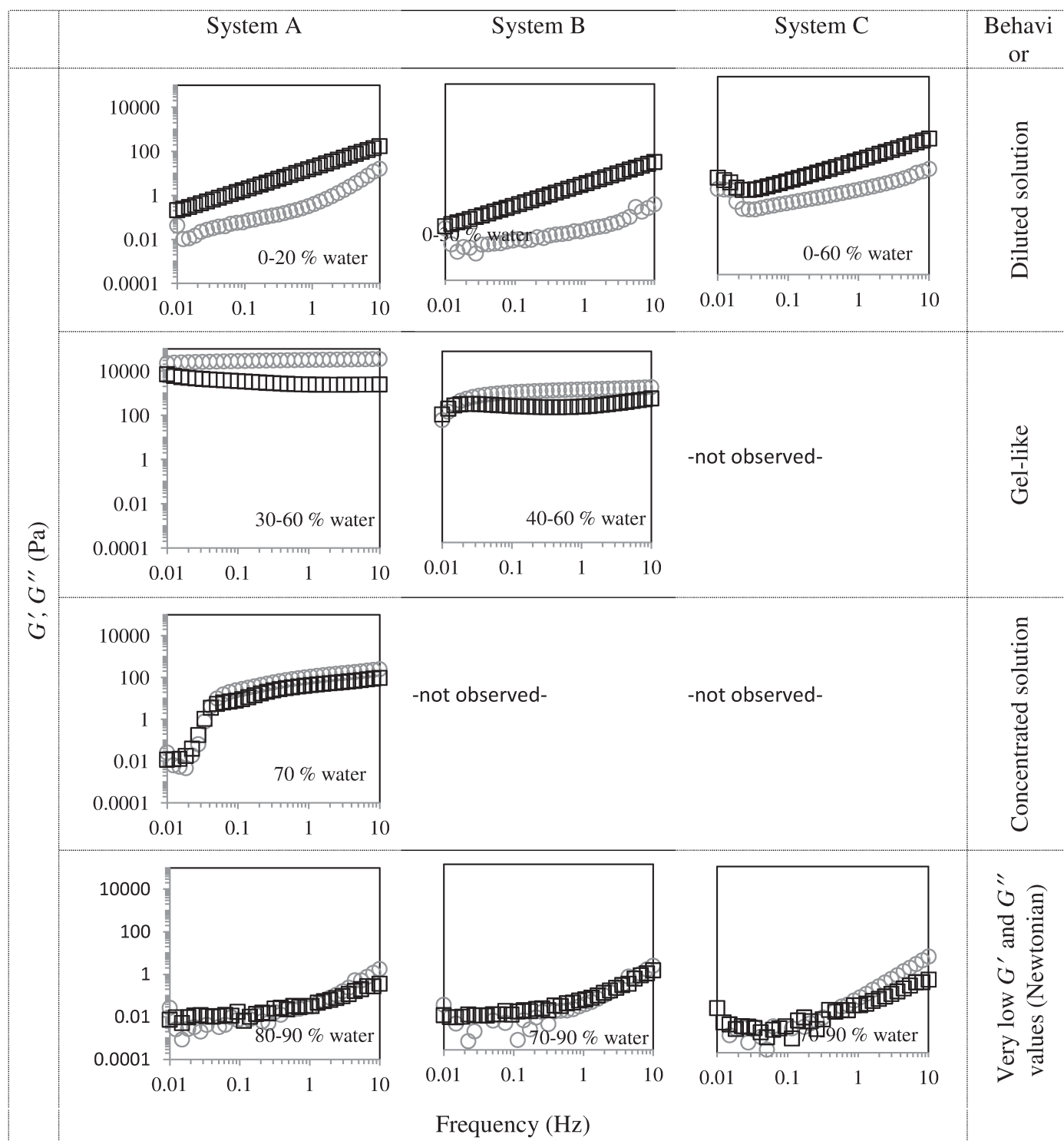


Fig. 8. Representative mechanical spectrum of systems A, B, and C. Viscoelastic moduli: loss modulus G'' (\square) and storage modulus G' (\circ).

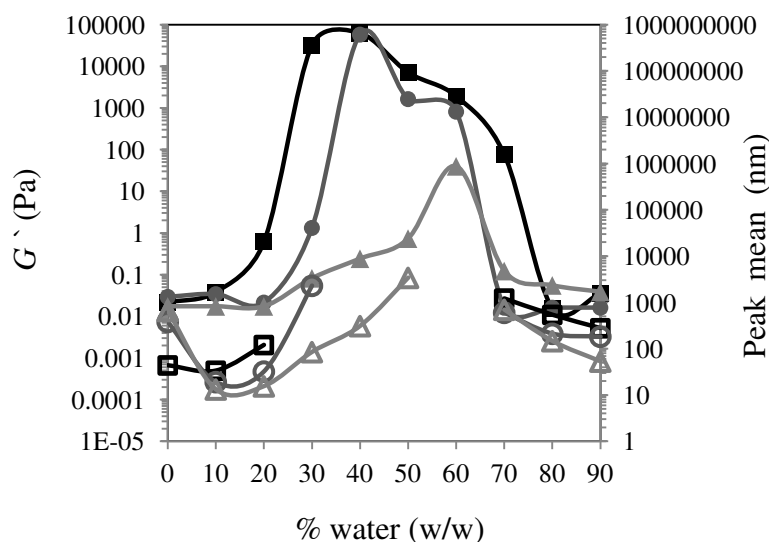


Fig. 9. Elastic modulus (G') (filled symbols) and main peak mean from intensity particle size distribution (open symbols) over the dilution line 7 of systems A (■, □), B (●, ○) and C (▲, △).

3.4. CONCLUSIONS

W/O and O/W MEs were obtained using water, MCT, Tween 80 and ethanol at extreme concentrations of oil and water, respectively. The addition of ethanol decreased the surfactant content necessary to produce W/O MEs and enabled the production of O/W MEs. Moreover, the presence of ethanol significantly affected particle size and rheology, producing less-structured systems with less shear thinning.

The structure transition from W/O ME to O/W ME was successfully analysed by conductivity, polarised light microscopy, particle size technique, but mainly and, in particular, rheology. Systems with distinct textures were produced depending on the combination of the ingredients used, which suggests a range of practical applications. MEs exhibited lower viscosities and less-structured systems, whereas LC phases exhibited higher viscosities and complex rheology under small and high deformations. In addition, rheological measurements identified structural changes with shear time. Systems rich in polar components (water and ethanol) exhibited anti-thixotropic behaviour and produced more organized systems under shear. However, systems with

prevailing nonpolar and amphiphilic components tended towards thixotropic behaviour because their gel-like structure was susceptible to shear.

Therefore, rheology was an effective technique for determining the phase transitions of the systems and showed the effects of ethanol and shear on the structures that could not be identified by other classical techniques. Moreover, the study of the rheological properties may significantly impact the determination of the most appropriate application for the systems.

3.5. ACKNOWLEDGEMENTS

The authors wish to acknowledge FAPESP (EMU 09/541371), CNPq (process 473412/20098, scholarship 143050/20095) and CAPES for their financial support.

3.6. REFERENCES

- [1] B.P. Binks, P.D.I. Fletcher, L. Tian, Influence of nanoparticle addition to Winsor surfactant microemulsion systems, *Colloids Surf., A* 363 (2010) 8–15.
- [2] I. Solè, A. Maestro, C. González, C. Solan, J.M. Gutiérrez, Optimization of nanoemulsion preparation by low-energy methods in an ionic surfactant system, *Langmuir* 22 (2006) 8326–8332.
- [3] L. Wolf, H. Hoffmann, K. Watanabe, T. Okamoto, Microemulsions from silicone oil with an anionic/nonionic surfactant mixture, *Phys. Chem. Chem. Phys.* 13 (2011) 3248–3256.
- [4] A. Spornath, A. Aserin, Microemulsions as carriers for drugs and nutraceutical, *Adv. Colloid Interface Sci.* 128 (2006) 47–64.
- [5] M.M. Alam, Y. Sugiyama, K. Watanabe, K. Aramaki, Phase behavior and rheology of oil swollen micellar cubic phase and gel emulsions in nonionic surfactant systems, *J. Colloid Interface Sci.* 341 (2010) 267–272.
- [6] M. Gradzielski, Recent developments in the characterization of microemulsions, *Curr. Opin. Colloid Interface Sci.* 13 (2008) 263–269.
- [7] S.P. Moulik, B.K. Pal, Structure, dynamics and transport properties of microemulsions, *Adv. Colloid. Interface* 78 (1998) 8–15.

- [8] C. Liu, J. Hao, Shear-induced structural transition and recovery in the salt-free cationic surfactant systems containing deoxycholic acid, *J. Phys. Chem. B* 115 (2011) 980–989.
- [9] M.G. Berni, C.J. Lawrence, D. Machin, A review of the rheology of the lamellar phase in surfactant systems, *Adv. Colloid Interface Sci.* 98 (2002) 217–243.
- [10] S. Furlanetto, M. Cirri, G. Piepel, N. Mennini, P. Mura, Mixture experiment methods in the development and optimization of microemulsion formulations, *J. Pharm. Biomed. Anal.* 55 (2011) 610–617.
- [11] M. Fanun, Properties of microemulsions with mixed nonionic surfactants and citrus oil, *Colloids Surf., A* 369 (2010) 246–252.
- [12] C. Lin, H. Lin, H. Chen, M. Yu, M. Lee, Stability and characterization of phospholipid-based curcumin-encapsulated microemulsions, *Food Chem.* 116 (2009) 923–928.
- [13] A. Yagmur, A. Aserin, N. Garti, Phase behavior of microemulsions based on food-grade nonionic surfactants: effect of polyols and short-chain alcohols, *Colloids Surf., A* 209 (2002) 71–81.
- [14] J. Feng, Z. Wang, J. Zhang, Z. Wang, F. Liu, Study on food-grade vitamin E microemulsions based on nonionic emulsifiers, *Colloids Surf., A* 339 (2009) 1–6.
- [15] N. Patel, U. Schmid, M.J. Lawrence, Phospholipid-based microemulsions suitable for use in foods, *J. Agric. Food Chem.* 54 (2006) 7817–7824.
- [16] H. Zhang, Y. Cui, S. Zhu, F. Feng, X. Zheng, Characterization and antimicrobial activity of a pharmaceutical microemulsion, *Int. J. Pharm.* 395 (2010) 154–160.
- [17] M. Lee, M. Yu, L. Kao, C. Lin, Enhancement of the encapsulation and transmembrane permeation of isoflavone-containing red clover extracts in phospholipid-based microemulsions using different extraction process, *J. Agric. Food Chem.* 57 (2009) 9489–9495.
- [18] Y.H. Cho, S. Kim, E.K. Bae, C.K. Mok, J. Park, Formulation of a cosurfactant-free o/w microemulsions using nonionic surfactant mixture, *J. Food Sci.* 73 (2008) 115–121.
- [19] M.E. Leser, L. Sagalowicz, M. Michel, H.J. Watzke, Self-assembly of polar food lipids, *Adv. Colloid Interface Sci.* 123–126 (2006) 125–136.

- [20] P. Guo, R. Guo, Ionic liquid induced transition from wormlike to rod or spherical micelles in mixed nonionic surfactant systems, *J. Chem. Eng. Data* 55 (2010) 3590–3597.
- [21] S.K. Metha, G. Kaur, K.K. Bhasin, Analysis of Tween based microemulsion in the presence of TB drug rifampicin, *Colloids Surf. B* 60 (2007) 95–104.
- [22] S. Peltola, P. Saarinen Savolainen, J. Kiesvaara, T.M. Suhonen, A. Urtili, Microemulsions for topical delivery of estradiol, *Int. J. Pharm.* 254 (2003) 99–107.
- [23] J. Flanagan, H. Singh, Microemulsions: a potential delivery system for bioactives, *Crit. Rev. Food Sci. Nutr.* 46 (2006) 221–237.
- [24] N. Garti, A. Yaghmur, M.E. Leser, V. Clement, H.J. Watzke, Improved oil solubilization in oil/water food grade microemulsions in the presence of polyols and ethanol, *J. Agric. Food Chem.* 49 (2001) 2552–2562.
- [25] A. Yaghmur, A. Aserin, B. Antalek, N. Garti, Microstructure considerations of new five-component Winsor IV food-grade microemulsions studied by pulsed gradient spin-echo NMR, conductivity, and viscosity, *Langmuir* 19 (2003) 1063–1068.
- [26] J.F. Steffe, *Rheological Methods in Food Process Engineering*, Freeman Press, Michigan, 1996.
- [27] S.K. Mehta, K. Bala, Tween-based microemulsions: a percolation view, *Fluid Phase Equilib.* 172 (2000) 197–209.
- [28] M. Fanun, A study of the properties of mixed nonionic surfactants microemulsions by NMR, SAXS, viscosity and conductivity, *J. Mol. Liq.* 142 (2007) 103–110.
- [29] L. Djordjevic, M. Primorac, M. Stupar, D. Krajisnik, Characterization of caprylocaproyl macroglycerides based microemulsion drug delivery vehicles for an amphiphilic drug, *Int. J. Pharm.* 271 (2004) 11–19.
- [30] A.M. Seddon, G. Lotze, T.S. Plivelic, A.M. Squires, A highly oriented cubic phase formed by lipids under shear, *J. Am. Chem. Soc.* 133 (2011) 13860–13863.
- [31] C. John, A.K. Rakshit, Effects of mixed alkanols as cosurfactants on single phase microemulsion properties, *Colloids Surf., A* 95 (1995) 201–210.

- [32] C.R.B. Mendonça, Y.P. Silva, W.J. Böckel, E.F. Simó-Alfonso, G. Ramis Ramos, C.M.S. Piatnicki, C.I.D. Bica, Role of the cosurfactant nature in soybean w/o microemulsions, *J. Colloid Interface Sci.* 337 (2009) 579–585.
- [33] M.A. Thevenin, J.L. Grossiord, M.C. Poelman, Sucrose esters/cosurfactant microemulsion systems for transdermal delivery: assessment of bicontinuous structures, *Int. J. Pharm.* 137 (1996) 177–186.
- [34] M. Trotta, R. Cavalli, E. Ugazio, M.R. Gasco, Phase behaviour of microemulsion systems containing lecithin and lysolecithin as surfactants, *Int. J. Pharm.* 143 (1996) 67–73.
- [35] M.A. Polizelli, V.R.N. Telis, L.Q. Amaral, E. Feitosa, Formation and characterization of soy bean oil/surfactant/water microemulsions, *Colloids Surf., A* 281 (2006) 230–236.
- [36] R. Efrat, A. Aserin, E. Kesselman, D. Danino, E. Wachtel, N. Garti, Liquid micellar discontinuous cubic mesophase from ternary monoolein/ethanol/water mixtures, *Colloids Surf., A* 299 (2007) 133–145.
- [37] H. Yue, P. Guo, R. Guo, Phase behavior and structure properties of sodium dodecyl sulfate (SDS)/Brij 30/Water system, *J. Chem. Eng. Data* 54 (2009) 2923–2929.
- [38] R. DeutchKlevzon, A. Aserin, N. Garti, Synergistic cosolubilization of omega3 fatty acid esters and coQ10 in dilutable microemulsions, *Chem. Phys. Lipids* 164 (2011) 654–663.
- [39] M. Fanun, Properties of microemulsions based on mixed nonionic surfactants and mixed oils, *J. Mol. Liq.* 150 (2009) 25–32.
- [40] D.J. McClements, *Food Emulsions: Principles, Practice, and Techniques*, CRC Press, Washington, 2005.
- [41] V.M. Sadtler, M. Guely, P. Marchal, L. Choplin, Shear-induced phase transitions in sucrose ester surfactant, *J. Colloid Interface Sci.* 270 (2004) 270–275.
- [42] J. Zipfel, J. Berghausen, P. Lindner, W. Richering, Influence of shear on lyotropic lamellar phases with different membrane defects, *J. Phys. Chem. B* 103 (1999) 2841–2849.
- [43] J.I. Escalante, M. Gradzielski, H. Hoffmann, K. Mortensen, Shear-induced Transition of originally undisturbed lamellar phase to vesicle phase, *J. Phys. Chem. B* 16 (2000) 8653–8663.

- [44] S. Muller, C. Borschig, W. Gronski, C. Schimidt, Shear-induced states of orientation of the lamellar phase of C12E4/Water, *Langmuir* 15 (1999) 7558–7564.
- [45] M.M. Alam, K. Ushiyama, K. Aramaki, Phase behavior, formation, and rheology of cubic phase and related gel emulsion in Tween 80/water/oil systems, *J. Oleo Sci.* 58 (2009) 361–367.
- [46] G. Montalvo, M. Valiente, E. Rodenas, Rheological properties of the L phase and the hexagonal, lamellar, and cubic liquid crystal of the CTAB/benzyl alcohol/ water system, *Langmuir* 12 (1996) 5202–5208.
- [47] M. Zheng, Z. Wang, F. Liu, J. Wu, Study on the microstructure and rheological property of fish oil lyotropic liquid crystal, *Colloids Surf., A* 385 (2011) 47–54.
- [48] Z. Németh, L. Halász, J. Pálinkás, A. Bóta, T. Horányi, Rheological behavior of a lamellar liquid crystalline surfactant-water system, *Colloids Surf., A* 145 (1998) 107–119.

- CAPÍTULO 4 -
EFEITO DA CONCENTRAÇÃO DE ETANOL E DA
TEMPERATURA EM SISTEMAS COMPOSTOS POR
TWEEN 80, ÁGUA E TRIACILGLICEROL DE CADEIA
MÉDIA

SIMULTANEOUS EFFECT OF COSURFACTANT
CONCENTRATION AND TEMPERATURE ON THE
STRUCTURE OF BIOCOMPATIBLE MICROEMULSIONS
AND LIQUID CRYSTALLINE PHASES

Rejane de Castro Santana, Luiz Henrique Fasolin, Rosiane Lopes da
Cunha. A ser submetido na Colloids and Surfaces a.

**SIMULTANEOUS EFFECT OF COSURFACTANT CONCENTRATION AND
TEMPERATURE ON THE STRUCTURE OF BIOCOMPATIBLE
MICROEMULSIONS AND LIQUID CRYSTALLINE PHASES**

Rejane de Castro Santana, Luiz Henrique Fasolin, Rosiane Lopes da Cunha*

Department of Food Engineering, Faculty of Food Engineering, University of
Campinas – UNICAMP, 13083862, Campinas, SP, Brazil

* Corresponding author. Tel.: +55 19 3521 40407, fax: +55 19 3521 4027.

Email address: rosiane@fea.unicamp.br (R.L. da Cunha).

ABSTRACT

Microemulsions and liquid crystalline phases have gained increasing interest due to their differentiated structure and rheology. For a better understanding of the phase behavior of these systems, it is essential to evaluate the effect of composition, as water and co-surfactant concentration, and different temperatures, simulating industrial processes and biological conditions. In this paper, we evaluated the structure and thermal behavior of systems composed by water, medium chain triglycerides (MCTs), polyoxyethylene sorbitan monooleate (Tween 80) and ethanol by small-angle scattering (SAXS), calorimetric and thermal rheological measurements. Ethanol content extended reverse micelles region to higher water content and produced systems with smaller repeat spacing (d). Systems containing intermediary water content and low or without ethanol showed a temperature transition around 50 °C. Hexagonal and cubic phases with a gel-like behavior were produced at 25 °C, while disordered systems with lower repeat spacing (d) and liquid behavior were observed at higher temperatures. These results are crucial for understanding the systems structures and enable the design of nanostructures with potential applications in food, pharmaceutical and cosmetic industries.

Keywords: microemulsions, liquid crystals, phase transition, SAXS, rheology

4.1. INTRODUCTION

Microemulsions (ME) and liquid-crystals (LC), such as lamellar, hexagonal, or cubic structures, can be produced by the surfactant molecules self-assemble (Binks, Fletcher and Tian, 2010) using low-energy methods, showing ease and low cost of preparation. In addition, these systems have oil and water domains with well-defined interfaces from surfactants, which leads to the ability to solubilise a large quantity of both polar and non-polar additives (Wolf, Hoffmann, Watanabe and Okamoto, 2011), including food ingredients, nutraceuticals, flavors, cosmetic components, and drugs (Spernath and Aserin, 2006).

Microemulsions are optically isotropic, translucent and thermodynamically stable systems with low viscosity. They are formed by swollen micelles (L_1 and L_2) with 1–200 nm stabilised by surfactants, usually in combination with a cosurfactant (Binks and Fletcher, 2010). In contrast, liquid-crystal phases exhibit a more complex structure and intermediary properties between ordered solids and disordered liquids. Surfactant molecules form bilayers that are regularly stacked in the lamellar phase (L_α), whereas cylinders are organised onto a triangular lattice in the hexagonal phase (H_1 and H_2) (Binks and Fletcher, 2010). More complex well-ordered geometry cubic phases can also be formed (Alam, Sugiyama, Watanabe and Aramaki, 2010), including gyroid ($Im3d$), double diamond ($Pn3m$) and primitive ($Im3m$) types.

The structure of ME and LC phases depends on the system's composition and external factors, as temperature (Liu and Hao, 2011; Berni, Lawrence and Machin, 2002). Medium-chain triglycerides (MCT) have been widely used to form biocompatible microemulsions (Patel, Schmid and Lawrence, 2006; Garti, Yaghmur, Leser, Clement and Watzle, 2001) since they are more stable than the cyclic oils. Moreover, solubilisation of MCT is easier than long-chain triglycerides (vegetable oils) because they show a more nonpolar structure with lower molar mass (Flanagan and Singh, 2006; Yaghmur, Aserin, Antalek and Garti, 2003). Medium-chain triglycerides have rapid digestion, being interesting to food applications (Matsaridou, Barmplexis, Salis and Nikolakakis, 2012). Short-chain alcohols are the most commonly used cosurfactants in microemulsion

formulations, but ethanol is the most suitable for use in drugs and food products, such as alcoholic beverages (Flanagan and Singh, 2006). Non-ionic surfactants are less toxic than ionic, less affected by pH and ionic strength and show improved dissolution and adsorption of drugs (Matsaridou, Barmpapalexis, Salis, Nikolakakis and 2012). Polyoxyethylene sorbitan monooleate (Tween 80) are polysorbates derived from PEG-ylated sorbitan (hydrophilic group) esterified with fatty acids (hydrophobic group) with a total of 20 ethylene oxide per molecule. They are non-ionic, soluble in water, but insoluble in oil (Feng, Wang, Zhang, Wang and Liu, 2009; Patel, Schmid and Lawrence, 2006).

de Castro Santana, Fasolin and Cunha (2012) have reported the pseudo-ternary diagram, particle size distribution, and rheology of systems composed by MCT, ethanol, water and Tween 80 at 25°C. However, the structure parameters were not determined, as well as the thermal and rheological behavior at different temperatures. It is particularly important to understand the systems structures under varied conditions of temperature, which could be further used to modulate and design systems composition and process conditions to specific industrial and biological applications (Kulkarni, 2011).

In this way, this study aimed the evaluation of the effect of ethanol concentration and water content on biocompatible systems composed by water, ethanol, MCT and Tween 80 by small-angle scattering (SAXS) and calorimetric analysis. In addition, the effect of temperature (25 °C to 70°C) on phase transitions was evaluated by SAXS and oscillatory rheology.

4.2. MATERIAL AND METHODS

4.2.1. MATERIAL

Delios V, a medium-chain triglyceride (MCT) rich in caprylic and capric glycerides, was kindly donated by Cognis (Germany). Tween 80 (polyoxyethylene sorbitan monooleate) and 99.5% ethanol were purchased from Synth (Brazil).

4.2.2. METHODS

4.2.2.1. Spontaneous emulsification method

The systems were produced by spontaneous emulsification method at 25 °C. Different MCT:ethanol ratios (1:0, 2:1, and 1:2, w/w) were used. Firstly, an initial mixture of Tween 80 and MCT + ethanol (at 70:30 ratio) was prepared under continuous magnetic stirring. Deionised water was then titrated under constant stirring in increments of 10% (w/w). Each formulation was kept stirring for 30 min, and the samples were then stored at 25 °C for at least 15 days before they were examined for characterization measurements. The samples were named according to the MCT:ethanol ratio used: A (1:0), B(2:1) or C (1:2). In addition, the samples were designated according to the water content. For example, an initial sample that contained 70% (w/w) Tween 80, 20% (w/w) MCT and 10% (w/w) ethanol (MCT:ethanol = 2:1) diluted with 50% (w/w) water was named as B50.

4.2.2.2. Small-angle scattering (SAXS)

Structure of liquid crystalline phases and microemulsions was evaluated by SAXS. The measurements were performed at (25, 50 and 70) °C using the beam line of the National Synchrotron Light Laboratory (LNLS, Campinas, Brazil), with X-ray source of wavelength $\lambda = 1.54 \text{ \AA}$. A position-sensitive X-ray detector and a multichannel analyzer were used to record the SAXS intensity, $I(q)$, as a function of modulus of scattering vector $q = (4\pi/\lambda) \sin(\theta/2)$, θ being the scattering angle. Each SAXS pattern corresponds to a data collection time of 100 s.

Structure type was determined according to scattering peaks position. For lamellar phases (L_α) the distance in relation to the first peak is 1:2:3:4, while for normal or reverse hexagonal phases (H_1 or H_2) the distance is given by 1: $\sqrt{3}$: $\sqrt{4}$: $\sqrt{7}$. Gyroid bicontinuous cubic ($Ia3d$) is identified by the peak positions at Bragg values $\sqrt{6}$: $\sqrt{8}$: $\sqrt{14}$: $\sqrt{16}$: $\sqrt{20}$: $\sqrt{22}$: $\sqrt{24}$, while bicontinuous cubic phases double diamond ($Pn3m$) presented distance relation to the first peak as 1: $\sqrt{2}$: $\sqrt{3}$: $\sqrt{4}$: $\sqrt{6}$: $\sqrt{8}$: $\sqrt{9}$: $\sqrt{10}$, and primitive bicontinuous cubic phase ($Im3m$) shows peak positions at 1: $\sqrt{2}$: $\sqrt{4}$: $\sqrt{6}$: $\sqrt{8}$: $\sqrt{10}$: $\sqrt{12}$.

Structural parameters were calculated from the peaks of SAXS spectra. The correlation distance (d) between the scattering centers of the structures was determined as $d=2\pi/q$. Here d is the center-to-center distance between neighboring scattering centers and q is the position of the correlation peak.

The distance between the centers of two hexagonal structures, known as lattice parameter (a), was calculated by Equation 1. The radius of the hydrophobic core of cylindrical aggregate (r_0) was calculated by Equation 2.

$$a = \frac{4\pi}{q_{100}\sqrt{3}} \quad (1)$$

$$r_0 = \sqrt{\frac{2\phi_{hc}}{\sqrt{3}\pi}} d \quad (2)$$

where q_{100} is the first peak position and ϕ_{hc} is the volume fraction of the hydrocarbon portion.

For cubic phases the lattice parameter (a) was obtained by plotting $(q/2\pi)^2$ as a function of the Miller index according to the Equation 3:

$$\left(\frac{q_{hkl}}{2\pi}\right)^2 = \left(\frac{1}{a}\right)^2 (h^2 + k^2 + l^2) \quad (3)$$

where q_{hkl} is the scattering vector of $[hkl]$ reflection and h, k, l are Miller indexes.

4.2.2.3. Differential scanning calorimeter (DSC)

Calorimetric measurements were performed using a DSC equipment (TA Instruments, Model 2920, New Castle, USA). The systems were weighted (5 to 10 μ g) in hermetic aluminium capsules. The pans were closed and cooled between 25°C and -60 °C and heated between -60 °C and 25 °C under an inert atmosphere (100 mL/min of N₂) at 2° C/min. The reference used was an empty aluminum capsule. The data was analyzed using the Universal Software Analysis V1.7F (TA Instruments). Freezing and melting (onset) temperature peaks were associated with thermal transitions and the water state (free or bounded). The enthalpies were evaluated by integrating the area of each DSC peak.

4.2.2.4. Rheological measurements

Oscillatory rheology was performed on a Physica MCR301 rheometer (Anton Paar, Austria) using a stainless steel cone-plate geometry (5.0 cm, 2° angle, truncation 208 μm). The measurements were performed within the linear viscoelastic region. Three sweeps (Heating 1 – Cooling 1 – Heating 2) were carried out between 25 °C and 75 °C at 2 °C/min, at a constant frequency (0.1 Hz) and deformation (1 %). Complex viscosity (η^*) vs temperature curves were evaluated and the temperatures of rheological transitions (or gel point) was determined by the maximum value in the (absolute) slope of $\log(\eta^*)$. Changes in the slope of η^* were maximized from the derivation of the data using the Savitzky and Golay filter (Savitzky and Golay, 1964).

4.3. RESULTS AND DISCUSSION

4.3.1. SAXS

SAXS pattern of systems changed with the water and co-surfactant content (Figure 1). The scattering vector (or the first peak position) decreased with water content up to intermediary concentration (40-50 % w/w) and increased again at higher water content. On the other hand, systems with higher ethanol content showed higher scattering vector and a reduced number of peaks which were less defined.

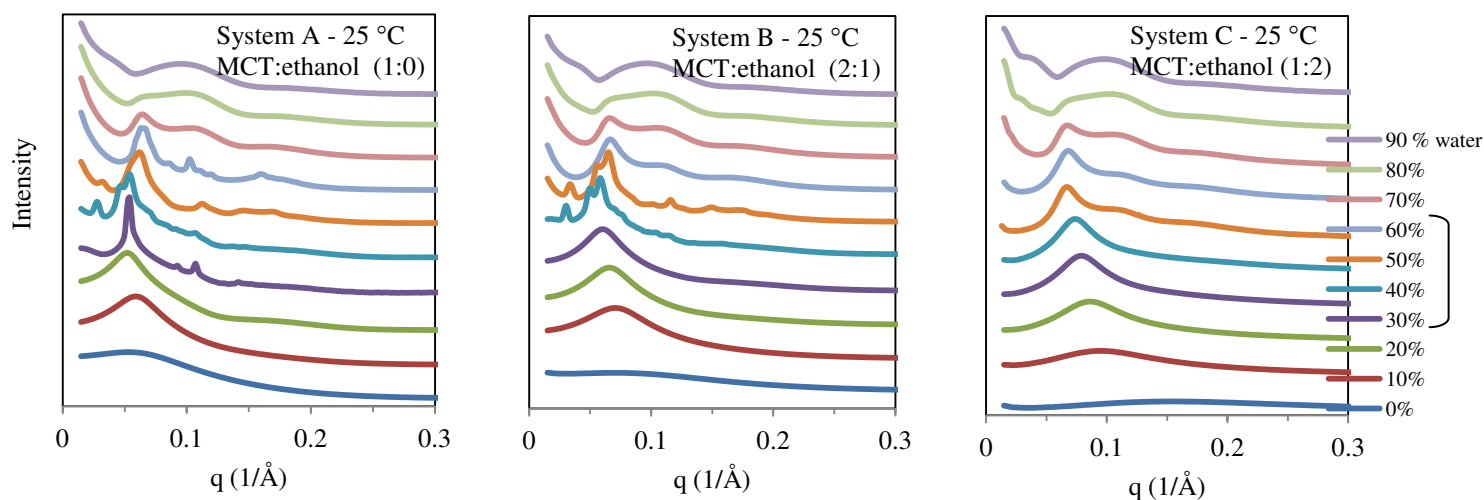


Figure 1. SAXS patterns of systems with different MCT:ethanol ratios, A (1:0), B (2:1), and C (1:2), at 25 °C.

Different types of structures were observed depending on the systems composition (Table 1). Reverse micelle structures (L_2) were produced at low water content, while liquid crystalline phases were observed at intermediary and high water contents. Hexagonal structure (H_1 and H_2) was the liquid crystalline phases (LC) most commonly found, but cubic structures, including $Ia3d$, $Im3m$ and $Pn3m$, were also observed in the systems with water content between 40 and 80 % (w/w). However, the structure transition from reverse micelle to liquid crystalline phases was hard to identify in some systems with low water content (as B30), since they showed a very small secondary peak that probably means an intermediary structure between an elongated micelle and a LC phase. In the same way, liquid crystalline (hexagonal and cubic phases) can coexist in some conditions, since they showed characteristic peaks of both phases or only a limited number of characteristic peaks, being not possible to identify a specific phase. Probably a partial disorder structure was produced.

Table. 1. Structural parameters obtained from SAXS measurements. d : structure repetition distance, a : lattice parameter of H_1 , H_2 , $la3d$, $Pn3m$ and, $Im3m$, and r_{hc} : radius of cylindrical micelle of H_1 or H_2 .

Systems (MCT:ethanol)	Parameters (Å)	% (w/w) water									
		0	10	20	30	40	50	60	70	80	90
A (1:0)	Type	L_2	L_2	L_2	H_2	H_1	$Pn3m$	$Pn3m$	H_1	$Pn3m / Im3m$	H_1
	d	117.5	106.3	120.5	117.7	224.2	197.9	98.2	98.2	87.8	65.2
	a	-	-	-	135.9	258.9	101.5	98.1	113.3	87.8	75.3
	r_{hc}	-	-	-	53.0	93.6	-	-	29.1	-	11.2
B (2:1)	Type	L_2	L_2	L_2	H_2 / L_2	$H_1 / la3d$	$H_1 / la3d$	H_1	H_1	$Im3m / Pn3m$	H_1
	d	88.0	88.0	96.2	102.6	208.1	187.7	94.6	95.6	90.9	65.4
	a	-	-	-	118.5	240.3	216.7	109.2	110.4	90.9	75.6
	r_{hc}	-	-	-	40.1	75.5	62.3	28.1	24.7	19.2	9.8
C (1:2)	Type	L_2	L_2	L_2	L_2	L_2	H_1	H_1	H_1	$Im3m / Pn3m$	H_1
	d	40.5	66.3	73.4	80.3	85.2	94.1	92.5	93.1	84.5	64.2
	a	-	-	-	-	-	108.6	106.8	107.5	84.4	74.2
	r_{hc}	-	-	-	-	-	25.9	22.8	19.9	14.8	8.0

Systems structure: reverse micelles (L_2), reverse hexagonal (H_2), lamellar (L_α), normal hexagonal (H_1), gyroid bicontinuous cubic ($la3d$), double diamond bicontinuous cubic ($Pn3m$), and primitive bicontinuous cubic ($Im3m$).

The structure type observed in each water concentration depended on the ethanol concentration. Ethanol content increased L_2 phase region, extending this structure type up to 40 % (w/w) of water in system C. However, this co-surfactant did not favor L_1 phases in systems composed by MCT, Tween 80 and water, as it was not observed in any system evaluated. In addition, cubic phases (Ia3d, Im3m, Pn3m) were less observed in systems with higher ethanol content. Alcohols interact at the interface between oil and water causing the swelling of aqueous channels and the relaxation of surfactant layers, which leads to a disordering of the cubic phase and to the formation of phases with flatter interfaces (Seddon, Lotze, Plivelic and Squires, 2011). As a result, ethanol can avoid the formation of rigid structures, including gels, liquid crystals and precipitates (John and Rakshit, 1995). Structural parameters (d , a , and r_{hc}) were lower in the systems with higher ethanol content at extreme conditions of water content (low and high) (Table 1). The displacement of SAXS peaks to lower q values as the water concentration rose to intermediary water content (40 - 50 % w/w) led to an increase in d , a , and r_{hc} values, which means higher distances between the repeated structures.

SAXS patterns of systems A, B and C with intermediary water content (30-60 % w/w) at (50 and 70) °C are shown in Figure 2. The systems observed at high temperatures showed a disordered structure (with no specific peaks correlation of a known structure), thus only d values were calculated (Figure 3). This behavior was also observed by Pouzot et al. (2007) in which cubic phases were melted to an isotropic fluid (L_2) at 45 °C, what means that both structures (cubic and micelle) coexisted at intermediary temperatures. Overall, the systems evaluated in the present paper tended to lose their liquid crystalline phase at high temperatures (Figure 2). However they still showed more than one broad peak which probably means meta-stable phases coexisting and disordered structures. In addition, systems A and B with intermediary water content (40 and 50 % w/w) still showed larger structural parameters than systems with (30 and 60) % (w/w) of water at (50 and 70) °C, showing that liquid crystalline structure are partially present even at high temperatures.

The main structural changes occurred at temperatures lower than 50 °C, since structural parameters decreased drastically when the temperature increased from (25 to 50) °C, while at 70 °C no significant changes occurred on

d values (Figure 3). The decrease of lattice parameter (a) and characteristic length (d) with temperature increase is a typical behavior in LC phases (Kulkarni, 2011; Mezzenga et al., 2005; Mohammady, Pouzot and Mezzenga, 2009; Pouzot et al., 2007). This structural parameter decrease is explained by the increased flexibility and rearrangement of the lipid hydrophobic tails with temperature, the progressive dehydration of polar heads groups (Mohammady, Pouzot and Mezzenga, 2009).

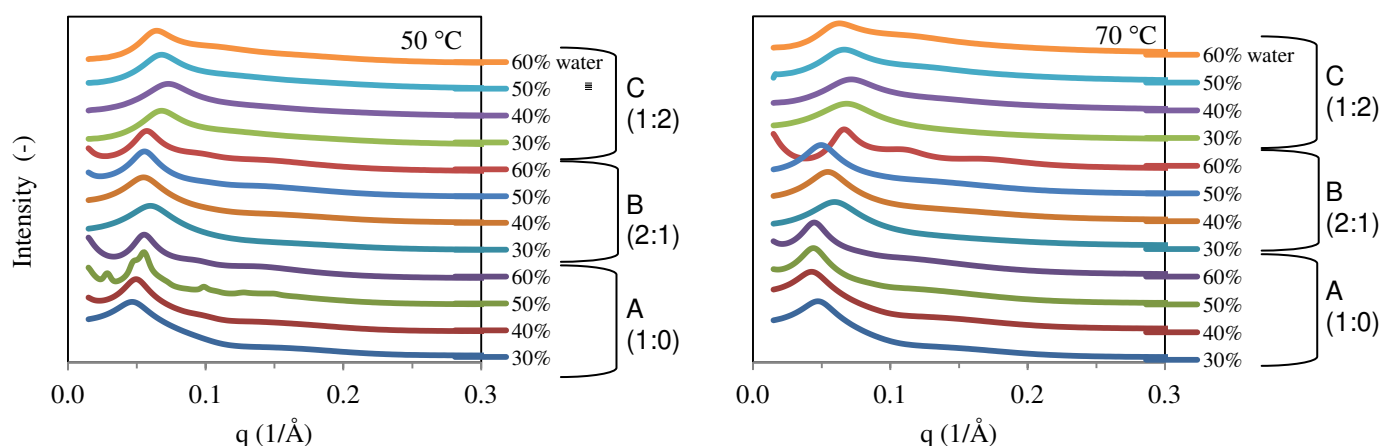


Figure 2. SAXS patterns of systems composed by different MCT:ethanol ratios, A (1:0), B (2:1), and C (1:2), with (30, 40, 50 and 60) % (w/w) of water at 50 °C and 70 °C.

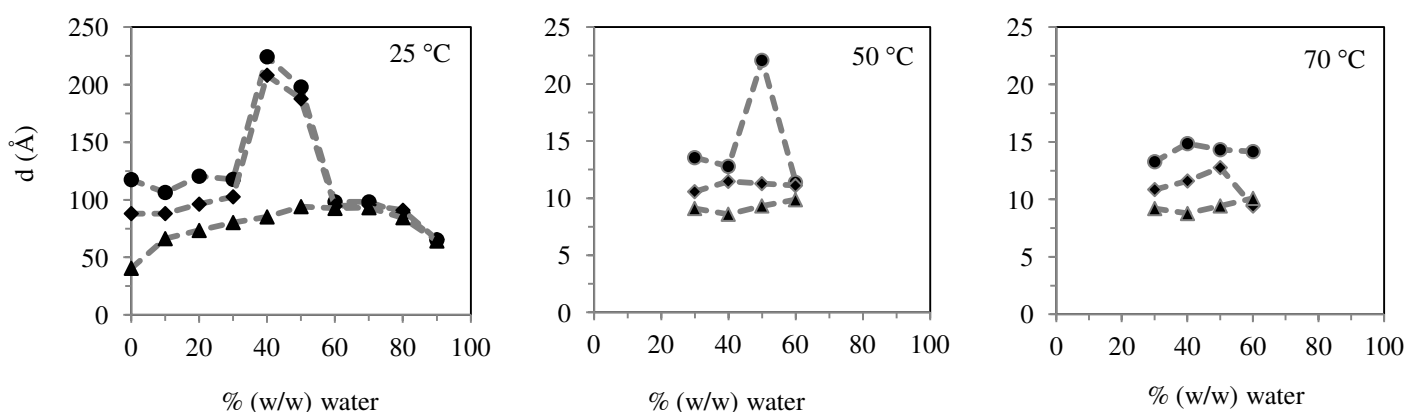


Figure 3. Characteristic length of structure ($d / \text{Å}$) obtained from SAXS of systems with different MCT:ethanol ratio A (1:0) (●), B (2:1) (◆), and C (1:2) (▲) at 25, 50, and 70 °C.

4.3.2. DIFFERENTIAL SCANNING CALORIMETRY (DSC)

DSC peaks were associated with the water state: free (weakly bound) or interfacial (strongly bound) water. Interfacial water is the water confined between the region separating the aqueous core and the oil dispersing phase in a W/O structure. This region is considered to be finite in extent and not just an imaginary line which serves as a border between the two phases (Garti, Aserin, Tiunova and Fanun, 2000). According to water state, and consequently components interactions and miscibility, differences in the melting and freezing behavior can be detected by DSC measurements (Boonme et al., 2006).

Exothermic and endothermic peaks of pure components (water, MCT and Tween 80) are shown in Figure 4 and Table 2. Pure water showed a big exothermic peak with onset peak temperature at $-20\text{ }^{\circ}\text{C}$ in cooling curve, which represents the freezing of supercooled water (Podlogar et al., 2004). The heating curve of pure water showed an endothermic peak with onset temperature at $0.5\text{ }^{\circ}\text{C}$ (melting temperature). The others components, MCT and Tween 80, showed smaller exothermic and endothermic peaks. Their corresponding freezing and melting temperatures are shown in Table 2.

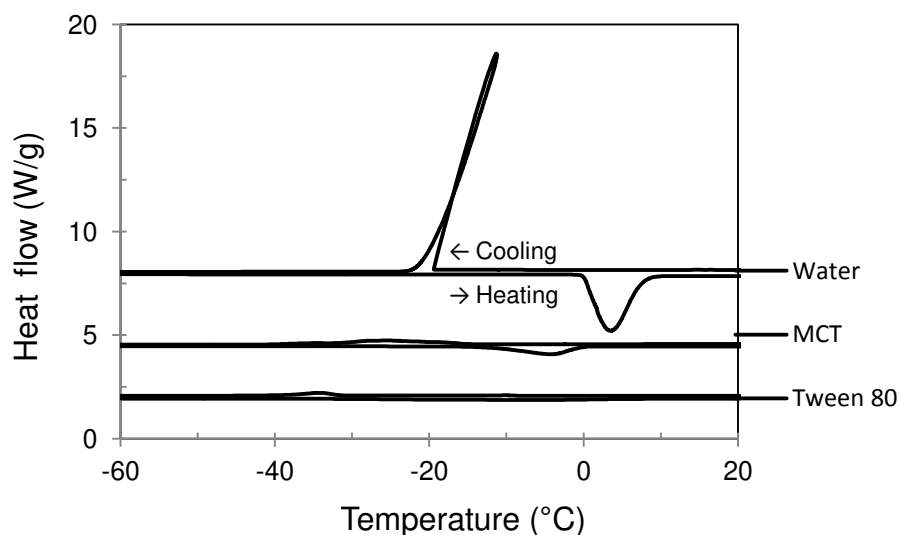


Figure 4. Thermal behavior of pure components (water, MCT and Tween 80).

Table. 2. Freezing and melting temperatures and enthalpy of pure components and systems (A, B, and C) with different MCT:ethanol ratios and water content.

Systems (MCT:ethanol)	% (w/w) Water	T _{freezing}	ΔH _{freezing} (J/g)	T _{melting}	ΔH _{melting} (J/g)
A (1:0)	0	-45.0	24.0	-24.6	2.3
	10	-46.4	8.2	-6.0	20.3
	20	-49.9	10.1	-10.8	21.1
	30	-41.9	19.8	-13.5	34.0
	40	-28.7	38.4	-13.2	49.0
	50	-23.6	70.2	-6.2	76.5
	60	-21.0	107.9	-2.5	111.9
	70	-23.6	138.8	-1.5	146.5
	80	-19.7	179.5	-0.6	186.6
	90	-19.1	250.0	-0.4	270.0
B (2:1)	0	-44.0	16.0	-35.3	5.2
	10	-47.2	6.6	-6.6	5.2
	20	-52.3	6.9	-4.1	12.0
	30	-50.4	6.5	-34.9	11.6
	40	-41.7	36.9	-18.1	35.7
	50	-29.2	65.4	-10.1	68.4
	60	-26.4	99.0	-5.8	103.0
	70	-16.1	137.0	-3.7	139.1
	80	-22.2	173.6	-2.5	186.0
	90	-20.0	212.1	-1.3	111.4
C (1:2)	0	-47.0	12.4	-39.6	4.3
	10	-46.7	3.2	-41.5	2.3
	20	-55.4	2.7	-7.5	2.8
	30	-54.1	2.6	-11.7	4.6
	40	-50.5	32.6	-25.0	35.8
	50	-40.5	52.9	-17.2	50.0
	60	-25.6	79.7	-10.9	77.6
	70	-26.3	123.3	-5.8	117.4
	80	-20.3	164.0	-4.4	159.5
	90	-19.4	173.2	-2.0	216.4
Water		-19.6	301.7	0.5	344.7
MCT (oil)		-21.7	72.6	-12.8	80.7
Tween 80		-31.4	19.7	-29.7	35.8

Calorimetric behavior of systems A, B, and C are shown in Figure 5 and Table 2. Freezing onset peaks were observed between -16 and -55 °C, while melting onset peaks varied between -42 °C and -0.4 °C. Generally, freezing and melting enthalpy showed a first decrease from (0 to 10) % (w/w) of water, followed by an increase at higher water content. At low water content, the systems showed lower freezing and melting temperatures. At this condition, the

amount of surfactant is high and the water molecules are strongly bound to the surfactant polar head groups, decreasing the freezing temperature (Yaghmur et al., 2002). The presence of a nearby surface will alter the thermodynamic properties of bound (interfacial) water, such as freezing point, melting point, enthalpy, and heat capacity such as freezing point, melting point, enthalpy, and heat capacity (Boonme et al., 2006). In this context, a small broadened peak at very low temperatures (below $-40\text{ }^{\circ}\text{C}$) has been suggested to be either internal water or water that is interacting strongly with the surfactants (Podlogar et al., 2004, 2005). This behavior was observed in the system containing lower than (30, 40 and 50) % (w/w) of water in the systems A, B, and C (Table 2), respectively. In addition, systems with low water content (between 0 and 30 % w/w) showed secondary endothermic and exothermic peaks, probably related to solidification and melting of oil and Tween 80, which are in high concentrations in these systems. The absence of secondary peaks at higher water content means that the oil changed from external to internal phase (Boome et al., 2006).

At higher water content, the peaks were shifted towards higher temperatures tending to pure water behavior. Free water is assumed to have similar physicochemical properties to those of pure water (Bonme et al., 2006). The decrease followed by an increase of melting and freezing temperature peaks is enables to identify phase behavior transition. Evaluating SAXS and DSC results, it can be assumed that water changes from the internal pseudo phase to the external pseudo phase closed to these water concentrations. The systems showed bounded water at low water content, including micelle and hexagonal phases, while the transition from water-in-oil to oil-in-water, or bicontinuous structures, occurred at higher water content.

In the same way, melting and freezing temperatures and enthalpies were lower in the systems with higher ethanol content and this behavior was observed up to higher water concentrations in systems with higher ethanol, suggesting that ethanol increased the interaction between water and others components (MCT and Tween 80). The decrease in peak temperatures with ethanol addition was expected. Alcohols are traditionally used as an antifreeze component in refrigeration systems due to their ability to reduce the aqueous solutions freezing and viscosity (Lucas and Raoult-Wack, 1998). Moreover, water and ethanol interaction was observed in SAXS results, which showed the

higher water solubilization by the increase of L₂ phase in systems with higher ethanol content.

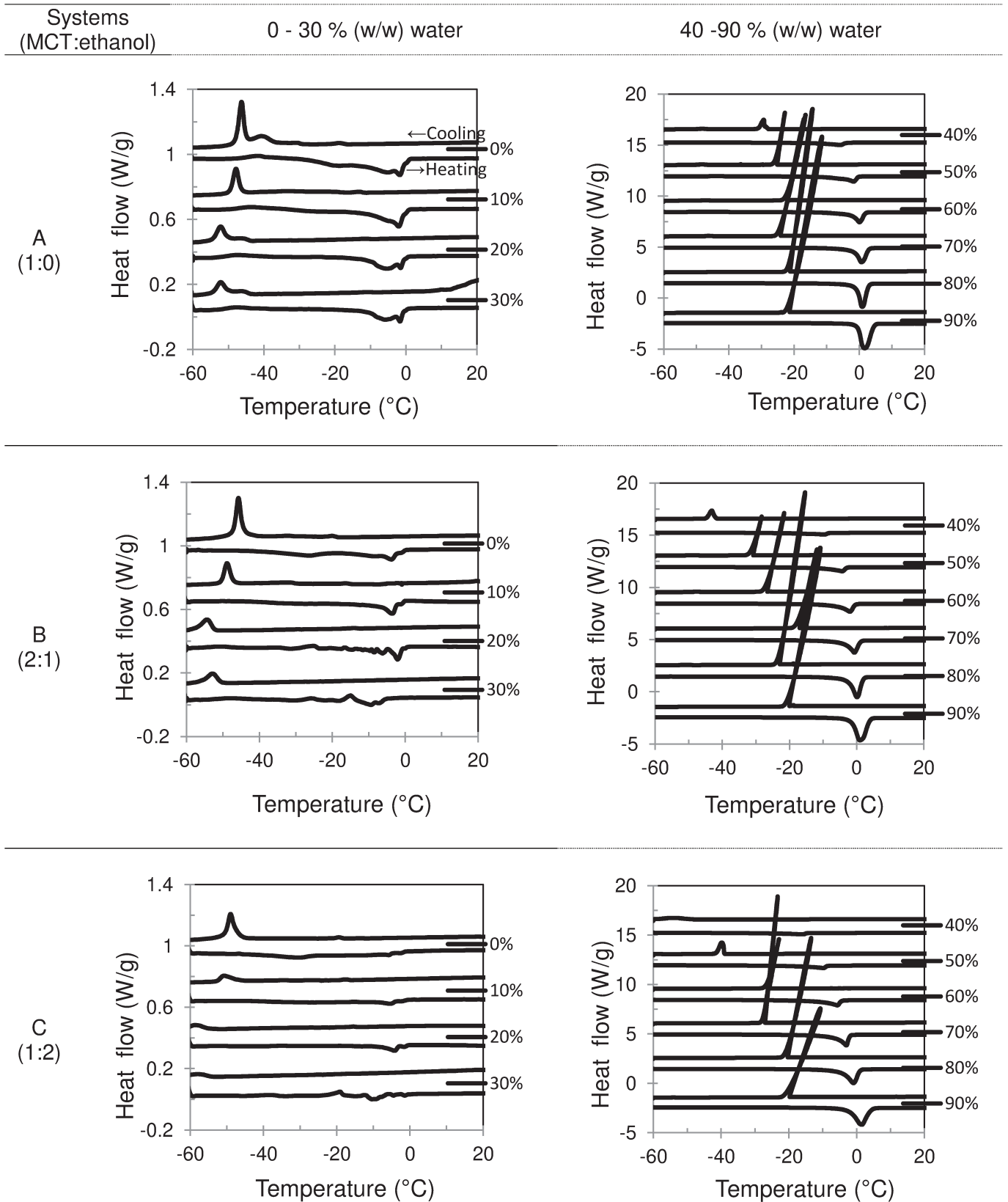


Figure 5. Thermal behavior of systems A, B, and C with low (0 to 30 % w/w), and intermediary to high (40 to 90 % w/w) water concentration.

4.3.3. RHEOLOGY

Figure 6 shows the temperature-dependent viscoelastic properties of the systems A, B, and C during temperature sweeps: first heating (H1), first cooling (C1) and second heating (H2). As observed in our previous work (de Castro Santana, Fasolin, Cunha, 2012), viscoelastic properties increased for water content up to intermediate levels (40, 50 % w/w) and decreased at higher water content. Moreover, the increment of ethanol produced less structured systems.

Temperature of structure transition (liquid crystalline to isotropic solution) was obtained from the viscoelastic properties (Figure 6). Depending on the systems composition different thermo-behavior was observed. System C, with higher ethanol content, was less affected by temperature. Even samples with intermediary water content only showed continuous decrease of η^* with temperature increase, without temperature transition (G' and G'' crossover). All samples of system C showed a diluted solution behavior ($G'' > G'$) along the temperature range evaluated.

Systems with high (more than 70 % w/w) or very low (lower than 30 % w/w) water content were little affected by temperature changes, while viscoelastic properties of systems with intermediate water content decreased with temperature increase. In addition, systems with low and high water content showed a reversible restructuration, since their η^* remained at similar values after heating and cooling cycles.

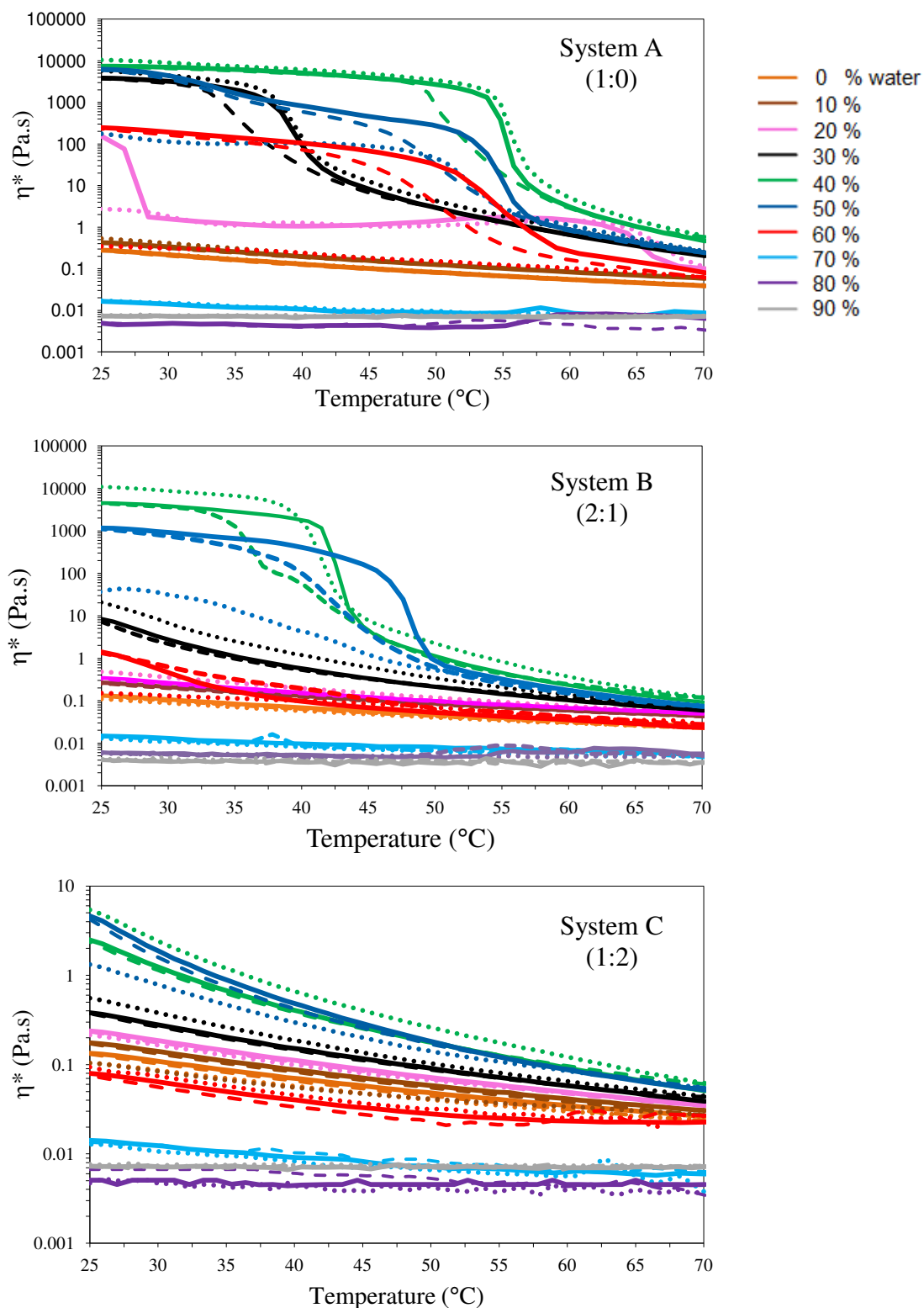


Figure 6. Effect of temperature on complex viscosity (η^*) of systems A, B and C. Process: first heating H1 (.....), first cooling C1 (— —), second heating H2 (—). Water concentration % (w/w): 0 (■), 10 (■), 20 (■), 30 (■), 40 (■), 50 (■), 60 (■), 70 (■), 80 (■) and 90 (■).

Systems showing intermediary water content with low or without ethanol (systems A and B) were highly affected by temperature, since a pronounced slope in curves was observed at intermediary temperatures (between 35 and 55 °C). Systems A (from 30 to 60 % w/w of water) and B (with 40 and 50 % w/w of water) showed three distinct regions during heating. The first region was observed at a temperature lower than the onset of the steep decrease of η^* , showing gel viscoelastic behavior (G' higher than G''). The second region is characterized by an abrupt decrease of η^* within a narrow temperature range. Transition temperatures of these systems are shown in Table 3. At this point, liquid crystalline phases are reorganized in a less structured system. In the third region, viscoelastic properties are very low, exhibiting a common behavior of a liquid with higher values of G'' than G' . The reduction of η^* during heating can be due to the viscosity decrease of the continuous phase and to the thermally induced fluidization of the liquid crystalline phase (Ahmed and Aramaki, 2009).

The system with 30 % (w/w) of water and without ethanol (A30) showed transition temperatures at 39 °C in the both heating process (H1 and H2), while the systems with 40, 50 and 60 % (w/w) showed temperature transition at higher temperatures in second heating (H2) (55 – 56 °C) when compared to H1. In the same way, system B with higher water content (B50) showed higher temperature transition than system with lower water content (B40). However, system B showed lower temperature transition than system A, since system B was less structured and needed less energy to phase transition. Transition temperature during cooling (C1) was always lower than in heating processes (H1 and H2) for both A and B systems, suggesting that the structure transition during cooling need more energy than in heating process. Hysteresis is identified as the difference between the viscoelastic properties during the cooling ascending curve and the heating descending curve and it suggests that a more structured, continuous and homogeneous gel was formed during cooling (Funami et al., 2008). Moreover, an irreversible process can be noticed in these systems, as can be noticed by different η^* values observed after the heating and cooling processes (Table 3). However, this mismatch of viscoelastic properties after successive heating and cooling cycles can be better explained by a macroscopic phase separation at high temperatures that prevents the

system from recovering the thermodynamically stable configuration, unless external mixing is carried out (Pouzot et al., 2007).

Table. 3. Viscoelastic properties (η^*) and transition temperatures of the first heating (H1), first cooling (C1), and second heating (H2) cycles.

System (MCT:ethanol) / water content	Process	Transition temperatures ($^{\circ}\text{C}$)	η^* before H1, C1, and H2
A (1:0) / 30% water	H1	39 ± 0.7	5700.00
	C1	35 ± 0.7	0.24
	H2	39 ± 0.7	3870.00
A (1:0) / 40% water	H1	56 ± 0.7	10500.00
	C1	52 ± 0.0	0.58
	H2	56 ± 0.0	7410.00
A (1:0) / 50% water	H1	52 ± 0.6	175.00
	C1	50 ± 0.0	0.25
	H2	55 ± 0.0	6270.00
A (1:0) / 60% water	H1	-	0.35
	C1	52 ± 0.7	0.06
	H2	56 ± 0.9	250.00
B (1:2) / 40% water	H1	42 ± 0.7	10900.00
	C1	37 ± 1.5	0.12
	H2	43 ± 0.7	4560.00
B (1:2) / 50% water	H1	45 ± 1.8	36.90
	C1	43 ± 1.2	0.74
	H2	49 ± 2.9	1170.00

The phase transition suggested by the drastic decrease of η^* around 50 $^{\circ}\text{C}$ (Figure 6 and Table 3) was consistent with SAXS results. The hexagonal and cubic phases observed at 25 $^{\circ}\text{C}$ (Figure 1 and Table 1) were partially melted and less structured phases were produced at 50 $^{\circ}\text{C}$ and 70 $^{\circ}\text{C}$ (Figure 2). Ahmed and Aramaki (2009) reported a similar behavior in systems composed of water, Tween 80 and C14EO3 (tri-ethyleneglycol mono n-tetradecyl ether), in which lamellar and hexagonal phase produced at low temperatures were replaced by an isotropic phase at 60 $^{\circ}\text{C}$. Moreover, the temperature phase transition observed on rheology was confirmed by the decrease of the distance between repeated structures (d parameter) when the temperature was increased from 25 $^{\circ}\text{C}$ to 50 $^{\circ}\text{C}$ (Figure 3). High temperatures cause non-ionic surfactant dehydration, making it more soluble in the oil phase and favoring negative spontaneous curvature of the surfactant film. In addition, temperature can increase the thermal motion of the surfactant film and enhance

the interfacial flexibility, which could lead to a decrease in the molecular organization of the surfactant and favor microemulsion formation (Fanun, 2010; Santana, Perrechil and Cunha 2013).

4.4. CONCLUSION

The present study showed the phase transition of systems composed by water, MCTs, Tween 80 and ethanol in a dilution line water and with different oil:ethanol ratios (1:0, 2:1, and 1:2). Correlation between freezing and melting peaks with the water state (free and bound) was used to identify the phase transition from water-in-oil to oil-in-water structure. In the same way, oscillatory measurements showed the increase of viscoelastic properties with water addition up to intermediary water content, suggesting the phase transition from O/W to O/W structures. SAXS results identified the kind of structure and its characteristics parameters according to phase composition and temperature condition. Systems with intermediary water content showed hexagonal and cubic phases and higher repeat spacing (d). Systems with higher ethanol content extended L_2 phase region to higher water content and produced systems with smaller repeat spacing (d) and low viscoelastic properties without temperature transition. In addition, systems with higher ethanol content showed lower exothermic and endothermic peaks and enthalpies due to components interaction.

The temperature dependence of structural and rheological properties was investigated using SAXS and oscillatory rheology. Systems with low and high water content and/or high ethanol content were less susceptible to temperature changes, did not showing significant rheological change with temperature increase. However, systems with intermediary water content and low or without ethanol showed a temperature transition around 50 °C, since they showed structured liquid crystalline phases. Hexagonal and cubic phases with a gel-like behavior were produced at 25 °C, while coexisting liquid crystalline and micelles phases with lower repeat spacing (d) and liquid behavior were observed at higher temperatures (50 and 70 °C). This study might be crucial for understanding the systems structure and design of nanostructures for potential applications in food, pharmaceutical and cosmetic with different compositions and temperature conditions.

4.5. ACKNOWLEDGEMENTS

The authors wish to acknowledge FAPESP, CNPq and CAPES for their financial support. We thank the Brazilian Synchrotron Laboratory, LNLS, for the use of the SAXS beamline.

4.6. REFERENCES

- Alam, M. M., Sugiyama, Y., Watanabe, K., and Aramaki, K. (2010). Phase behavior and rheology of oil-swollen micellar cubic phase and gel emulsions in nonionic surfactant systems. *Journal of Colloid and Interface Science*, 341, 267-272.
- Ahmed, T., Aramaki, K. (2009). Temperature sensitivity of wormlike micelles in poly(oxyethylene) surfactant solution: Importance of hydrophilic-group size. *Journal of Colloid and Interface Science* 336, 335–344.
- Binks, B.P., Fletcher, P.D.I., Tian, L. (2010). Influence of nanoparticle addition to Winsor surfactant microemulsion systems. *Colloids and Surfaces A: Physicochemical and Engineering Aspects*, 363, 8–15.
- Berni, M.G., Lawrence, C.J., Machin, D. (2002). A review of the rheology of the lamellar phase in surfactant systems. *Advances in Colloid Interface Science*, 98, 217–243.
- Boonme P, Krauel K, Graf A, Rades T, Junyaprasert VB. (2006). Characterization of microemulsion structures in the pseudoternary phase diagram of isopropyl palmitate/water/Brij 97:1-Butanol, *AAPS Pharm Sci Tech*, 7, E99-E104.
- De Castro Santana, R., Fasolin, L. H., Cunha, R. L. (2012). Effects of a cosurfactant on the shear-dependent structures of systems composed of biocompatible ingredients. *Colloids and Surfaces A: Physicochemical and Engineering Aspects*, 398, 54-63.
- Fanun, M. (2010) Properties of microemulsions with mixed nonionic surfactants and citrus oil. *Colloids and Surfaces A: Physicochemical and Engineering Aspects*, 382:226–231.
- Feng, J., Wang, Z., Zhang, J., Wang, Z., Liu, F. (2009). Study on food grade vitamin E microemulsions based on nonionic emulsifier. *Colloids and Surfaces A: Physicochemical and Engineering Aspects*, 339, 1–6.

- Flanagan, J., Singh, H. (2006). Microemulsions: a potential delivery system for bioactives, *Critical Reviews in Food Science and Nutrition*, 46, 221–237.
- Funami, T., Noda, S., Nakauma, M., Ishihara, S., Takahashi, R., Al-Assaf, S., Ikeda, S., Nishinari, K., & Phillips, G. O. (2008). Molecular structures of gellan gum imaged with atomic force microscopy in relation to the rheological behavior in aqueous systems in the presence or absence of various cations. *Journal of Agricultural and Food Chemistry*, 56, 8609-8618.
- Garti, N., Aserin, A., Tiunova I., Fanun, M. (2000). A DSC study of water behavior in water-in-oil microemulsions stabilized by sucrose esters and butanol. *Colloids and Surfaces A: Physicochemical and Engineering Aspects*, 170, 1-18
- Garti, N., Yagmur, A., Leser, M. E., Clement, V., Watzke, H. J. (2001). Improved oil solubilization in oil/water food grade microemulsions in the presence of polyols and ethanol. *Journal of Agricultural and Food Chemistry*, 49, 2552–2562.
- John, C., Rakshit, A. K. (1995). Effects of mixed alkanols as cosurfactants on single phase microemulsion properties. *Colloids and Surfaces A: Physicochemical and Engineering Aspects*, 46, 95, 201–210.
- Kulkarni, C. V. (2011). Nanostructural studies on monoelaidin – water systems at low temperatures. *Langmuir*, 27, 11790-11800.
- Liu, C., Hao, J. (2011). Shear-induced structural transition and recovery in the salt-free catanionic surfactant systems containing deoxycholic acid. *Journal of Physical Chemistry B*, 115, 980–989.
- Lucas, T., Raoult-Wack, A.L. (1998). Imersion chilling and freezing in aqueous refrigerating media: review and future trends. *International Journal of Refrigeration*, 21, 419-429.
- Matsaridou, I., Barmapalexis, P., Salis, A., Nikolakakis, I. (2012). The influence of surfactant HLB and oil/surfactant ratio on the formation and properties of self-emulsifying pellets and microemulsion reconstitution. *AAPS PhamSciTec*, 13:1319-1330.
- Mezzenga, R., CMeyer, C., Servais, C., Romoscanu, A. I., Sagalowicz, L., et al. (2005). Shear rheology of lyotropic liquid crystals: a case study. *Langmuir*, 21, 3322-3333.

- Mohammady, S. Z., Pouzot, M., Mezzenga, R. (2009). Oleoylethanolamide-Based lyotropic liquid crystals as vehicles for delivery of amino acids in aqueous environment. *Biophysical Journal*, 96, 1537-1546.
- Patel, N., Schmid, U., Lawrence, M.J. (2006). Phospholipid-based microemulsions suitable for use in foods. *Journal of Agricultural and Food Chemistry*, 20, 7817-7824.
- Podlogar, F., Gagperlin, M., Tomsic, M., Jamnik, A., Rogac, M.B., (2004). Structural characterisation of water-Tween 40((R))/Imwitor 308((R))-isopropyl myristate microemulsions using different experimental methods. *International Journal of Pharmaceutics*, 276, 115-128.
- Podlogar, F., Rogac, M.B., Gagperlin, M., (2005). The effect of internal structure of selected water-Tween 40 (R)-Imwitor 308 (R)-IPM microemulsions on ketoprofen release. *International Journal of Pharmaceutics*, 302, 68-77.
- Pouzot, M., Mezzenga, R., Leser, M., Sagalowicz, L., Guillot, S., Glatter, O. (2007). Structural and rheological investigation of Fd3m inverse micellar cubic phases. *Langmuir*, 23, 9618-9628.
- Santana, R. C., Perrechil, F. A., Cunha, R. L. (2013). High- and low-energy emulsifications for food applications: a focus on process parameters. *Food Engineering Reviews*, 5, 107-122.
- Savitzky, A., & Golay, M. J. E. (1964). Smoothing + differentiation of data by simplified least squares procedures. *Analytical Chemistry*, 36, 1627.
- Seddon, A. M., Lotze, G., Plivelic, T. S., Squires, A.M. (2011). A highly oriented cubic phase formed by lipids under shear. *Journal of the American Chemical Society*, 133, 13860–13863.
- Spernath, A., Aserin, A. Microemulsions as carriers for drugs and nutraceutical. *Advance in Colloid and Interface Science*, 128 (2006) 47–64.
- Wolf, L., Hoffmann, H., Watanabe, K., Okamoto, T. (2011). Microemulsions from silicone oil with an anionic/nonionic surfactant mixture. *Physical Chemistry Chemical Physics*, 13, 3248–3256.
- Yagmur, A. Aserin, N. Garti, (2002). Phase behavior of microemulsions based on food grade nonionic surfactants: effect of polyols and short chain alcohols. *Colloids and Surfaces A: Physicochemical and Engineering Aspects*, 209, 71–81.

Yagmur, A., Kriechbaum, M., Amenitsch, H., Steinhart, M., Laggner, P., Rappolt, M. (2009). Effects of pressure and temperature on the self-assembled fully hydrated nanostructures of monoolein-oil systems. *Langmuir*, 26, 1177-1185.

- CAPÍTULO 5 -

**EFEITO DO TIPO DE SURFACTANTE NA ESTRUTURA E
REOLOGIA DE SISTEMAS COMPOSTOS POR ÁGUA,
TRIACILGLICEROL DE CADEIA MÉDIA E ETANOL.**

STRUCTURE AND RHEOLOGY OF MICROEMULSIONS
AND LIQUID CRYSTALLINE PHASES COMPOSED OF
BIOCOMPATIBLE SURFACTANT MIXTURES.

Rejane de Castro Santana, Luiz Henrique Fasolin, Rosiane
Lopes da Cunha. Submetido na Colloids and Surfaces A.

STRUCTURE AND RHEOLOGY OF MICROEMULSIONS AND LIQUID CRYSTALLINE PHASES COMPOSED OF BIOCOMPATIBLE SURFACTANT MIXTURES.

Rejane de Castro Santana, Luiz Henrique Fasolin, Rosiane Lopes da Cunha

Department of Food Engineering, Faculty of Food Engineering, University of Campinas – UNICAMP, 13083862, Campinas, SP, Brazil

* Corresponding author. Tel.: +55 19 3521 40407, fax: +55 19 3521 4027.

Email address: rosiane@fea.unicamp.br (R.L. da Cunha).

ABSTRACT

Mixtures composed by Tween 80 and others surfactants (Tween 20, lecithin, Span 20 or Span 80) were used to obtain varied self-assembled structures in systems formed by medium-chain triglyceride (2.7-9.3 % w/w), ethanol (5.3-18.7 w/w) and water (30-60 % w/w). These systems were evaluated by rheological and small angle X-ray scattering measurements in order to identify the relation between the composition and the corresponding structural and rheological behaviour. Micelle and hexagonal phases prevailed in Tween systems, while Tween/Span and Tween/lecithin systems also presented lamellar phases. Cubic phases were observed only in Tween 80 + lecithin systems. A relationship among structural parameters, rheological behavior and surfactant mixture properties (critical packing parameter - CPP, and hydrophilic-lipophilic balance - HLB) was observed. Surfactant mixtures with lower HLB tended to produce shear thinning and viscoelastic liquid crystalline phases at high surfactant content. The high pseudoplasticity was associated to an ordered liquid crystalline structure susceptible to breakage or reorientation under shear. Moreover, partition phenomenon of ethanol changed with surfactant mixture properties leading to higher lattice parameter in systems with lower HLB. Thus, results showed that different systems structures and rheological properties could be produced depending on the components characteristics, concentration and interactions.

5.1. INTRODUCTION

Surfactant molecules can self-assemble into a large variety of morphologies, including microemulsions (ME) (or swelling micelles) and liquid-crystal (LC), such as lamellar, hexagonal, or cubic structures (Binks, Fletcher and Tian, 2010). These systems are prepared using low-energy methods, showing easy and low cost of preparation. In addition, since these systems show oil and water domains with well-defined interfaces, they have the ability to solubilise both polar and non-polar additives (Wolf, Hoffmann, Watanabe and Okamoto, 2011) including food ingredients, nutraceuticals, flavors, cosmetic components, and drugs (Spernath and Aserin, 2006).

Microemulsions are optically isotropic, translucent and thermodynamically stable systems that show low viscosity. They are formed by small swollen micelles (1–200 nm) stabilised by surfactants, usually in combination with a cosurfactant (Binks and Fletcher, 2010). In contrast, liquid-crystal phases exhibit a more complex structure. Surfactant molecules form bilayers that are regularly stacked in the lamellar phase, whereas cylinders are organised onto a triangular lattice in the hexagonal phase (Binks and Fletcher, 2010). Cubic phases are characterized by an optically isotropic and highly viscous three-dimensional structure (Alam, Sugiyama, Watanabe and Aramaki, 2010). The bicontinuous cubic phase consists of two continuous but non-intersecting water channels separated by the surfactant. These systems are named as gyroid ($Ia3d$), double diamond ($Pn3m$) and primitive ($Im3m$) curvatures depending on the corresponding space groups (Kulkarni, 2011).

The structure of ME and LC phases is strongly dependent of the systems composition. Medium-chain triglycerides (MCT) have been widely used to form biocompatible microemulsions (Patel, Schmid and Lawrence, 2006; Garti, Yaghmur, Leser, Clement and Watzle, 2001) since they are more stable than the cyclic oils. Moreover, medium-chain triglycerides show a more nonpolar structure and lower molecular weight than long-chain triglycerides (vegetable oils), making easier oil solubilisation (Flanagan and Singh, 2006; Yaghmur, Aserin, Antalek and Garti, 2003). Short-chain alcohols are the most commonly used cosurfactants in microemulsion formulations, but ethanol is the most suitable for use in drugs and some food products, such as alcoholic beverages

(Flanagan and Singh, 2006).

Surfactant structure, such as the length of hydrophobic chain tail and the characteristic of the head group, affects liquid crystalline microstructure and rheological properties, as well as their applicability. The food-grade emulsifiers evaluated in this study were sorbitan monooleate (Span 80), sorbitan monolaurate (Span 20), soybean lecithin, polyoxyethylene sorbitan monooleate (Tween 80), and polyoxyethylene sorbitan monolaurate (Tween 20), which show a hydrophilic-lipophilic balance (HLB) of 4.3, 8.6, 9.0, 15.0 and 16.7, respectively (Walstra, 2003; Araújo, 2001).

Lecithin is a mixture of phospholipids with an amphoteric character generally recognized as safe (GRAS). Its main component is the phosphatidylcholine (PC) (Figure 1a), followed by phosphadylethanolamine (PE), phosphatidylinositol (PI), phosphatidic acid (PA) and other minorities. Span 80 and Span 20 are monosorbates (Figure 1b), while Tween 20 and Tween 80 are polysorbates (Figure 1c). The different monosorbates and polysorbates vary in the length of the polyoxyethylene chain, type of fatty acid, and degree of esterification (Zhang, Cui, Zhu, Feng and Zheng, 2010). Such structural variations result in different self-assembly mechanisms and structures.

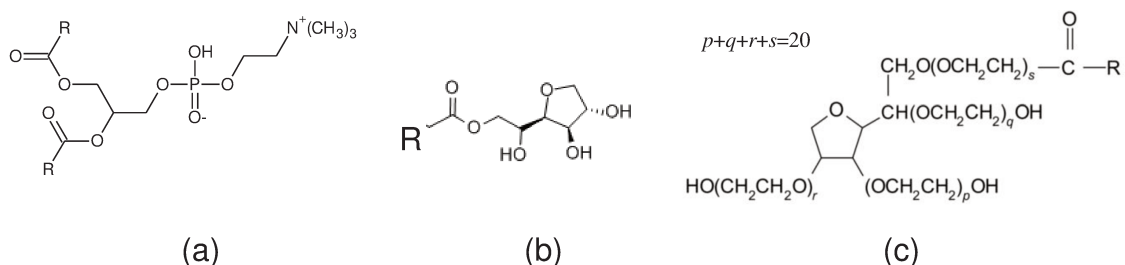


Figure. 1. Formula of (a) phosphatidylcholine, (b) Span 20 and Span 80 monosorbates and (c) Tween 20 and Tween 80 polysorbates. R is C_nH_{2n+1} with $n=11$ for Span 20 and Tween 20 and $n=17$ for Span 80 and Tween 80.

The combination of both lipophilic and hydrophilic surfactants could lead to a special self-assembly since it would change the spontaneous curvature and the elasticity or rigidity of the interfacial film formed by only one surfactant type (Paul and Mitra, 2005). As a result, the morphology of liquid crystalline phases is modified, showing changes in their lattice parameter and transition among the

phases, as well as the system capability to solubilise other molecules and the partition phenomenon within hydrophilic or hydrophobic domains (Mohammady, Pouzot and Mezzenga, 2009). Surfactant mixtures are also been used in order to decrease the surfactant and co-surfactant content necessary to microemulsion formation, increasing the water and oil co-solubilisation due to a synergistic effect (Paul and Mitra, 2005). Moreover, some preliminary studies showed that the use of surfactant mixtures can result in a microemulsion that can be diluted without altering or destroying their micellar structure (Spernath, Yaghmur, Aserin, Hoffman and Garti, 2003).

Therefore, the effect of surfactants mixtures on the self-assembled structures in systems composed by medium-chain triglyceride (MCT), ethanol and water was evaluated by rheological and SAXS measurements. To our knowledge, no studies about the relationship between surfactant mixture properties, structural parameters and rheological behaviour of this type of system have been reported.

5.2. MATERIAL AND METHODS

5.2.1. MATERIAL

Delios V, a medium-chain triglyceride (MCT) rich in caprylic and capric glycerides, was kindly donated by Cognis (Germany). Tween 80 (polyoxyethylene sorbitan monooleate), Tween 20 (polyoxyethylene sorbitan monolaurate) and ethanol 99.5 % were purchased from Synth (Brazil). Sorbitan monooleate (Span 80) and sorbitan monolaurate (Span 20) were obtained from Sigma-Aldrich (USA). Lecithin Lipoid S45, composed of not less than 45 % (w/w) of phosphatidylcholine, 10-18 % (w/w) of phosphatidylethanolamine, no more than 4 % (w/w) of lysophosphatidylcholine and 3 % (w/w) of triglycerides, was purchased from Lipoid GmbH (Germany).

5.2.2. METHODS

5.2.2.1. Surfactants mixture properties

Mixtures of Tween 80 with Tween 20, Span 80, Span 20 or lecithin (ratio 3:1) were used to in the systems preparation. The different surfactants mixtures

were characterized according to their effective hydrophilic-lipophilic balance (HLB) and the critical packing parameter (CPP). CPP is inversely related to HLB, but the CPP concept considers bulkiness of the hydrophobic tail.

CPP of each surfactant is shown in Table 1 (Pottirayil, Kailas and Biswas (2011)). CPP is defined as $V/(a_0l_c)$, where V is the hydrocarbon volume, l_c is the chain length and a_0 is the head group area of the surfactants. Equations 1, 2 and 3 were used to calculate the parameters l_c , a_0 , and V of monosorbates and polysorbates surfactants. Phosphatidylcholine molecule properties were considered in CPP determination of lecithin, since it was the major fraction of the Lipoid S45. For phosphatidylcholine, a_0 is equal to 0.7170 nm^2 , V was calculated according to Equation 4 and CPP was calculated using 80 % of chain length (l_c) (Kumar, 1991).

Tab. 1. Critical packing parameter (CPP) of surfactants.

Surfactant	n	$l_c \text{ (nm)}$	$V \text{ (nm}^3\text{)}$	j	$a_0 \text{ (nm}^2\text{)}$	CPP
Tween 20	11	1.5455	0.3233	20	1.5330	0.1365
Tween 80	17	2.3045	0.4847	20	1.5330	0.1372
Lecithin	17	2.3045	1.0506	-	0.7170	0.7948
Span 20	11	1.5455	0.3233	3	0.4790	0.4367
Span 80	17	2.3045	0.4847	3	0.4790	0.4391

$$l_c \text{ (nm)} = (0.154 + 0.1265n) \quad (1)$$

$$a_0 \text{ (nm}^2\text{)} = (29.3 + 6.20j) \quad (2)$$

$$V \text{ (nm}^3\text{)}_{\text{monol polysorbates}} = (27.4 + 26.9n)10^{-3} \quad (3)$$

$$V \text{ (nm}^3\text{)}_{\text{lecithin}} = (0.0309n) \quad (4)$$

where n is the number of CH_2 groups in the hydrophobic tail, and j is the number of oxyethylene groups of monosorbates and polysorbates.

HLB and CPP of surfactant mixtures of each system (Table 2) were calculated according to additive principle, taking into account the HLB or CPP values and the molar fraction of each surfactant in the mixture.

Tab. 2. Surfactant mixtures properties (*HLB* and *CPP*).

System	<i>CPP</i>	<i>HLB</i>
Tween 80 (T8)	0.1372	15.00
Tween 80 + Tween 20 (T8T2)	0.1370	15.45
Tween 80 + Lecithin (T8Lec)	0.3740	12.84
Tween 80 Span 20 (T8S2)	0.3042	11.43
Tween 80 + Span 80 (T8S8)	0.2896	9.60

5.2.2.2. Phase-diagrams construction and characterisation

The five-component systems were described by pseudo-ternary diagrams with the following corners: MCT + ethanol, water and surfactant mixtures of Tween 80 with Tween 20, Span 80, Span 20 or lecithin (ratio 3:1). The diagrams were produced using a spontaneous emulsification method at 25 °C. Firstly, an initial system containing the surfactants mixture and MCT+ethanol (ratio 1:2) was prepared at different ratios (10:90; 20:80; 30:70; 40:60; 50:50; 60:40; 70:30; 80:20; 90:10 w/w). Deionised water was then titrated under constant stirring using increments of 10 % (w/w). Each formulation was kept under stirring for 15 min, and the samples were then stored at 25°C for at least 15 days before they were examined for the diagram construction.

Each system produced by spontaneous emulsification was characterised according to its visual appearance in order to construct the pseudo-ternary phase diagrams. Systems with one phase (including opaque and translucent appearance) were named as “1 phase” (1-P), which included microemulsions and some liquid crystalline phases. The total area of “1-phase” region (A_{1-P}) was calculated as a characteristic parameter. Systems showing phase separation with translucent phases were classified as “2 transparent phases” (2-TP), which represented Winsor I, Winsor II or Winsor III systems. Systems with one or two phases showing a white (opaque) appearance were named as “white phase” (WP), which included macro, mini, nanoemulsions, or liquid crystalline phases.

5.2.2.3. Characterisation of ME and LC phases

The samples obtained from water titration (30, 40, 50 and 60 % w/w of water) in an initial mixture composed by 60, 70 and 80 % (w/w) of the surfactant

mixtures and, consequently 40, 30 and 20 % (w/w) of MCT+ethanol (dilution lines 6, 7 and 8), respectively, were analysed by rheological and SAXS measurements. The composition of these systems is shown in Table 3. Each sample was named according to its formulation: two first numbers corresponding to the final water content (30, 40, 50 or 60 % w/w), followed by the initial surfactant concentration (60, 70 or 80% w/w). In addition, the samples were classified according to the surfactants combination: Tween 80 (T8), Tween 80+Tween20 (T8T2), Tween 80+Span 20 (T8S2), Tween 80+Span 80 (T8S8) and Tween 80+Lecithin (T8Lec). For example, an initial sample that contained 70 % (w/w) of Tween 80:Tween 20 (3:1) and 30 % (w/w) of MCT+ethanol, which was diluted with 50 % (w/w) water was named as 5070T8T2.

Tab. 3. Composition (% w/w) of the systems evaluated by rheological and SAXS measurements.

Systems	Water	Oil	Ethanol	Surfactant mixture
3060	30	9.3	18.7	42
4060	40	8.0	16.0	36
5060	50	6.7	13.3	30
6060	60	5.3	10.7	24
3070	30	7.0	14.0	49
4070	40	6.0	12.0	42
5070	50	5.0	10.0	35
6070	60	4.0	8.0	28
3080	30	4.7	9.3	56
4080	40	4.0	8.0	48
5080	50	3.3	6.7	40
6080	60	2.7	5.3	32

5.2.2.4. Small angle X-ray scattering (SAXS)

Structure information of liquid crystalline and microemulsions was obtained from SAXS. The measurements were performed at room temperature using the beam line of the National Synchrotron Light Laboratory (LNLS, Campinas, Brazil), with X-ray source of wavelength $\lambda = 1.54 \text{ \AA}$. A position-sensitive X-ray detector and a multichannel analyzer were used to record the SAXS intensity, $I(q)$, as a function of modulus of scattering vector $q = (4\pi/\lambda) \sin(\theta/2)$, θ being the scattering angle. Each SAXS pattern corresponds to a data

collection time of 100 s.

Structure type was determined according to the scattering peaks positions. For lamellar phases (L_α) the distance in relation to the first peak is 1:2:3:4, while for normal or reverse hexagonal phases (H_1 or H_2) the distance ratio is given by 1: $\sqrt{3}$: $\sqrt{4}$: $\sqrt{7}$. Bicontinuous cubic phases double diamond ($Pn3m$) presents distance ratio of 1: $\sqrt{2}$: $\sqrt{3}$: $\sqrt{4}$: $\sqrt{6}$: $\sqrt{8}$: $\sqrt{9}$: $\sqrt{10}$.

The correlation distance (d) between the scattering centers of the structures was determined as $d=2\pi/q$. Here d is the center-to-center distance between neighboring scattering centers and q is the position of the correlation peak.

The distance between the centers of two hexagonal or lamellar structures, known as lattice parameter (a), was calculated from Equation 5. The radius of the hydrophobic core of cylindrical aggregate (r_{hc}) was calculated from Equation 6, while lamella thickness formed by hydrophobic tail (d_{hc}) or hydrophilic tail (d_w) were calculated from Equations 7 and 8.

$$a = \frac{4\pi}{q_{100}\sqrt{3}} \quad (5)$$

$$r_{hc} = \sqrt{\frac{2\phi_{hc}}{\sqrt{3}\pi}} d \quad (6)$$

$$d_{hc} = d\phi_{hc} \quad (7)$$

$$d_w = d - d_{hc} \quad (8)$$

where q_{100} is the first peak position, ϕ_{hc} is the volume fraction of the hydrocarbon portion and d is the correlation distance.

For cubic phases the lattice parameter (a) was obtained by plotting $(q/2\pi)^2$ as a function of the Miller indexes according to Equation 9:

$$\left(\frac{q_{hkl}}{2\pi}\right)^2 = \left(\frac{1}{a}\right)^2 (h^2 + k^2 + l^2) \quad (9)$$

where q_{hkl} is the scattering vector of $[h/k]$ reflection and h, k, l are Miller indexes.

5.2.2.5. Rheology

Flow curves and oscillatory measurements were performed on a Physica MCR301 rheometer (Anton Paar, Austria) at 25 °C using a stainless steel cone-plate geometry (5.0 cm, 2° angle, truncation 208 μ m).

Flow curves were obtained from an up–down–up steps program using a

shear-rate range between 0 and 100 s⁻¹. Newtonian viscosity (μ) or the apparent viscosity at 3 s⁻¹ (η_3) obtained from the first step (transient state) were also evaluated. Such shear rate was chosen because it showed minor effect of shear on the structure behaviour.

Oscillatory measurements were performed within the linear viscoelastic region. The complex (G^*), storage (G') and loss (G'') moduli and complex viscosity (η^*) were evaluated using a frequency sweep between 0.01 and 10 Hz.

5.3. RESULTS

5.3.1. PHASE DIAGRAM AND VISUAL APPEARANCE

The systems with different surfactants composition were visually observed to construct the pseudo-ternary diagrams (Figure 2).

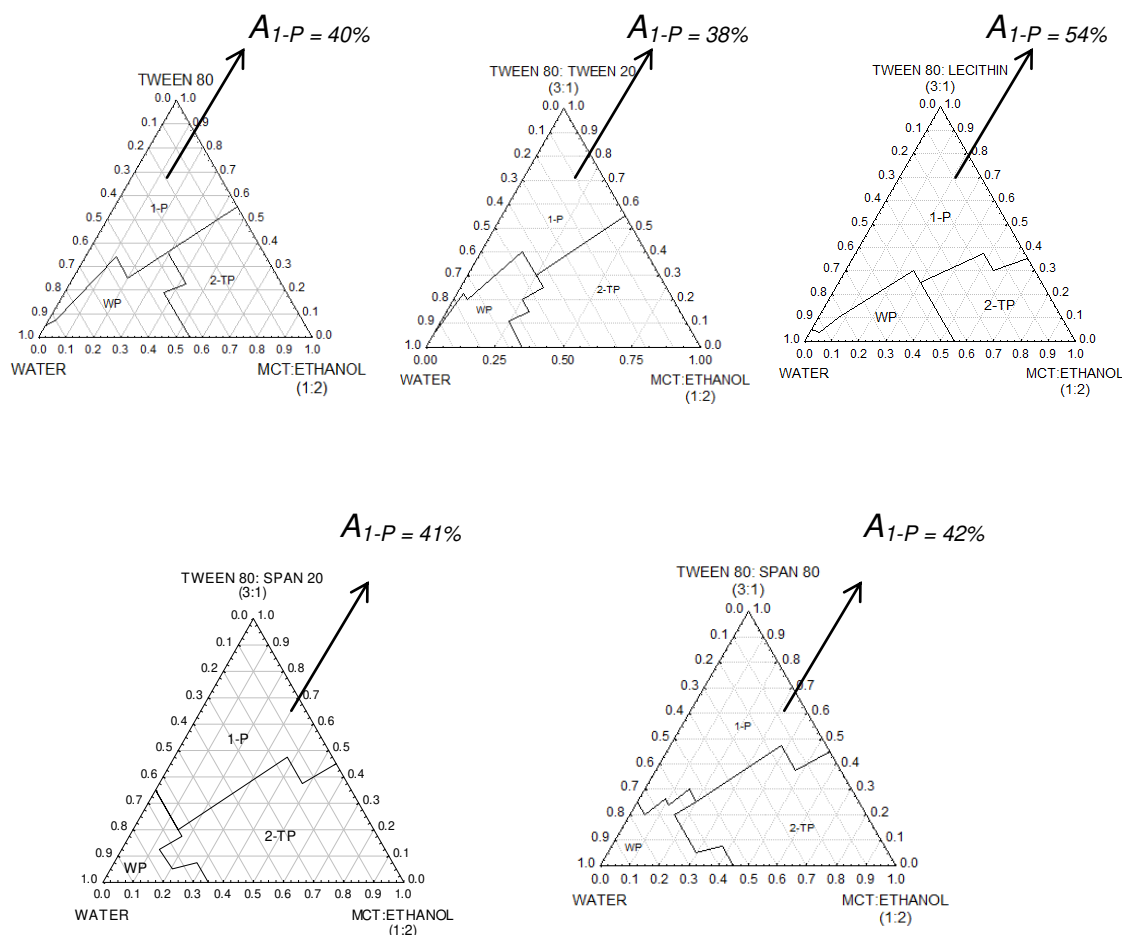


Figure. 2. Pseudo-ternary diagrams of systems composed by water, MCT, ethanol, and surfactant mixtures. 1-P: one phase; 2-TP: two transparent phases, WP: white phase. A_{1-P} : area of one-phase region obtained from pseudo-ternary diagrams.

Microemulsions and liquid crystal phases (one-phase region) were obtained at dilutions lines produced with an initial high surfactant content. Systems containing lecithin or monosorbates showed one-phase with an initial surfactant concentration from 40 and 50 % (w/w), respectively, while polysorbates needed at least 60 % (w/w) of initial surfactant content to produce one-phase systems. However, polysorbates could form one-phase at higher water content than the mixtures with monosorbates. Figure 2 show that the area of one-phase region (A_{1-P}) was the biggest in the system T8Lec, while the others showed around 40 % of A_{1-P} . The one-phase region of T8Lec system consisted only of liquid crystal, and microemulsions were not observed according to polarized light microscopy (results not shown).

At low surfactant concentration and high MCT:ethanol concentration,

two-transparent phases (2-TP) were formed in which a ME phase coexisted with an oil and/or an aqueous phase (Winsor I, II or III). In contrast, at low surfactant, MCT and ethanol content and high water concentration, a system with milked-like appearance (WP) with phase separation (or not) was formed.

The systems chosen to be evaluated by SAXS and rheological measurements showed different visual appearance (Figure 3), including one translucent phase, one opaque phase and phase separated systems. In general, higher surfactant content increased the opacity of the systems and disfavored the phase separation, while the water addition enhanced the phase separation.

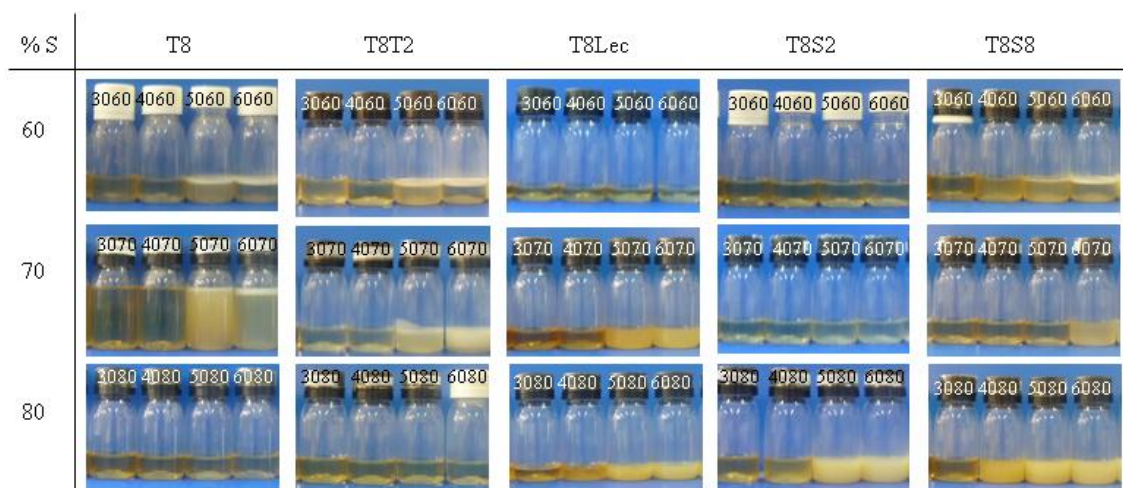


Figure. 3. Visual appearance of the different systems formed by surfactants mixtures, MCT, ethanol and water. Final water concentration from 30 to 60 (% w/w) and initial surfactant mixture concentration (% S) varied from 60 to 80 % (w/w).

5.3.2. SAXS

Most samples presented well-defined correlation peaks that changed position and shape as the water concentration increased (Figure 4). The scattering vector or the first peak position tended to decrease at higher water content, while the peaks number and definition rose as the surfactant content increased.

Different types of structures were observed depending on the systems composition (Table 4). Reverse structures were produced at low water content,

while normal structures were observed from 50 % (w/w) of water content. Normal hexagonal structure (H_1) was the liquid crystalline (LC) most commonly found, but lamellar structures (L_α) were also observed for most of the systems with higher surfactant content. Systems containing lecithin also showed cubic phase ($Pn3m$) at the higher surfactant content. More hydrophobic systems (T8Lec, T8S2 and T8S8) showed a larger number of LC structures than polysorbates (T8 and T8T2) systems, decreasing L_2 region and extending their LC region. In addition, structural parameters of the systems d , a , and r_{hc} were lower in more hydrophilic systems, showing the following order: T8T2 < T8 < T8Lec < T8S2 < T8S8 (Table 4).

The displacement of SAXS peaks to lower q values as the water concentration rose (30 – 60 % w/w) indicated an increase in d and a values or a higher distance between the repeated structures. In the same way, higher water content increased the thickness of the hydrophilic phase (d_w), while the hydrophobic phase thickness (d_o) was higher in systems with lower HLB, being around 10, 15 and 20 Å in T8, T8Lec/T8S2 and T8S8 systems, respectively. The slight decrease of a and d values of some polysorbates systems at high water content (as 6060T8, 6060T8T2, and 6070T8T2 systems), can be attributed to the non well-defined or overlapping peaks. In addition, the structure transition from reverse micelle to liquid crystalline phases (H_2 , L_α and H_1) was hard to identify in some systems, since they showed a very small secondary peak that probably means a structure between an elongated micelle and a LC phase.

Generally, d values decreased with the increase of surfactant concentration at the same water content in more hydrophobic systems, while the more hydrophilic systems (T8 and T8T2) did not show any tendency probably because of the presence of less defined peaks.

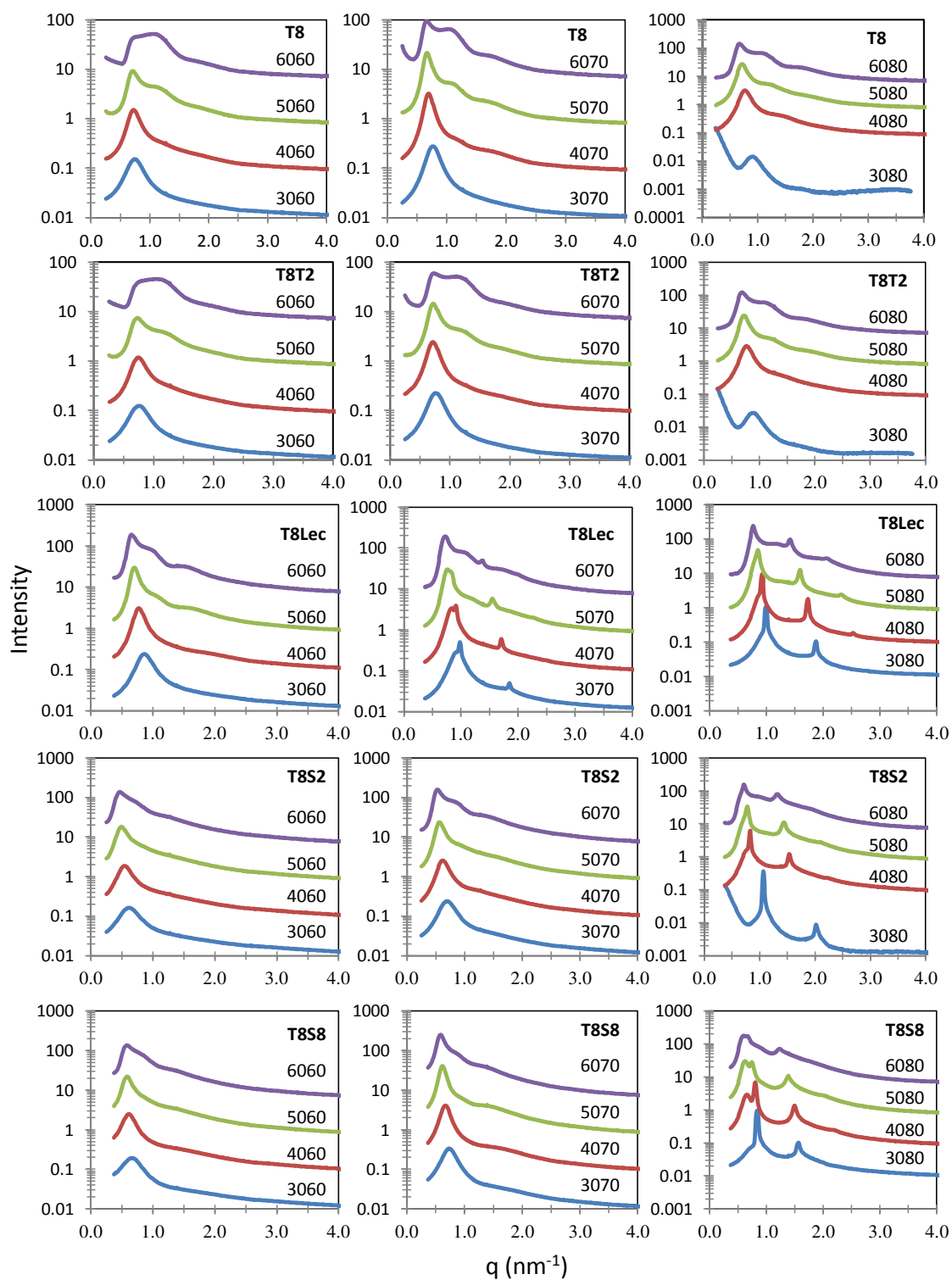


Figure. 4. SAXS patterns of T8, T8T2, T8Lec, T8S2 and T8S8 systems at different water concentrations

Tab. 4. Structural parameters obtained by SAXS measurements. d : structure repetition distance, a : lattice parameter of H_1 , H_2 , L_α or $Pn3m$, d_{hc} : hydrophobic thickness of L_α , d_w : hydrophilic thickness of L_α and r_{hc} : radius of cylindrical micelle of H_1 or H_2 .

% S	Structure parameters (Å)	T8				T8T2				T8Lec				T8S2				T8S8			
		% (w/w) water				% (w/w) water				% (w/w) water				% (w/w) water				% (w/w) water			
		30	40	50	60	30	40	50	60	30	40	50	60	30	40	50	60	30	40	50	60
60	Type	L ₂	L ₂	H ₁	H ₁	L ₂	L ₂	H ₁	H ₁	H ₂	H ₂	H ₁	H ₁	L ₂	L ₂	L ₂	H ₁	L ₂	L ₂	L ₂ /H ₁	H ₁
	d	85.0	87.2	89.6	86.4	83.8	85.7	86.3	76.9	84.9	96.6	109.7	118.2	101.5	115.4	127.8	138.2	115.4	129.0	137.5	139.5
	a	-	-	103.4	99.8	-	-	99.6	88.8	-	111.53	126.69	136.49	-	-	-	159.5	-	-	158.8	161.1
	r_{hc}	-	-	25.3	21.9	-	-	24.3	19.4	-	31.25	32.48	31.38	-	-	-	38.5	-	-	43.4	39.5
	d_{hc}	-	-	-	-	-	-	-	-	-	-	-	-	-	-	-	-	-	-	-	-
	d_w	-	-	-	-	-	-	-	-	-	-	-	-	-	-	-	-	-	-	-	-
70	Type	L ₂	H ₂	H ₁	H ₁	L ₂	L ₂	H ₁	H ₁	L _α	L _α	Pn3m	Pn3m	L ₂	L _α	H ₁	H ₁	L ₂	L ₂	H ₁	H ₁
	d	82.2	90.8	94.1	94.7	82.0	87.6	87.6	86.5	77.7	86.9	98.7	103.7	89.7	101.8	112.9	121.2	101.8	115.4	127.0	137.5
	a	-	104.9	108.6	109.4	-	-	101.1	99.9	77.7	86.9	129.6	132.0	-	101.8	130.4	139.9	-	-	146.6	158.8
	r_{hc}	-	27.3	25.8	24.0	-	-	24.0	21.2	-	-	-	-	-	-	34.8	33.5	-	-	39.9	38.7
	d_{hc}	-	-	-	-	-	-	-	-	14.5	14.0	-	-	-	17.8	-	-	-	-	-	-
	d_w	-	-	-	-	-	-	-	-	63.22	71.9	-	-	-	84.0	-	-	-	-	-	-
80	Type	L ₂	L _α	H ₁	H ₁	L ₂	L ₂	H ₁	H ₁	Pn3m	Pn3m	Pn3m	Pn3m	L _α	L _α	L _α	L _α	L _α	L _α	L _α	L _α
	d	69.3	81.5	87.7	93.9	71.2	81.5	87.4	92.6	71.1	78.0	86.1	96.7	71.3	88.9	95.5	105.5	87.3	117.1	124.8	132.2
	a	-	81.5	101.3	108.4	-	-	101.0	106.9	103.7	112.6	115.9	134.3	71.3	88.9	95.5	105.5	87.3	117.1	124.8	132.2
	r_{hc}	-	-	23.4	22.4	-	-	23.1	21.9	-	-	-	-	-	-	-	-	-	-	-	-
	d_{hc}	-	10.6	-	-	-	-	-	-	-	-	-	-	14.4	15.4	13.7	12.1	18.3	21.1	18.7	15.9
	d_w	-	70.9	-	-	-	-	-	-	-	-	-	-	57.0	73.6	81.7	93.4	69.0	109.3	106.0	116.3

Systems structure: (L₂) reverse micelles, (H₂) reverse hexagonal, (L_α) lamellar, (H₁) normal hexagonal and (Pn3m) cubic phases

5.3.3. FLOW CURVES

Different rheological behavior (Table 5 and Figure 5) was observed depending of the systems composition. Systems using only Tween 80 as surfactant showed Newtonian behavior. However, the partial substitution of Tween 80 by others biocompatible surfactants increased the rheological complexity of the systems.

Mixed polysorbates system (T8T2) showed shear-thinning behavior at the highest water content (60 % w/w) or with the combination of a lower water concentration (50 % w/w) and a lower surfactant content (5060T8T2). Systems with lecithin or Span 20 showed shear-thinning behavior at the highest surfactant content, and the more pronounced pseudoplasticity was observed in systems with lower water content. T8S8 or the more hydrophobic mixture led to a higher number of conditions showing shear-thinning behavior.

Apparent viscosity of the different systems was evaluated at low shear rate and from the first-up flow curve in order to observe the structure minimally disturbed (Table 5). In general, the highest viscosity was observed for lecithin systems, but systems with Span 80 presented higher values at high surfactant content and water content lower than 50 % (w/w). Moreover, the higher viscosity values were observed at intermediary water concentration (40 and 50 % w/w).

Tab. 5. Rheological properties of systems. n : behavior index, k : consistency index, η_3 : apparent viscosity at 3 s^{-1} , μ : Newtonian viscosity.

Systems	water content % (w/w)	% (w/w) Initial surfactant content											
		60				70				80			
		n	k (Pa.s ^{n})	R^2	μ or η_3 (mPa.s)	n	k (Pa.s ^{n})	R^2	μ or η_3 (mPa.s)	n	k (Pa.s ^{n})	R^2	μ or η_3 (mPa.s)
T8	30	1	-	0.99	249	1	-	0.99	461	1	-	0.99	839
	40	1	-	0.99	515	1	-	0.99	1547	1	-	0.99	3053
	50	1	-	0.99	181	1	-	0.99	2363	1	-	0.99	2450
	60	1	-	0.99	33	1	-	0.99	66	1	-	0.99	167
T8T2	30	1	-	0.99	196	1	-	0.99	411	1	-	0.99	443
	40	1	-	0.99	279	1	-	0.99	1017	1	-	0.99	1143
	50	0.796	0.467	0.99	130	1	-	0.99	425	1	-	0.99	820
	60	0.467	0.619	0.92	26	0.635	0.558	0.98	55	0.856	0.229	0.99	85
T8Lec	30	1	-	0.99	294	0.802	0.566	0.99	659	0.545	2.055	0.99	1560
	40	1	-	0.99	3615	1	-	0.99	3020	0.445	45.02	0.87	5805
	50	1	-	0.99	1735	1	-	0.99	7393	0.796	6.958	0.99	8520
	60	1	-	0.99	63	1	-	0.99	111	1	-	0.99	349
T8S2	30	1	-	0.99	109	1	-	0.99	219	0.580	2.092	0.99	1648
	40	1	-	0.99	205	1	-	0.99	438	0.718	2.221	0.97	1860
	50	1	-	0.99	128	1	-	0.99	537	0.712	1.274	0.99	1437
	60	1	-	0.99	23	1	-	0.99	60	0.687	0.307	0.99	383
T8S8	30	1	-	0.99	167	1	-	0.99	293	0.629	2.791	0.99	3035
	40	0.835	0.805	0.99	337	1	-	0.99	1105	0.592	15.674	0.97	7165
	50	0.758	0.443	0.98	106	0.763	4.943	0.98	2055	0.803	1.396	0.99	1145
	60	1	-	0.99	23	0.637	0.734	0.96	310	0.634	0.372	0.99	158

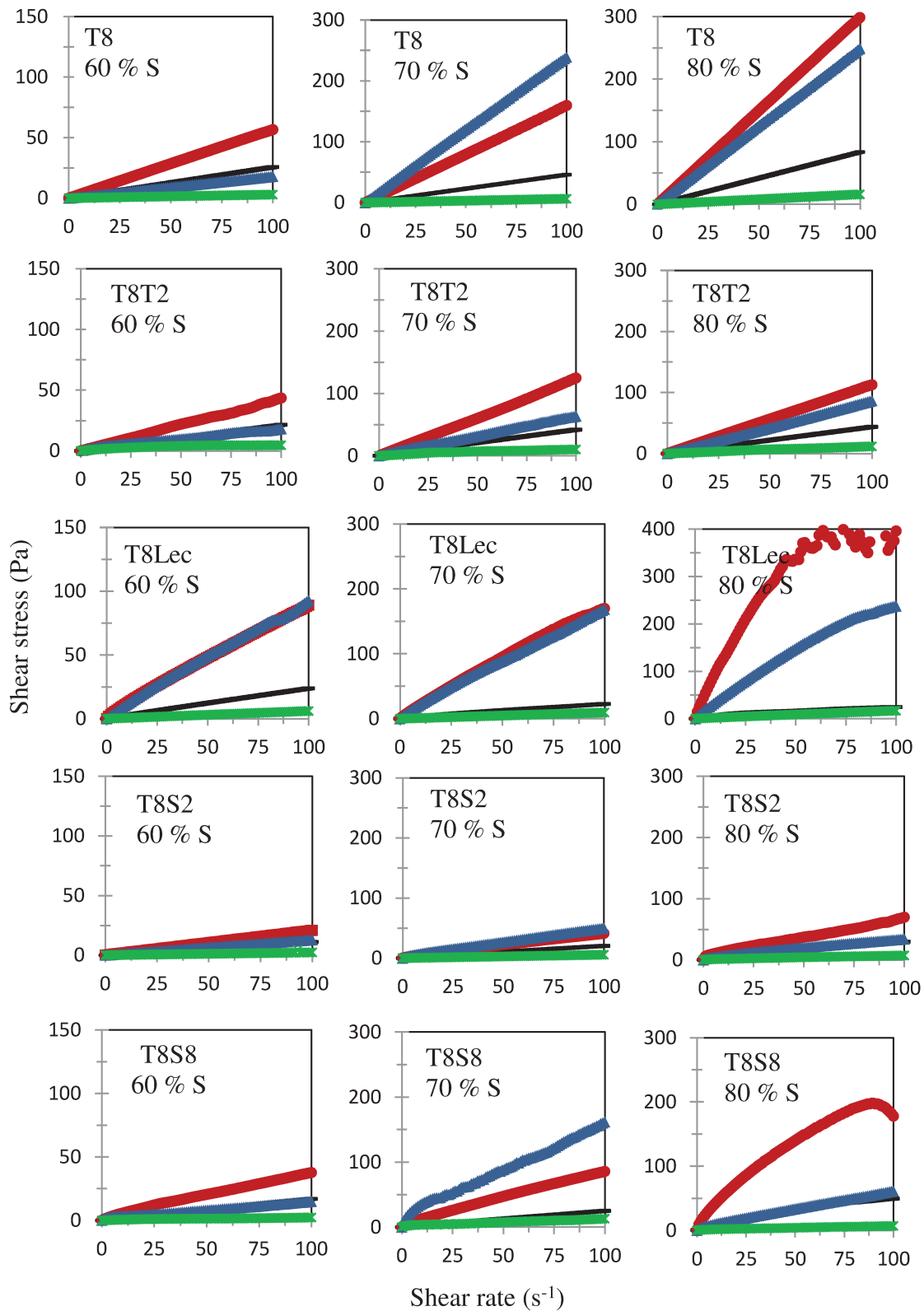


Figure. 5. Flow curves of systems composed by different surfactants mixtures (T8, T8T2, T8S2, T8S8 and T8Lec), with 60, 70 and 80 % (w/w) of initial surfactant

concentration and 30 (—), 40 (●), 50 (▲) and 60 (×) % (w/w) of water. S: initial surfactant concentration.

5.3.4. OSCILLATORY RHEOLOGY

Oscillatory tests also contributed to evaluate the structural transition of the colloidal mixture of MCT, water, ethanol and surfactant mixtures. Figure 6 shows the frequency dependency of complex viscosity (η^*) of T8, T8T2, T8Lec, T8S2 and T8S8 systems. Generally, η^* increased for water content up to 40 and 50 % (w/w) and decreased at higher water content.

Systems containing Tween 20 (more hydrophilic systems) were the less structured, showing lower η^* values and a diluted solution behavior (G' lower than G'' , data not shown). Systems containing only Tween 80 showed diluted solution behavior, excepted systems 5070T8 and 6080T8, which showed concentrated solution behavior ($G'-G''$ crossover point, data not shown) and a frequency-dependent η^* .

The systems with lecithin showed gel-like behavior at higher surfactant content (80 % w/w) and for 4060 (lower surfactant and high water content), while 4070T8Lec showed concentrated solution behavior and the others systems showed a diluted solution behavior.

T8S2 systems showed concentrated solution or gel-like behavior at the highest surfactant concentration, while the others systems showed diluted solution behavior. T8S8 systems showed the most frequency-dependent behavior and more structured systems, with gel-like and concentrated solution behavior for the systems with high initial surfactant content and/or 50 and 60 % (w/w) of water.

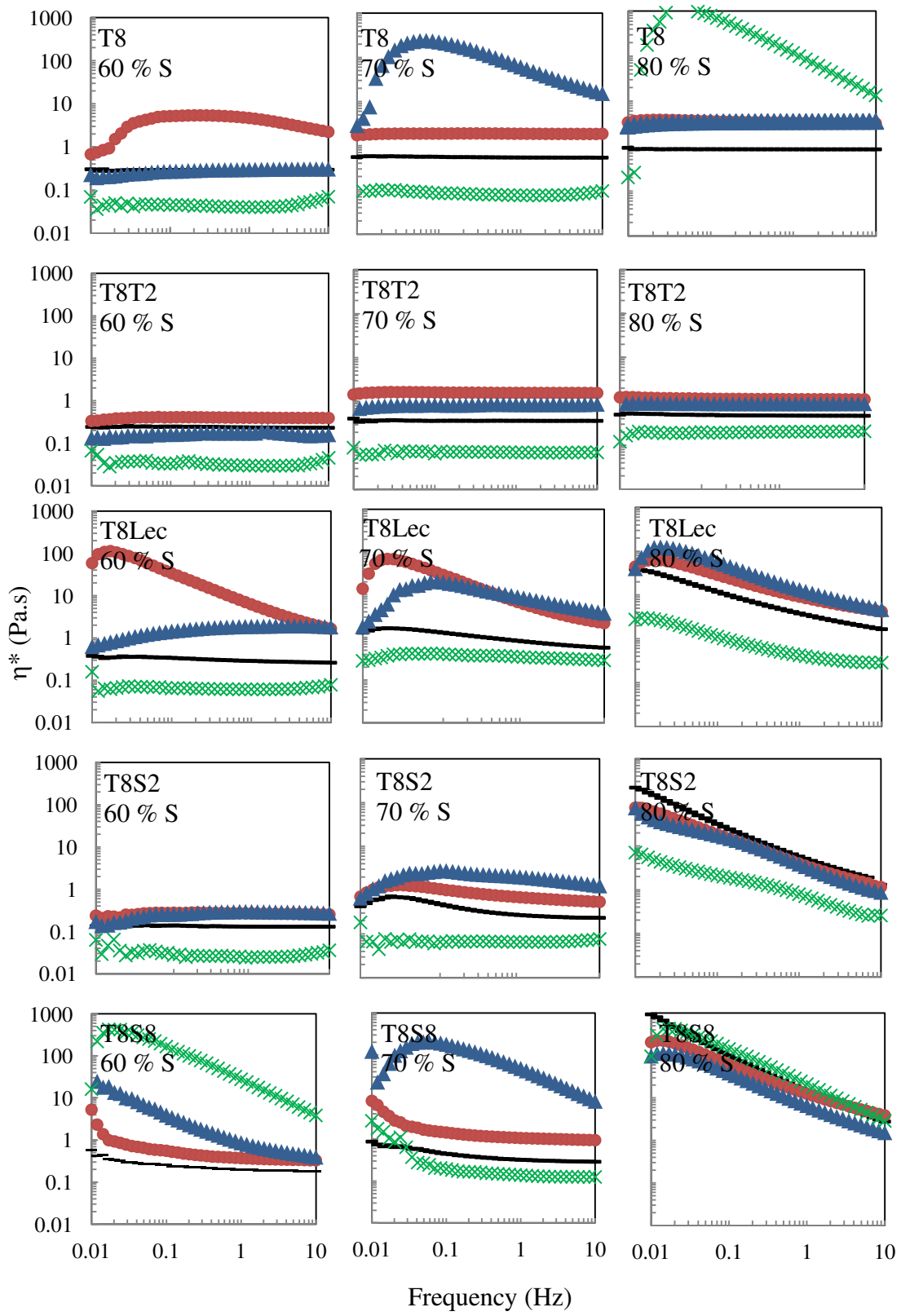


Figure. 6. Complex viscosity of systems T8, T8T2, T8S2, T8S8 and T8Lec with 60, 70 and 80 % (w/w) of initial surfactant concentration and 30 (—), 40 (●), 50 (▲) and 60 (×) % (w/w) of water. S: initial surfactant concentration.

5.4. DISCUSSION

The wide range of structures and rheological behavior observed could be explained by the water and surfactant concentrations, as well as the chemical properties of surfactants mixture. Moreover, the partition phenomenon and diffusion mechanism of cosurfactant (ethanol) between the oil, water and surfactants tails was affected by surfactants combination and components concentration, exerting influence on the self-assembly and the corresponding systems structure.

5.4.1. Effect of water and surfactant concentration on system structure and rheology

The transition from W/O (reverse) to O/W (normal) structures was observed with the water increase from 30 to 60 % (w/w) of water and it was identified by the maximal viscosity (Table 5) or viscoelastic properties (Figure 6), as observed in other works (De Castro Santana, Fasolin and Cunha, 2012; Deutch-Klevzon, Aserin and Garti, 2011; Fanun, 2009; Yaghmur, Aserin, Antalek and Garti, 2003).

Generally, d and a increased with water addition (Table 4). Probably it occurred because of the water binding to the “dry” structure that swells (Feitosa, Cavalcante and Amaral, 2009). In the same way, the increase of a and d_w and the decrease of d_o with water addition in lamellar phases indicated that the surfactant bilayer was compressed by the expanding water channel (Li et al., 2009). In hexagonal phases, r_{hc} decreased with water increment probably because the water was the outer phase.

Hydrophobic systems showed a bigger LC region than hydrophilic systems, and consequently they showed enhanced viscoelastic properties at higher water content even at lower surfactant content. The more structured systems observed at higher surfactant content could be associated with their smaller d and a (Table 4),

revealing that the surfactant molecules would be aggregated more densely in the lamella or cylinder of hexagonal phase, and/or the lamellas or cylinders aggregated more densely in the lamella or hexagonal phase (Li et al., 2009).

5.4.2. Effect of surfactant type on systems structure and rheology

Chemical affinity (*CPP* and *HLB*) of surfactants mixture determined the tendency of the structural characteristics. Polysorbates mixtures (T8 and T8T2) showed *HLB* near 15, tending to form normal (O/W) structures at water concentration higher than 50 % (w/w) (Table 4). Moreover, these O/W systems did not show phase separation over a bigger area of phase diagram and with higher water content than systems containing monosorbates (Figure 2). *CPP* of T8 and T8T2 mixtures were 0.1372 and 0.1370 (Table 2), respectively, which should tend to form normal micelles (L_1) (Tadros, 2008). Observation of H_1 instead of L_1 phase could be explained by changes in apparent *CPP* with the global systems composition. Since *CPP* is a measure of the preferred geometry adopted by the surfactant, it may change with the addition of water, oil and co-surfactant. Oil molecules can penetrate between surfactant hydrocarbon tails increasing the effective hydrophobic volume and consequently the real *CPP* of the mixture. On the other hand, the presence of hydrophilic molecules (as water and ethanol) can influence optimal head group area by altering the solubility of the surfactant head group in the aqueous phase (Lawrence and Rees, 2000). In this way, L_1 phases probably could be observed only at water content higher than 60 % (w/w).

Monosorbates mixtures (T8S8 and T8S2) showed lower *HLB* values (9.6 and 11.43) or higher *CPP* than polysorbates systems (Table 2), disfavoring the production of normal structure and tending to produce reverse structures depending on the overall system composition. Indeed a higher number of L_2 systems at lower surfactant and water content (Table 4) was observed when compared to the others systems. However, the presence of ethanol and oil molecules resulted in the production of L_α systems in more hydrophobic systems and higher surfactant content.

Unlike behavior of systems containing lecithin can be explained by its amphoteric character. The presence of electric charges increased the repulsion between surfactant layers, prevented the coalescence of aggregates (Rodríguez et al, 2003) and expanded the water domain in the one phase (1-P) region (Figure 2). In addition, lecithin shows CPP near to 0.8, tending to produce structures with surfactant layer curvature close to zero (Israelachvili, 1994), as the numerous lamellar (L_α) and cubic phases ($Pn3m$) observed in our study (Table 4). Despite of the low lecithin:Tween 80 ratio used, the presence of lecithin induced a small but considerable change on *HLB* and *CPP* of these systems (Table 2), which led to significant changes on systems structure and rheology. T8Lec showed structured and viscous systems, which can be explained by the repulsion between amphoteric molecules, so that they cannot move freely but tended to be fixed within some array (Rodríguez et al. 2003).

Moreover, surfactants mixture properties showed a clear effect on structural parameters of the systems. Lower *HLB* led to higher distance between scattering centers of the structure (d and a values) (Table 4). In the same way, hydrophobic radius (r_{hc}) of hexagonal phases (H_1 and H_2) phases and hydrophilic thickness (d_w) of lamellar phase (L_α) were usually bigger on systems with lower *HLB*. Such increase of structural distance is associated to the increase of the surfactant hydrophobic chain (Li et al., 2009).

Probably, the poor interaction between more hydrophobic surfactants and ethanol (polar molecule) makes the alcohol more susceptible to the partition phenomenon. Therefore, in more hydrophobic systems with low water content, ethanol migrates to water droplets, or water channels of hexagonal phases, resulting in structures with higher interfacial area, bigger and with higher distance between structures. In the same way, in more hydrophobic systems with high water content, the ethanol migrates to the continuous water phase increasing the distance between the structures.

Non-Newtonian behavior was observed mainly in LC systems (H_1 , L_α and $Pn3m$). Shear-thinning behavior was associated with system components interactions, which determine the flexibility of the surfactant layer and structure

resistance under shear. Pseudoplasticity of LC can be attributed to the reversible orientation of the particles and/or particle size reduction caused by shear flow, such as the breaking of the wormlike micellar network (Guo and Guo, 2010; Yue, Guo and Guo, 2008).

Generally, more hydrophobic systems showed a higher number of shear thinning systems, a higher viscosity (Table 5) and a more viscoelastic structure (Figure 6), probably because of the lower interaction between hydrophobic surfactant and ethanol, especially at high surfactant content. The more rigid structure produced on hydrophobic systems were reversibly broken under shear, showed by the shear-thinning behavior. Moreover, the viscosity and viscoelastic properties were higher in systems composed by surfactant with longer chain length (monooleate fatty acid) than in systems composed by surfactant with smaller chain length (monolaurate fatty acid), as observed by Li et al. (2009).

Lower n and higher k values were observed on systems with well-defined and with a number of peaks in SAXS measurements (Figure 4), which was associated to a more ordered structure that reorganized under shear. Therefore, more complex structures as lamellar (L_{α}) phases of lecithin and monosorbates systems as well as cubic phases ($Pn3m$) of T8Lec systems showed shear thinning behavior. The realignment of the disordered lamellar phase under shearing explains its shear-thinning behaviour (Liu and Hao, 2011).

5.5. CONCLUSIONS

The partial substitution of Tween 80 (25 % w/w) by different biocompatible surfactants showed a strong effect on the structure and rheology of the systems. According to surfactants mixture properties, as CPP and HLB, the mixture layer curvature changed and a variety of structures were produced. Micelle and hexagonal were the main phases observed in more hydrophilic systems, while lamellar phases were produced in monosorbates and lecithin systems. Cubic phases were only observed in lecithin systems.

In addition, rheological-structural behavior depended of the interactions between systems components as well as the partition phenomenon which changed

with characteristics of surfactants mixture. Higher lattice parameters observed on systems with lower HLB were explained by the partition phenomenon of ethanol to water phase. Moreover, a relationship between pseudoplasticity and more structured systems was observed on more hydrophobic LC systems. The higher pseudoplasticity was associated with a structure susceptible to reorientation or to the structure broken under shear. On the other hand, the pseudoplasticity observed in more hydrophilic systems was associated to the structure reorganization of flexible structures. At last, the concentration of components also influenced systems properties. At intermediary water content, LC with high viscosity and viscoelastic properties were produced, while at higher surfactant content, it was observed pseudoplastic and structured LC systems. This discussion concerning the effects of surfactant properties and components concentration on systems structure and rheology could be used to improve the stability and efficiency of food, pharmaceutical or cosmetic products.

5.6. ACKNOWLEDGEMENTS

The authors wish to acknowledge FAPESP, CNPq and CAPES for their financial support. We thank the Brazilian Synchrotron Laboratory, LNLS, for the use of the SAXS beamline.

5.7. REFERENCES

- M.M. Alam, Y. Sugiyama, K. Watanabe, K. Aramaki (2010). Phase behavior and rheology of oil swollen micellar cubic phase and gel emulsions in nonionic surfactant systems, *J. Colloid Interface Sci.*, 341, 267–272.
- M.G. Berni, C.J. Lawrence, D. Machin (2002). A review of the rheology of the lamellar phase in surfactant systems, *Adv. Colloid Interface Sci.* 98 217–243.
- B.P. Binks, P.D.I. Fletcher, L. Tian, (2010). Influence of nanoparticle addition to Winsor surfactant microemulsion systems, *Colloids Surf., A.* 363. 8–15.
- R. Deutch-Klevzon, A. Aserin, N. Garti (2011). Synergistic cosolubilization of omega-3 fatty acid esters and coQ₁₀ in dilutable microemulsions *Chem. Phys. Lipids*, 654–663.

- M. Fanun, (2010). Properties of microemulsions with mixed non-ionic surfactants and citrus oil, *Colloids Surf., A*, 369, 246–252.
- Fanun, M. (2009). Properties of microemulsions based on mixed nonionic surfactants and mixed oils, *J. Mol. Liq.* 150, 25–32.
- Fasolin, L. H., Santana, R. C., Cunha, R. L. (2012). Microemulsions and liquid crystalline formulated with triacylglycerols: effect of ethanol and oil unsaturation, *Colloids Surf., A*, 415, 31-40.
- J. Feng, Z. Wang, J. Zhang, Z. Wang, F. Liu, (2009). Study on food grade vitamin E microemulsions based on nonionic emulsifiers, *Colloids Surf., A*, 339, 1–6.
- J. Flanagan, H. Singh, (2006). Microemulsions: a potential delivery system for bioactives, *Crit. Rev. Food Sci. Nutr.*, 46, 221–237.
- Garti, N., Yaghmur, A., Leser, M. E., Clement, V., Watzke, H. J. (2001). Improved oil solubilization in oil/water food grade microemulsions in the presence of polyols and ethanol, *J. Agric. Food Chem.* 49, 2552–2562.
- Guo, P., Guo, R. (2010). Ionic liquid induced transition from wormlike to rod or spherical micelles in mixed nonionic surfactant systems, *J. Chem. Eng. Data*, 55, 3590–3597.
- Israelachvili, J. (1994). The science and applications of emulsions – an overview, *Colloids Surf., A*, 91, 1-8.
- Kulkarni, C. V. (2011). Nanostructural studies on monoelaidin – water systems at low temperatures, *Lagmuir*, 27, 11790-11800.
- Kumar, V. V. (1991). Complementary molecular shapes and additivity of the packing parameter of lipids. *Proceeding of the National Academy of Sciences*, 88, 444-448.
- Lawrence, M. J., and Rees, G. D. (2000). Microemulsion-based media as novel drug delivery systems, *Adv Drug Deliver Review*, 45, 89–121.
- Li, X.-W, Zhang, J., Dong, B., Zheng, L.-Q., Tung, C.-H. (2009). Characterization of lyotropic liquid crystals formed in the mixtures of 1-alkyl-3-methylimidazolium bromide/p-xylene/water, *Colloids Surf., A*, 335, 80-87.

- C. Lin, H. Lin, H. Chen, M. Yu, M. Lee (2009). Stability and characterization of phospholipid based curcuminencapsulated microemulsions, *Food Chem.* 116, 923–928.
- Liu, C., Hao, J. (2011). Shear-induced structural transition and recovery in the salt-free cationic surfactant systems containing deoxycholic acid, *J. Phys. Chem. B* 115, 980–989.
- Patel, N., Schmid, U., Lawrence, M.J. (2006). Phospholipid-based microemulsions suitable for use in foods, *J. Agric. Food Chem.*, 20, 7817-7824.
- Paul, B. K., Mitra, R. K. (2005). Water solubilization capacity of mixed reverse micelles: Effect of surfactant component, the nature of the oil, and electrolyte concentration. *J. Colloid Interface Sci.*, 288, 261-279.
- Pottirayil, A., Kailas, S. V., Biswas, S. K. (2011). Lubricity of an oil in water emulsion in metal cutting: The effect of hydrophilic/lipophilic balance of emulsifiers. *Colloids Surf., A*, 384, 323-330.
- Rodríguez, C., Acharya, D. P., Hinata, S., Ishitobi, M., Kunieda, H. (2003). Effect of ionic surfactants on the phase behavior and structure of sucrose ester/water/oil systems. *Journal of Colloid and Interface Science*, 262, 500-505.
- A. Spornath, A. Aserin, (2006). Microemulsions as carriers for drugs and nutraceutical, *Adv. Colloid Interface Sci.*, 128, 47–64.
- Spornath, A.; Yaghmur, A.; Aserin, A.; Hoffman, R. E.; Garti, N. (2003). Self-diffusion nuclear magnetic resonance, microstructure transitions, and solubilization capacity of phytosterols and cholesterol in Winsor IV food-grade microemulsions. *Journal of Agricultural and Food Chemistry*, 51, 2359-2364.
- Tadros, T. F. *Applied Surfactants: Principles and Applications*. Weinheim: Wiley – VCH.
- Zhang, H., Cui, Y., Zhu, S., Feng, F., Zheng, X. (2010). Characterization and antimicrobial activity of pharmaceutical microemulsions. *International Journal of Pharmaceutics*, 395, 154-160.
- L. Wolf, H. Hoffmann, K. Watanabe, T. (2011). Okamoto, Microemulsions from silicone oil with an anionic/nonionic surfactant mixture, *Phys. Chem. Chem. Phys.* 13, 3248–3256.

Yaghmur, A., Aserin, A., Antalek, B., Garti, N. (2003). Microstructure considerations of new five-component Winsor IV food-grade microemulsions studied by pulsed gradient spin-echo NMR, conductivity, and viscosity, *Langmuir* 19, 1063–1068.

Yaghmur, A. Aserin, N. Garti, (2002) Phase behavior of microemulsions based on food grade nonionic surfactants: effect of polyols and short chain alcohols, *Colloids Surf., A*, 209, 71–81.

Yue, H., Guo, P., Guo, R. (2008). Phase behavior and structure properties of sodium dodecyl sulfate (SDS)/Brij 30/Water system, *J. Chem. Eng. Data*, 54, 2923–2929.

**CAPÍTULO 6 -
CONCLUSÕES GERAIS**

Sistemas com diferentes estruturas e comportamentos reológicos foram produzidos a partir da auto-organização de compostos biocompatíveis. A transição estrutural com a adição de água foi claramente observada a partir de diagramas pseudo-ternário, microscopia de luz polarizada, DSC, DLS, reologia, e SAXS. Entretanto, somente a técnica de SAXS foi capaz de identificar a estrutura e os parâmetros estruturais de sistemas com propriedades reológicas semelhantes.

Microemulsões A/O (ou micelas reversas inchadas) com baixa viscosidade foram produzidas em baixas concentrações de água, enquanto micelas normais e cristais líquidos menos estruturados foram produzidos em elevadas concentrações de água. Já em concentrações intermediárias de água, cristais líquidos com maiores distâncias entre os planos das estruturas (d), elevada viscosidade e reologia complexa sob grandes e pequenas deformações foram produzidos. Além disso, a reologia identificou mudanças estruturais com o tempo de cisalhamento. Sistemas ricos em componentes polares (água e etanol) mostraram comportamento anti-tixotrópico e produziram sistemas mais organizados sob cisalhamento. Sistemas com predomínio de componentes apolares e anfífilicos tenderam ao comportamento tixotrópico, devido à susceptibilidade da estrutura do tipo gel ao cisalhamento.

Já a avaliação dos sistemas com diferentes razões óleo:etanol mostrou que o incremento de etanol estendeu a região de microemulsões reversas (ou micelas reversas inchadas) para maiores concentrações de água, produziu sistemas com menor distância entre os planos das estruturas (d), baixos valores de propriedades viscoelásticas e pouco dependentes da temperatura. Além disso, sistemas com elevada concentração de etanol apresentaram pequenos picos endotérmicos e exotérmicos devido à interação entre os componentes.

O estudo do efeito da temperatura mostrou que sistemas com concentração intermediária de água e baixa concentração de etanol apresentaram uma transição de fases em torno de 50 °C. Fases hexagonais e cúbicas com comportamento do tipo gel foram produzidas a 25 °C, enquanto fases líquidas cristalinas de baixa organização e micelas coexistiram em temperaturas elevadas (50 e 70 °C), apresentando menor distância entre os planos das estruturas (d) e

comportamento do tipo líquido. Entretanto, sistemas com baixa e elevada concentração de água não apresentaram mudanças reológicas com o aumento da temperatura.

O estudo dos sistemas compostos por misturas de surfactantes revelou que as propriedades dos sistemas estão relacionadas com o PC (parâmetro crítico de empacotamento) e BHL (balanço hidrofílico-lipofílico) da mistura de surfactante. Fases micelares e hexagonais predominaram nos sistemas mais hidrofílicos, enquanto a fase lamelar foi produzida em sistemas contendo monosorbatos e lecitina. Fases cúbicas foram observadas somente em sistemas com lecitina. Maiores parâmetros estruturais lattice (a) foram observados em sistemas com menor BHL devido à partição do etanol na água. Além disso, sistemas mais hidrofóbicos apresentaram cristais líquidos pseudoplásticos com elevadas propriedades viscoelásticas. Por último, sistemas com maiores concentrações de surfactantes apresentaram pseudoplasticidade e cristais líquidos estruturados.

As diferentes estruturas e comportamentos reológicos avaliados neste trabalho apresentam potenciais aplicações nas indústrias alimentícia, farmacêutica e cosmética. Os resultados esclareceram os efeitos de cada componente (água, co-surfactante e surfactante) e da temperatura sobre as propriedades dos sistemas, viabilizando a adequada manipulação da composição e da temperatura na obtenção de estruturas com diferentes texturas (tanto na forma de géis quanto na forma líquida) e veiculadoras de bioativos com liberação controlada.

